The Chemistry and Technology of GYPSUM

R. A. Kuntze, editor

ASTM STP 861

THE CHEMISTRY AND TECHNOLOGY OF GYPSUM

A symposium sponsored by
ASTM Committee C-11 on
Gypsum and Related Building
Materials and Systems
Atlanta, GA, 14–15 April 1983

ASTM SPECIAL TECHNICAL PUBLICATION 861
Richard A. Kuntze, Ontario Research
Foundation, editor

ASTM Publication Code Number (PCN)
04-861000-07

1916 Race Street, Philadelphia, PA 19103

Library of Congress Cataloging in Publication Data

The Chemistry and technology of gypsum.

(ASTM special technical publication; 861)
"ASTM publication code number (PCN) 04-861000-07."
Includes bibliographies and index.
1. Gypsum—Congresses. I. Kuntze, Richard A.
II. ASTM Committee C-11 on Gypsum and Related Building Materials and Systems. III. Series.
TA455.G9C48 1984 666'.92 84-70880
ISBN 0-8031-0219-4

Library of Congress Catalog Card Number: 84-70880

Printed in Ann Arbor, MI
September 1984

Foreword

The symposium on The Chemistry and Technology of Gypsum and Gypsum Products was presented at Atlanta, GA, 14–15 April 1983. The symposium was sponsored by ASTM Committee C-11 on Gypsum and Related Building Materials and Systems. Richard A. Kuntze, Ontario Research Foundation, presided as chairman of the symposium and is editor of the publication.

Related ASTM Publications

Masonry: Materials, Properties, and Performance, STP 778 (1982), 04-778000-07

Extending Aggregate Resources, STP 774 (1982), 04-774000-08

Cement Standards—Evolution and Trends, STP 663 (1979), 04-663000-07

Significance of Tests and Properties of Concrete and Concrete-Making Materials, STP 169B (1978), 04-169020-07

A Note of Appreciation to Reviewers

The quality of the papers that appear in this publication reflects not only the obvious efforts of the authors but also the unheralded, though essential, work of the reviewers. On behalf of ASTM we acknowledge with appreciation their dedication to high professional standards and their sacrifice of time and effort.

ASTM Committee on Publications

ASTM Editorial Staff

Janet R. Schroeder
Kathleen A. Greene
Rosemary Horstman
Helen M. Hoersch
Helen P. Mahy
Allan S. Kleinberg
Susan L. Gebremedhin

Contents

Introduction

Recent advances in gypsum chemistry, analytical techniques, and manufacturing technologies have raised a number of issues of concern to producers and users of gypsum products alike. For example, the analysis of gypsum and gypsum products as covered by ASTM standards is based almost entirely on wet chemical methods. However, modern instrumental methods are now used routinely in most laboratories and institutions. They are capable of determining constituents and impurities of gypsum and its dehydration products more accurately and reliably than conventional methods.

In addition, by-product gypsums are increasingly considered as raw material in the manufacture of gypsum products as partial or complete replacement of natural gypsum. Present ASTM standards do not deal with these synthetic materials, which provide a number of analytical problems because of the presence of unusual impurities not normally found in natural gypsums. For the same reason, the manufacture and application of building materials containing by-product gypsums is affected by serious difficulties.

In order to address these questions and problems, this symposium was sponsored by ASTM Committee C-11 on Gypsum and Related Building Materials and Systems. The symposium was intended to provide a forum for discussions of theories, test methods and analyses, and basic information on gypsum and its products.

Richard A. Kuntze
Ontario Research Foundation, Sheridan Park, Mississauga, Ontario, Canada, L5K1B3, editor

Robert F. Acker[1]

Physical Testing of Gypsum Board Per ASTM C 473

REFERENCE: Acker, R. F., "**Physical Testing of Gypsum Board Per ASTM C 473,**" *The Chemistry and Technology of Gypsum, ASTM STP 861*, R. A. Kuntze, Ed., American Society for Testing and Materials, 1984, pp. 3–21.

ABSTRACT: This work was performed to investigate modernization of the equipment used for the physical testing of gypsum board that has not been basically changed over a period of many years and is not commercially available. A comprehensive study has been made using a commercially available machine for three strength tests, with the expectation that this type of equipment might be incorporated into ASTM methods and specifications in the future. Technical advances in the methods of evaluating gypsum board are desirable in a progressive industry.

The procedure used was to run the three major physical tests: flexural strength; core, end, and edge hardness; and nail pull resistance on a machine using constant strain rate loading and compare those results with those obtained on the commonly used ASTM specified machine that uses a constant stress rate. A TM 51008 tester made by Testing Machines, Inc. was used for the work reported in this paper. Comparative tests were made on equipment conforming to the specifications of ASTM Physical Testing of Gypsum Board Products, Gypsum Lath, Gypsum Partition Tile or Block, and Precast Reinforced Gypsum Slabs (C 473). Preliminary work was done in a research laboratory to develop the fixtures and procedures necessary to use the new equipment. The machine was then placed in a manufacturing plant and duplicate tests on all types of board products were run for a period of several months.

Data will be presented to show that the constant strain rate method of testing can give equally precise results with a very substantial saving in time and physical effort. For flexural strength, nail pull resistance, and core hardness there is a simple linear correlation between the results with the two machines. The constant strain rate machine can more accurately determine the maximum load causing failure than the constant stress rate machine. Correlation between the results of tests on either machine shows that the core hardness and nail pull resistance tests tend to duplicate information on core properties.

KEY WORDS: gypsum, physical tests, physical properties, gypsum board, constant stress, constant strain

About 1975 the ASTM specifications for gypsum board were changed to eliminate arbitrary weight limits and substitute performance tests. The tests added were humidified sag resistance; core, end, and edge hardness; and nail pull

[1]Research associate, United States Gypsum Company, Graham J. Morgan Research Center, 700 North Highway 45, Libertyville, IL 60048.

resistance. The flexure test that was already in the specifications was retained as a performance test.

With the exception of sag resistance, these tests are run by using a testing machine that can apply force to a specimen and measure the force applied. The device used was designed about 1922. It is slow and laborious to use and is not commercially available.

The test procedures are intended primarily for use by the purchaser or user. The product manufacturers voluntarily certify that their products meet the appropriate ASTM specifications. To do this, they must run sufficient tests by these procedures to determine that their products conform to the specifications. All of the tests require that specimens be conditioned for an extended period of time before testing, so the tests cannot be used for direct process control. It is desirable that the tests measure significant properties of the products so that they can be used for product evaluation.

This paper describes work done with a type of testing machine that is commercially available. It is much faster and easier to use than the presently approved type of unit, gives equal or better precision, and can furnish more information from some of the tests than the type of unit presently approved.

Testing Machines

The exact type of machine to be used is not specified in ASTM Physical Testing of Gypsum Board Products, Gypsum Lath, Gypsum Partition Tile or Block, and Precast Reinforced Gypsum Slabs (C 473). However, each procedure specifies that force be applied to a specimen at a controlled rate of 4.45 N/s (60 lb/min). A typical testing machine of the type commonly used in the industry is shown in Fig. 1. On this machine, the prescribed rate of loading is obtained by allowing lead shot to flow into a bucket through a variable size orifice.

The machine used by the United States Gypsum Company was designed in the early 1920s. Some original drawings, which are still used for basic features of the machine, are dated 1922. The method of loading by running lead shot into a bucket is simple and readily adaptable to construction in a plant shop. There is no theoretical reason for specifying constant stress rate loading. To the best of our knowledge, United States Gypsum Company built the first machine to be used for testing gypsum board, and this type of machine was specified in the ASTM procedures because it had been adopted by other manufacturers and was commonly used in the industry.

As best can be determined, other gypsum manufacturers still use similar machines including the shot-bucket method of loading, although other methods of loading are possible. The drawings in ASTM C 473 show a very similar machine, although the method of load application is not detailed.

When a test has been completed, the bucket of shot must be removed and weighed. The shot is then poured back into the supply bucket. This particular machine has a four to one lever arm ratio so the force applied to a specimen is

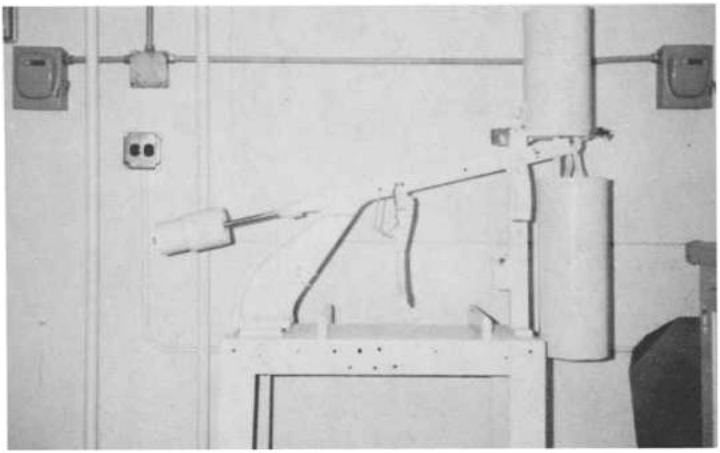

FIG. 1—*Testing machine commonly used for gypsum board.*

five times the mass of the shot. For 16-mm (⅝-in.) board, the minimum breaking load for the flexural strength test broken across the fiber is 667 N (150 lbf). Actual values can be much higher, particularly for tests across the fiber.

When using this testing machine, the operator must repeatedly lift and move a bucket with a mass up to or over 13.6 kg (30 lb). This is tiring at best and can be hazardous unless the person is robust. If this manual labor were eliminated, the job would be more suitable for less robust persons, including females or the physically handicapped.

We have not been able to locate a commercially available machine that uses constant stress loading and is adaptable to the tests of ASTM C 473. Many machines in a wide range of types and capacities are available that use constant strain rate loading. Typically the force is applied to a specimen by a head moving at a constant speed, and the force applied is measured by a sensing system that supports a platform on which the specimen is placed. Testing speeds can be varied over a wide range.

Figure 2 shows a high-capacity high-cost machine of this type that typically could be found in a research laboratory or testing agency. Figure 3 shows the TM 51008 made by Testing Machines, Inc. (TMI). This is a smaller, lower cost machine suitable for use in a plant laboratory. The work to be described was done on this machine, but obviously any machine that gives constant strain loading could be used. For convenience we will refer to the machines as constant stress and constant strain machines.

The TMI machine is equipped with a device for recording a stress-strain curve for tests. Such a device is normally available for any constant strain testing machine.

Figure 4 shows the accessories used for nail pull resistance, and core, end,

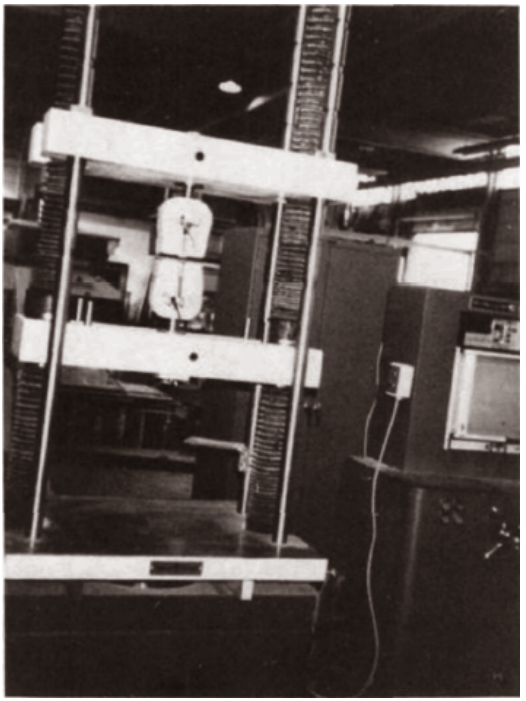

FIG. 2—*Commercial constant strain type testing machine.*

and edge hardness on the two machines. Since the weight of the specimen holder is included in the load measured on the TMI tester, it is convenient to have all accessories weigh the same to avoid frequent adjustment of tare load. The holes drilled in the TMI accessories were used to adjust the weight. The nail pull resistance specimen support for the TM tester has a slot cut in the face. This makes it convenient to remove the specimen by only retracting the sample head slightly and saves a good deal of time on this test.

Flexure Testing

On the TMI tester, the testing area is a little more than 305 mm (12 in.) square. For flexure testing, a 305- by 254-mm (12- by 10-in.) specimen tested on 254-mm (10-in.) centers was used. ASTM C 473 specifies that a 305- by 406-mm 12- by (16-in.) specimen tested on 356-mm (14-in.) centers be used. There is no particular significance to this specimen size other than that the predominant product made in 1922 was 406-mm (16-in.) wide, and the specimen size simplified specimen preparation.

A preliminary test of the TMI tester was run on a special run of board in which three thicknesses of board had been made with the same lots of face and

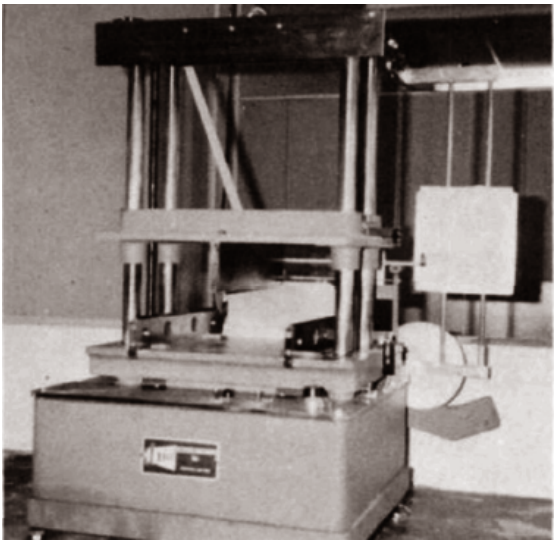

FIG. 3—*Testing Machines Inc. Model 51008 tester.*

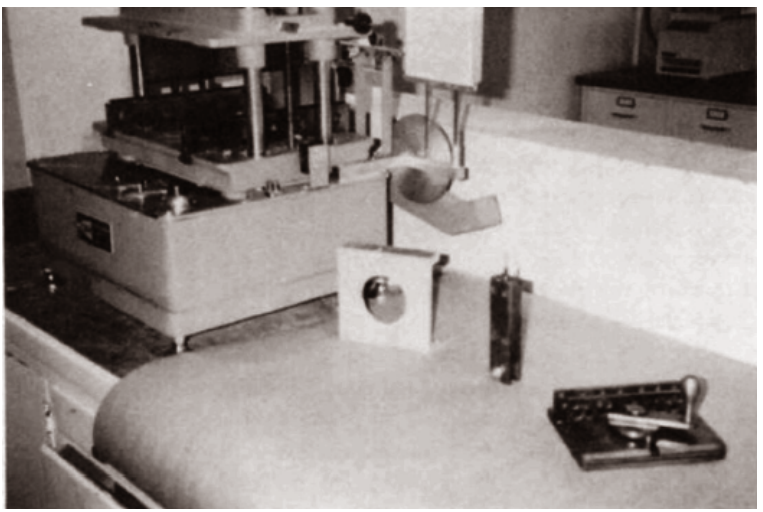

FIG. 4—*Accessories used for gypsum board testing.*

back paper. A number of specimens were run for each of the four variations of the flexure test and at two different speeds of the testing head.

Results are shown in Table 1. The main things to note are that, in the range used, the speed of the testing head had no noticeable effect and the standard deviations of the various specimens were essentially the same for both machines. The two machines have equal precision, and the variations measured are most likely in the product rather than the testing equipment.

A linear correlation of the average values from the two testing machines showed excellent agreement. A calculated correlation equation is $P = 0.08N + 6.9$ ($r = 0.999$). P stands for the value on the presently approved constant stress testing machine and N for the value by the new constant strain machine, and r for the statistical correlation coefficient.

It is obvious that flexure tests should be directly proportional to specimen width. Numerous tests on both types of machines have confirmed this. The modulus of rupture (MOR) formula predicts that flexural strength should be inversely proportional to the span. Combining these relationships we can calculate that the test on the 12 by 16 specimen should be $12/10 \times 10/14 = 0.857$ times the strength of the 10 by 12 specimen. This is reasonably close to the slope of 0.8 found for the correlation equation. Gypsum wallboard is not a homogeneous material as is assumed in the calculation of MOR.

The fact that the correlation equation contains a constant can be explained by considering the action of the two testing machines. The constant strain machine records only the maximum force exerted on the specimen. For flexure tests, this is usually the point where the core first cracks. Additional resistance to breaking occurs as the paper tears and in the case of a board containing glass fiber, as the fibers pull out of the core. The force required for this second break may even exceed that for the initial core crack.

The constant strain machine will record the maximum force whenever it occurs. In a shot-bucket machine, shot will continue to flow into the bucket until the specimen completely fails, and the lever arm falls. Almost invariably there is some shot flow after the point of maximum resistance by the specimen. As will be shown later, the shot-bucket type of machine gives higher numerical values than a maximum-recording constant-strain machine. The difference between the machines is generally quite uniform and predictable. Since the constant strain machine records the true maximum force resisted by a specimen, while the shot-bucket machine usually indicates a greater force, the constant strain machine can be considered more accurate.

The next step in the evaluation was to place a TMI testing machine in a plant and run duplicate tests on all types of products for a period of several months. Results of flexural strength tests are shown in Table 2. For clarity, only the averages are shown in this table, but standard deviations were calculated for each average and were very similar for the two machines. For example, on 12.7-mm (½-in.) regular wallboard where 129 sets of specimens were tested, the standard deviations were as shown in Table 3. This again shows that the two

TABLE 1—*Flexural strength tests various thicknesses.*[a]

Specimen	TM Tester			Board Test Unit		
	Number Tested	Average, lb	Standard Deviation	Number Tested	Average, lb	Standard Deviation
5/16 in. parallel FD	4	35.0	0[b]	...	...	...
	6	36.2	1.5[c]	10	34.7	0.4
5/16 in. parallel FU	2	40.0	0[b]	...	...	...
	3	37.2	0.3[c]	7	39.9	1.6
3/8 in. parallel FD	3	42.3	0.7[b]	...	...	...
	13	43.6	1.5[c]	10	42.6	1.5
3/8 in. parallel FU	3	46.2	1.0[b]	...	...	...
	9	48.5	2.4[c]	10	45.7	2.6
1/2 in. parallel FD	1	73.5	...[b]	...	...	...
	6	74.6	2.4[c]	6	66.5	2.6
1/2 in. parallel FU	1	88.6	...[b]	...	...	...
	3	82.2	10.1[c]	6	76.7	6.1
5/16 in. across FD	3	117.7	3.8[b]	...	...	...
	5	122.7	1.1[c]	11	101.2	3.8
5/16 in. across FU	3	127.3	3.8[b]	...	...	...
	6	131.2	4.7[c]	10	107.8	2.1
3/8 in. across FD	4	141.0	2.7[b]	...	...	...
	11	142.5	2.6[c]	10	118.8	2.2
3/8 in. across FU	3	149.0	6.9[b]	...	...	...
	8	151.6	6.8[c]	10	125.6	5.9
1/2 in. across FD	1	217.0	...[b]	...	...	...
	5	208.8	4.3[c]	7	177.9	5.5
1/2 in. across FU	2	224.0	1.0[b]	...	...	...
	5	225.0	22.4[c]	7	188.8	16.6

[a]1 in. = 25.4 mm and 1 lb = 4.448 N. FU is face up and FD is face down.
[b]Tested at 0.5 in./min.
[c]Tested at 2.0 in./min.

TABLE 2—*Flexural strength data averages.*[a]

Product, in.	Across FU, lb		Across FD, lb		Parallel FU, lb		Parallel FD, lb		Number of Tests
	Old	New	Old	New	Old	New	Old	New	
¼	88.5	88	94	95	26.5	23.5	26.5	24.5	2
5/16	123.2	129.2	136.3	135.8	38.2	35.4	36.7	36.0	6
⅜ A	100	110	100	100	37	30	31	31	1
⅜ B	132.2	141.1	131.6	138.9	35.1	34.8	36.3	34.6	14
7/16	153	155	146	152	43	42.5	31	40.6	1
½ A	172	187.5	183	189	47.25	57.1	52	58.5	4
½ B	212.1	227.9	207.9	226.4	63.2	67.6	59.3	59.8	11
½ regular	175.2	184.4	174.3	183.4	49.13	49.79	49.6	48.5	129
⅝ A	247.2	280.6	243.1	279.6	75.9	82.8	76.5	84.4	9
⅝ B	252.1	280.3	246.4	272	79.4	89.4	81.5	76.6	15
⅝ X	252.4	283.0	256.0	283.0	82.5	93.2	82.0	79.1	79
⅝ C	278.8	322.2	270	305.8	96.5	126.2	94.5	95.1	4

[a] 1 in. = 25.4 mm and 1 lb = 4.448 N. FU is face up and FD is face down.

TABLE 3—*Standard deviations for 12.7-mm (½-in.) regular wallboard.*

Test[a]	Standard Deviation	
	Old Tester	New Tester
Parallel FU	4.0	4.3
Parallel FD	3.9	3.7
Across FU	10.1	9.7
Across FD	10.1	9.6

[a]FU is face up and FD is face down.

machines have the same precision and that the variations measured are in the products.

Figure 5 is a graph of these results showing that there is obviously a very good correlation between the two machines. A calculated correlation equation using all the individual test results, except for a few to be discussed later, gave the equation $P = 0.88N + 7.07$ ($r = 0.99$). This is an excellent correlation, and the slope 0.88 is very close to the theoretical value of 0.857 calculated as explained earlier. This curve is shown as a solid line in Fig. 5. Theoretically, the relationship between the two testers should be a straight line. Experiments show that a slightly better correlation can be achieved by using the exponential formula for a curvilinear correlation.

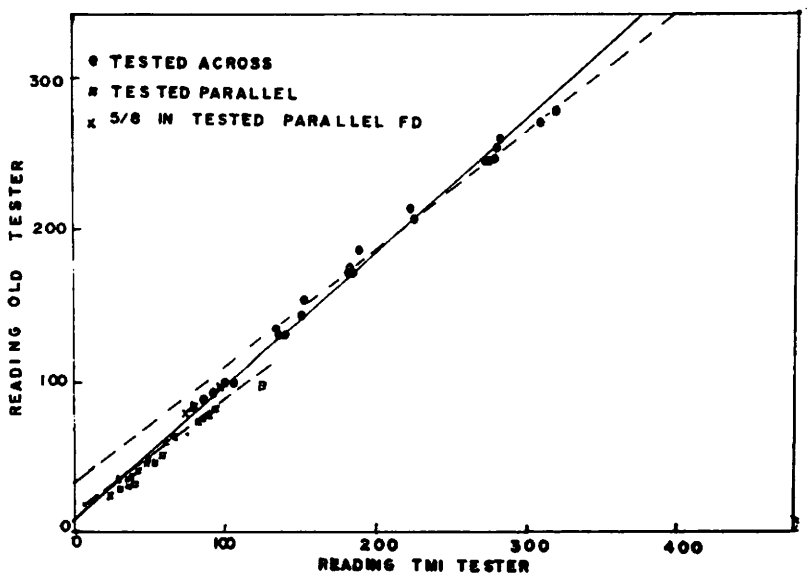

FIG. 5—*Flexure test—TMI tester versus old tester.*

Inspection of the graph suggests that the across the fiber and parallel to the fiber tests may fall on different curves. Calculating separate correlations for the two sets of data, we get the equations

$$P = 0.79N + 28.67 \ (r = 0.97) \text{ tests across}$$
$$P = 0.69N + 15.55 \ (r = 0.91) \text{ tests parallel}$$

These are still excellent correlations, but the parallel tests are not quite as consistent. These curves are shown as dotted lines in Fig. 5.

Inspection of the data in Table 2 shows some unusual results in the data for a 15.88-mm (⅝-in.) board tested parallel. On 15.88-mm (⅝-in.) Type X, where 79 sets of specimens were tested, the face-up and face-down tests have the same average when tested by the present tester. However, the face-up tests average higher and the face-down tests slightly lower on the new tester. The same trend is noticeable on the other types of 15.88-mm (⅝-in.) board tested, although there is more variation because of the smaller number of specimens tested. The face-down data do not fit the correlation curves and were omitted in calculating the correlation equations.

All of the 15.88-mm (⅝-in.) board tested in this study contained glass fibers. As mentioned previously, board containing glass fiber behaves differently in a flexure test than board containing only paper fiber. One of the advantages of the constant strain machine is that a stress-strain curve can be recorded. Figure 6 shows the stress-strain curves for several flexure tests. It is particularly obvious in the case of 15.88-mm (⅝-in.) Type X that the face-up and face-down curves are quite different. It may be that the action of the constant strain machine is revealing a difference that is not shown by the more violent action of the shot-bucket machine. A tentative explanation is that glass fiber distribution is not perfectly uniform through the thickness of the board. Additional data will be needed to clarify this point.

The stress-strain diagram gives considerably more information about the product tested than the single-value result, which is all that can be obtained from the present unit:

1. The test will show the actual value at which the board first cracks. The primary purpose of a flexural strength specification is to ensure that the board has enough strength to withstand normal handling. The force required to crack the core is probably a more practical measure of board utility than the force required to pull it apart after it is cracked.
2. The slope of the first part of the stress-strain curve is a measure of the flexibility of a board. Numerous attempts have been made to measure this property by measuring load versus deflection on the constant stress type of tester, but it is not practical on this type of machine. The area under the curve measures the total work required to break the board or the toughness of the board.

The stress-strain curve gives an accurate measure of these properties; and with

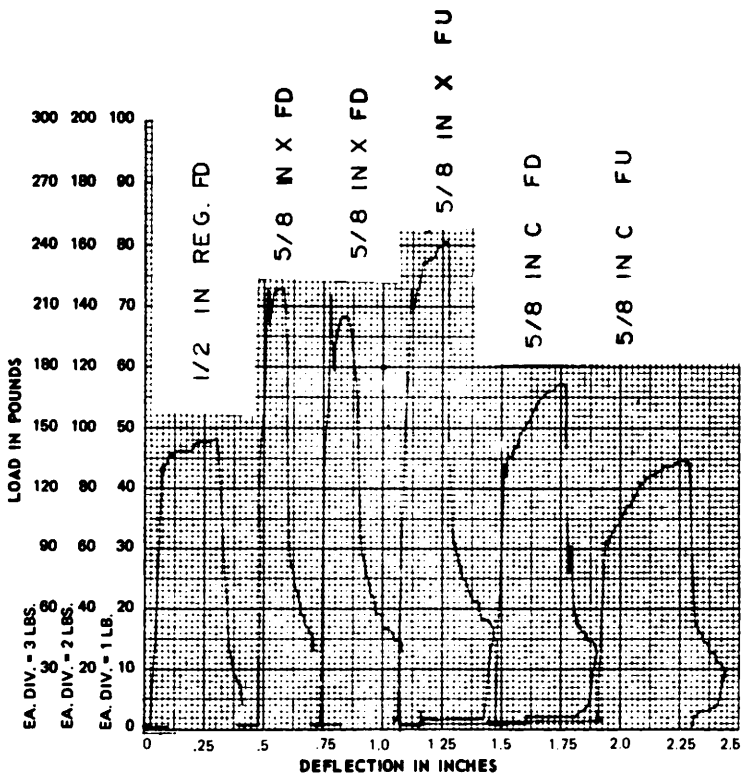

FIG. 6—*Flexure test—stress-strain curves.*

a good evaluation, it may be possible to learn to control them better and set meaningful specifications for them.

3. The complete stress-strain curve gives additional information about core properties. As noted previously, it may show something about fiber distribution, and additional knowledge about core properties may give us a chance to improve them.

The timesaving from running flexure tests on a constant strain machine is substantial. For 15.88-mm (⅝-in.) wallboard, the specifications are 667 N (150 lb) across and 222 N (50 lb) parallel. For a full sample of four specimens, the minimum load application time is 6⅔ min, and it can be substantially greater. On the constant strain machine, the total testing time is only a minute or two per sample regardless of the load required.

In view of the good correlation between the two types of machines, we do not believe that any plant or testing agency would have any difficulty in devel-

oping a correlation that would permit them to test on a constant strain machine and certify that the products would meet the appropriate specifications when tested according to ASTM C 473.

In view of the increased accuracy and the additional information that can be obtained by using the constant strain machine, we would recommend that ASTM Committee C-11 on Gypsum and Related Building Materials and Systems consider adopting it as a standard device for conducting strength tests on gypsum board. Some additional testing on various types of board from different plants would be required to determine the best values for specifications for tests run on the new machine.

Nail Pull Resistance Test

The constant strain machine can be readily adapted for running the nail pull resistance test. No change in sample size is required. The only change made in the equipment was the slot in the sample holder referred to previously. This makes inserting and removing a sample quicker and more convenient but is not absolutely necessary.

Table 4 shows comparative data obtained from plant tests on various types of board. Note that the standard deviations are very similar on the two machines. Possibly the constant strain tester is slightly more precise, but it is apparent that most of the variation is in the products.

The correlation equation for this data is $P = 0.98N + 6.3$ ($r = 0.93$). The correlations for any one type of board are not as good. For example, on 12.7-mm (½-in.) regular wallboard, the correlation coefficient is only 0.48. This is enough to show a significant relationship but not enough for prediction. The explanation is that this product is reasonably uniform, and most of the variations in each set of test results are random variations around an average. These variations will not necessarily correlate. When several types of board are included, there is a wider range of values and the averages for the various types of board do correlate well.

The slope of the correlation curve is very close to unity indicating that differences in results are the same on both machines. The absolute values differ slightly, and there is a constant term in the correlation equation because the shot-bucket machine always tends to overshoot the maximum value as explained previously. The maximum force occurs just as the paper starts to tear, but there is a noticeable delay in the fall of the lever arm on the shot-bucket machine before the sample fails completely.

The minimum values that should be specified for a constant strain testing machine to be equivalent to the ASTM C 473 specifications are shown in Table 5.

It would probably make little practical difference if specifications by a constant strain machine were rounded off at 20 N (4.5 lb) below the present specifications.

The timesaving on this test is also substantial. A minimum test of 355 N (80

TABLE 4—*Nail pull resistance tests.*[a]

Product, in.	Number of Tests	Old, lb		New, lb		Correlation Coefficient
		Average	Standard Deviation	Average	Standard Deviation	
½ regular	40	89.6	4.7	85.4	4.4	0.48
½ other	12	108.2	8.0	103.1	7.6	0.47
⅝ Type X	24	105.8	5.2	102.5	5.3	0.89
⅝ other	12	110.1	17.0	103.7	16.0	0.70
Less than ½	12	87.9	11.6	84.4	9.3	0.97

[a]1 in. = 25.4 mm and 1 lb = 4.448 N.

TABLE 5—*Minimum values that should be specified for a constant strain testing machine to be equivalent to ASTM C 473 specifications.*

Board Thickness		ASTM Specification		TM Specification	
mm	in.	N	lb	N	lb
6.4	¼	178	40	153.1	34.4
8	5/16	222	50	198.5	44.6
9.5	⅜	267	60	243.4	54.7
13	½	356	80	335.1	75.3
16	⅝	400	90	380.5	85.5

lb) on 12.7-mm (½-in.) wallboard requires a minimum of 6⅔-min shot flow time, for the five specimens in a sample, on the shot-bucket machine. On the constant strain tester, the time is only 1 or 2 min regardless of the load required.

The use of the stress-strain curve recorder does not give much additional information with this test. However, the timesaving that is possible would recommend the adoption of the constant strain type of tester by manufacturing plants, testing agencies, and ASTM.

Core, End, and Edge Hardness Tests

These tests can also be readily run on the constant strain machine. Equipment and technique are essentially the same.

Table 6 shows the results of comparative tests in a plant on various types of boards. Since this test does not vary with thickness, there is no need to separate the data by thickness. The correlation equation is $P = 1.03N + 3.6 (r = 0.92)$.

The standard deviations are similar with possibly a little better uniformity on the constant strain machine. The slope of the correlation curve is close to unity, again indicating that differences in results are equal on the two machines. The constant term shows a small difference in absolute values with the constant stress machine giving a larger numerical value for the same reasons as explained previously.

The reason for the higher reading is also clearly shown on a stress-strain diagram. Figure 7 shows a number of curves for this test. In most cases, the force required for penetration rises rapidly at first and then levels off. However, on the constant stress machine the load applied would continue to increase until the 12.7-mm (½-in.) penetration was achieved. The constant strain machine gives a more accurate or more realistic value.

The stress-strain curves also show that there can be numerous small-scale variations in core hardness. Most likely these represent small voids or lumps in the core. We believe that these local variations can cause some of the extreme variation between specimens that can occur in the nail pull resistance test. While these variations can affect the shape of the curve, in most cases the final value is quite consistent.

TABLE 6—*Core, end, and edge hardness tests.*[a]

Test	Number of Tests	Machine Reading				Correlation Coefficient
		Old		New		
		Average, lb	Standard Deviation	Average, lb	Standard Deviation	
Core hardness	87	29.8	5.8	25.5	4.6	0.80
End hardness	74	28.6	7.2	23.0	6.1	0.86
Edge hardness	77	44.7	17.4	39.9	15.0	0.90

[a] 1 lb = 4.448 N.

The use of the stress-strain recorder provides a method for measuring the penetration of the pin with greater accuracy than is possible on the constant stress machine. However, the shape of the curve indicates that there would be no great loss in accuracy if the penetration was judged by observing a mark on the pin as is common practice with the constant stress machine.

An exception to the uniformity of this test was noted on an unusually hard Sample H (Fig. 7). On this sample the readings did not level off until about 19.05-mm (¾-in.) penetration was achieved. This sample had small-scale variations in hardness and would have been judged quite variable when tested at 12.7-mm (½-in.) penetration. At 19.05-mm (¾-in.) penetration, the results were quite uniform. The stress-strain curve could provide considerably more information about a sample than the one-point test of the constant stress machine.

The timesaving on this test is not as great as on the other two. A minimum specification test takes about 15 s per specimen on the constant stress machine. On the constant strain machine, the test is conveniently run at 51 mm/min (2 in./min), which gives a 15-s testing time per specimen for any load.

In Fig. 7 Sample I shows a test of edge hardness. It is common in this industry to use some procedure to increase the hardness of board core at the edges. This particular sample shows considerable variation, particularly when penetration is increased beyond 12.7 mm (½-in.). It is quite possible that plants could do a good deal to evaluate the operation of their edge hardness device by using this test and the stress-strain recorder.

The probability of greater accuracy and the additional information available from a stress-strain curve would indicate the advantage of using a constant strain rather than a constant stress testing machine for this test.

In practice we believe that the test is not used very widely because a sample that meets the nail pull resistance specification will substantially exceed the core and end hardness specification. Further study and development of this test is warranted particularly if it is done on a constant strain machine.

Comparison of Nail Pull Resistance and Core Hardness Tests

Consideration of what is done to the core when conducting the two tests indicates that they are somewhat similar. True, the pin used for the nail pull resistance test has a larger diameter and must tear through the paper before it crushes the core, but the basic action is to crush the core by pushing a pin into it.

Two variable correlations were calculated for the various types of products where both tests had been run on samples from one board. Results are shown in Table 7. On individual products little correlation was shown. As explained previously this is because a single product is reasonably uniform and the variations in test results are random variations around an average which has no reason to be correlated.

Where a wider range of products was used, particularly the 12.7-mm (½-in.)

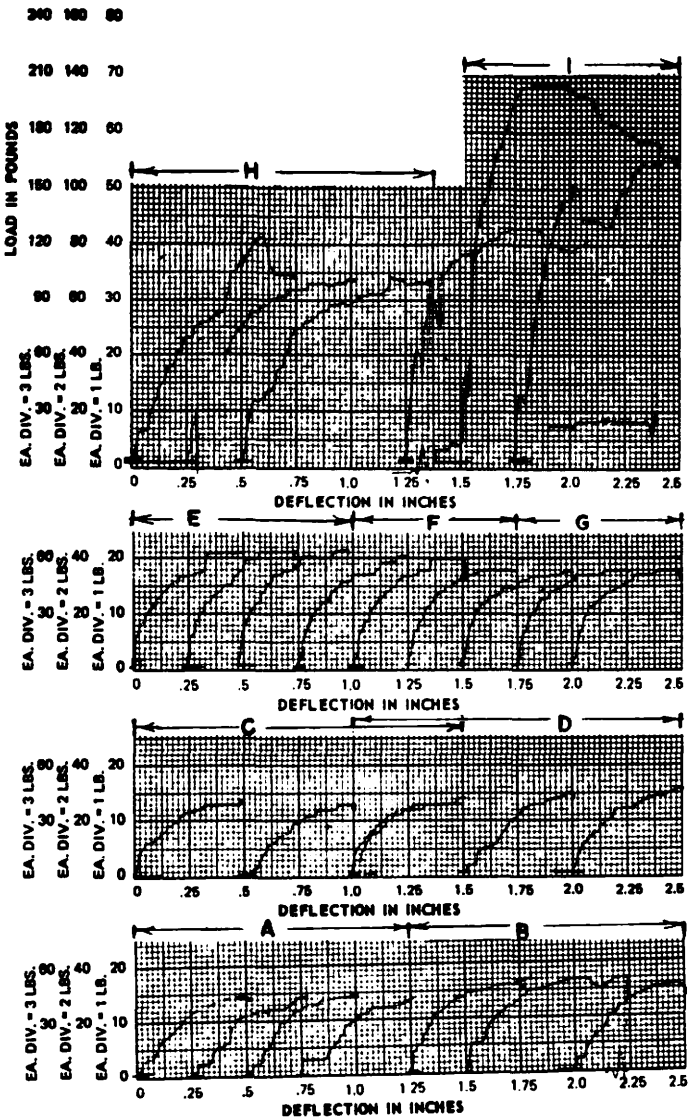

FIG. 7—*Core hardness stress-strain curves.*

TABLE 7—*Two-variable correlations nail pull and core hardness.*[a]

Type Board, in.	Correlation Coefficient
½ regular	0.35
½ other	0.87
⅝ Type X	0.18
⅝ other	0.59
Less than ½	0.36
All	0.65

[a]1 in. = 25.4 mm.

types, better correlation was obtained. However, when all the data were combined, poorer correlation was obtained than on 12.7-mm (½-in.) types alone. This is because the nail pull resistance test also varies with thickness, and another variable is introduced.

An additional evaluation was made by running a three-variable correlation using nail pull resistance as the dependent variable and core hardness and flexural strength as independent variables. The correlation coefficients are shown in Table 8.

Flexural strength varies primarily with thickness. It also varies with the tensile strength of the paper on the side tested, but the paper used on any one product is reasonably uniform. The correlation coefficients on individual products show slight increases indicating that there may be some correlation with the variations in paper strength, but the changes are hardly significant.

The combined correlation coefficient does increase significantly showing that nail pull resistance can be predicted reasonably well from core hardness and flexural strength. Since the major component of flexural strength variation is thickness, the correlation is really with core hardness and thickness. There may be a small effect of paper strength, but it is confounded with the effect of thickness.

A logical conclusion is that the core hardness and nail pull resistance tests give essentially duplicate information. The core hardness test has the potential

TABLE 8—*Three-variable correlations nail pull versus core hardness and transverse strength.*[a]

Type Board, in.	Correlation Coefficient
½ regular	0.45
½ other	0.88
⅝ Type X	0.33
⅝ other	0.66
Less than ½	0.68
All	0.84

[a]1 in. = 25.4 mm.

of giving more information about the product if run on a constant strain machine and is less time consuming to run on the present testing machine.

Conclusions

The testing machine commonly used on gypsum board is specified because it is something that was easy to build in the early days of the industry. It is now out-moded, very slow, laborious, and possibly dangerous to use. Now that more sophisticated machines are commercially available they should be considered for use in gypsum board. The use of a stress-strain recorder with a constant strain type of machine could give more information from the test procedures than the presently approved machine.

Consideration should also be given to what the tests tell a user about the utility of a product. The nail pull resistance and core hardness tests give very similar information. Possibly other types of tests should be devised to measure other properties of gypsum board.

George W. Green[1]

Gypsum Analysis with the Polarizing Microscope

REFERENCE: Green, G. W., "**Gypsum Analysis with the Polarizing Microscope,**" *The Chemistry and Technology of Gypsum, ASTM STP 861*, R. A. Kuntze, Ed., American Society for Testing and Materials, 1984, pp. 22–47.

ABSTRACT: The fastest and most accurate method for the qualitative analysis of gypsum is use of the polarizing microscope. Five bits of optical data can be used for identification of gypsum and its most common impurities such as natural anhydrite, calcite, dolomite, and silica. The optical data are morphology, refractive index, birefringence, angle of extinction, and dispersion staining. Gypsum can be identified by its refractive index of 1.521 and 1.530, its oblique extinction angle, its birefringes of 0.009, and a blue dispersion staining color when mounted in a refractive index liquid of 1.528. Natural anhydrite is normally seen as blocky crystals with a refractive indices of 1.570 and 1.614. The birefringence of 0.044 gives it much higher order polarizing colors than gypsum, and it has parallel extinction. Silica has the same birefringence as gypsum; so it is hard to distinguish with crossed polars. However its refractive index of 1.544 is higher than gypsum and has a yellow dispersion color to contrast with the blue of gypsum when mounted in 1.528. Limestone may be either calcite or dolomite. Limestone may be distinguished mainly by its very high birefringence of 0.172, which renders even very fine particles colorful with crossed polars—larger particles are high order white. Calcite may be distinguished from dolomite by mounting in a refractive index liquid of 1.660 rendering the dolomite orange with the calcite blue.

The phases of gypsum can be distinguished also. Beta hemihydrate has the same shape as the dihydrate from which it was made but is porous and cloudy rather than clear and solid. Alpha hemihydrate may be blocky or acicular and has a refractive index of 1.558 and 1.586. The birefringence is 0.028. When mounted in 1.564 liquid, the dispersion colors will change from orange to blue as the stage is rotated. Soluble anhydrite is difficult to identify, but dead-burned gypsum has a refractive index close to natural anhydrite, and the dispersion colors are red and blue when mounted in a liquid of 1.596. The qualitative analysis of natural anhydrite may be done by direct estimation, or by estimating a series of fields and averaging the results. A more precise method is to count and measure the diameters of all particles then calculate the weight percent of each.

KEY WORDS: gypsum, microscopes, polarization, birefringence, limestone, silicon dioxide, anhydrite, refractivity, extinction angle, dispersion staining

ASTM Chemical Analysis of Gypsum and Gypsum Products (C 471), Note 4, Section 14 reads "The presence of the different forms of $CaSO_4$ may be

[1]Senior product development engineer, Georgia-Pacific Corp., 2861 Miller Rd., Decatur, GA 30035.

corroborated by a microscopic examination." There is no further explanation or method for the corroboration. This paper suggests a method for this purpose along with other useful and hopefully interesting information.

The microscope is a great tool to have around a gypsum laboratory. The polarizing microscope in particular is perhaps the fastest and most accurate means for qualitative analysis of gypsum. It can also be put to work doing some quantitative analysis of anhydrite in gypsum.

There are five major clues to help us identify a particle. They are morphology, refractive index, birefringence, angle of extinction, and dispersion staining. These clues will help us identify impurities in gypsum, mainly, limestone, silica, and natural anhydrite. They will also help distinguish the different phases of gypsum: dihydrate, hemihydrate, alpha and beta, and anhydrite.

Background

Let me explain briefly what these clues mean for those who may not be familiar with microscopy.

Morphology

Simply ask: What does the particle look like? What shape is it? What kind of texture does it have? What is the crystal form? What structure does it have?

Refractive Index

The refractive index of a particle is a second clue to its identity. See Ref *1* for a good book of refractive indices and other optical properties of inorganic substances.

The refractive index of solid particles can be measured on the microscope by immersing the particle in liquids of known refractive index until a match is found. A match is found when the particle virtually disappears in the liquid.

Figure 1 shows some glass beads in a liquid of 1.600 refractive index (RI). They have good contrast. In Fig. 2 they are in 1.500 RI. Less contrast, so we are closer. In Fig. 3 they disappear completely in 1.516 RI; so we have a match. The only reason you can see them at all is because of the inclusion of air bubbles in the glass beads.

A set of refractive index liquids can be purchased from R. P. Cargille Laboratories.[2] You could make up your own set of liquids and calibrate them on a refractometer, but if you do a great amount of microscopy I highly recommend buying a set of calibrated liquids.

At first glance matching a particle to a liquid may seem like a time consuming and tedious task, but with practice it can usually be done in five tries or less. There are several methods of determining whether the particle has a higher or

[2]Obtained from R. P. Cargille Laboratories, Inc., 55 Commerce Rd., Cedar Grove, NJ 07009.

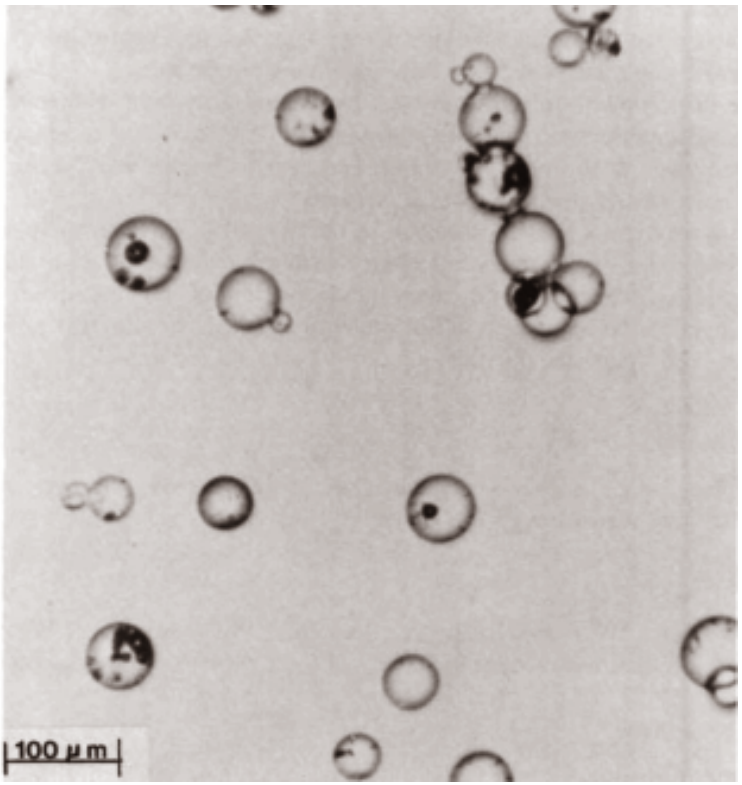

FIG. 1—*Glass beads in refractive index liquid 1.600.*

lower refractive index than the liquid, and of course the degree of contrast helps determine how far away it is.

One of the more useful methods is the Becke test. Becke noticed that when the microscope is focused up and down a bright halo near the boundary of a particle moves in and out. The halo will always move toward the higher refractive index as the focus is raised and toward the lower refractive index as the focus is lowered. Thus if the particle has a refractive index higher than the liquid, the Becke line will move from outside the boundary to the inside as the focus is raised and vice versa. Figures 4 and 5 show the bright Becke line outside and inside the boundary, respectively.

Refractive index liquids have another use besides identification. They can help get rid of the major component of a sample so we can more easily see the impurities. If a gypsum specimen is mounted in liquid that does not match, such as 1.600 RI (Fig. 6), we can see the gypsum crystals, but we already know there is a lot of gypsum in the specimen. What we want to see is how much other junk is there. Now if we mount the gypsum in a liquid with a 1.528 RI (Fig.

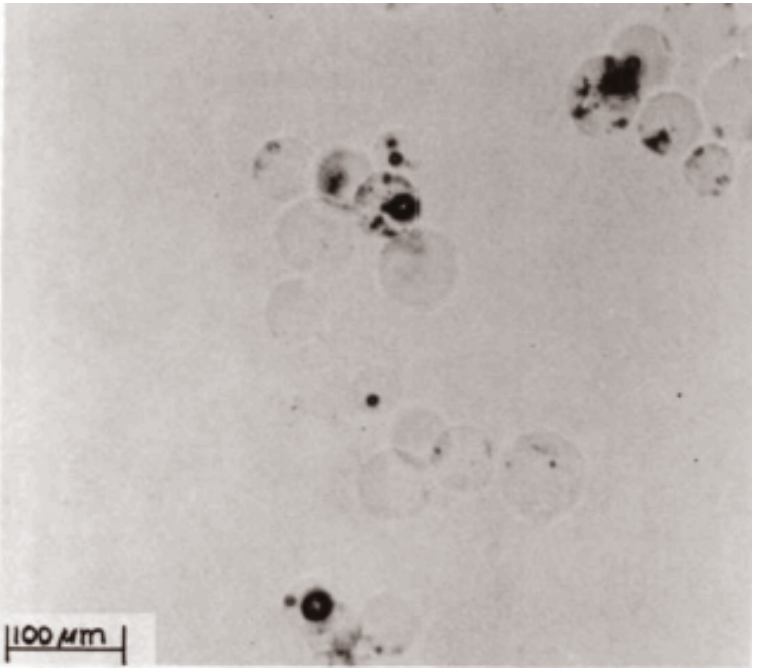

FIG. 2—*Glass beads in refractive index liquid 1.500.*

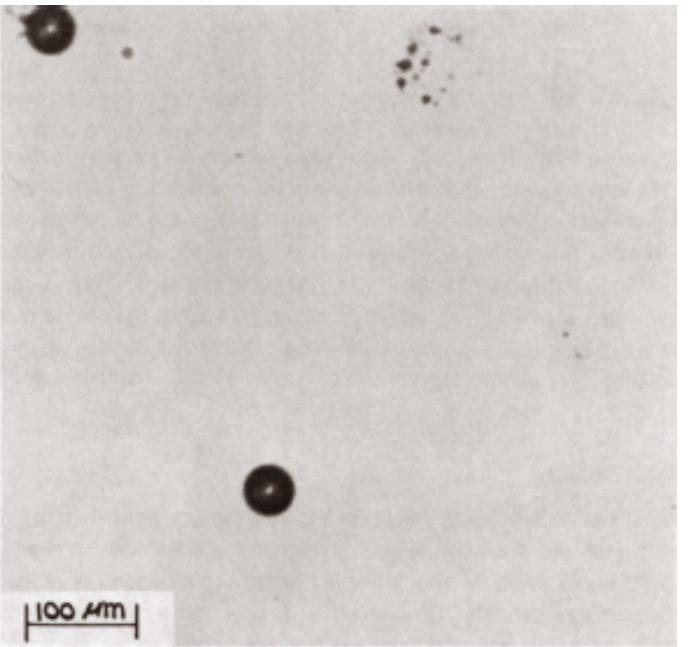

FIG. 3—*Glass beads in refractive index liquid 1.516.*

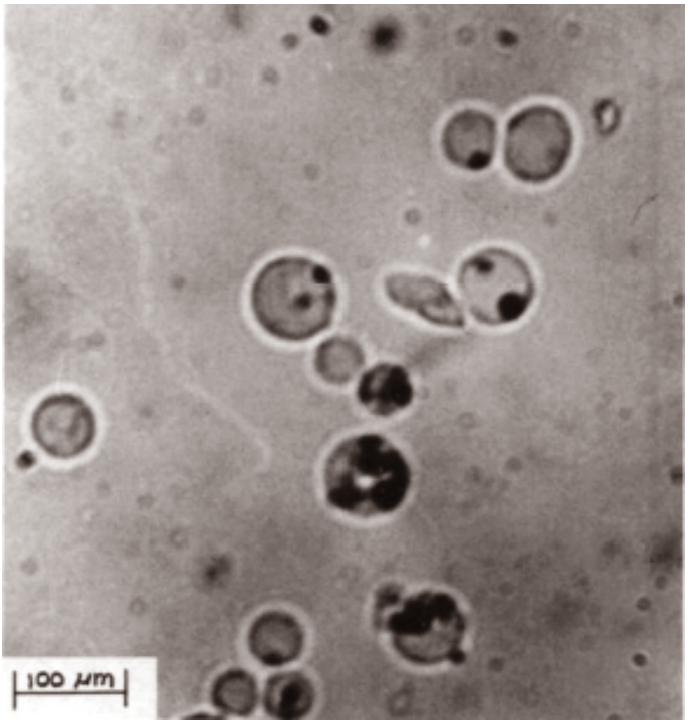

FIG. 4—*Becke line outside particles with lowered focus.*

7), the gypsum will virtually disappear making the impurities stand out. Notice that I said "virtually" disappear. There are two reasons why a particle may not disappear totally. First, only some solid substances have a single refractive index. These are glasses and crystalline substances that are in the cubic system such as potassium chloride. All other crystalline substances have either two or three refractive indices. What you see may be one of the indices or a combination of two indices, depending on how the crystal is oriented. This is called birefringence, which we will get to later. For instance, Figure 8 shows quartz, mounted in 1.544 RI, which matches one of its refractive indices. However, if we rotate the polarizing filter or the stage, we see that the other refractive index does not match (Fig. 9).

Dispersion Staining

A second reason why even isotropic substances may only virtually disappear is due to dispersion. We have all seen dispersion at work when a beam of white light is split into a rainbow of colors by a prism. The dispersion of the liquid is rarely the same as the solid. Therefore, although one wavelength of light may match up, others will not, and there will be faint color fringes around the edge

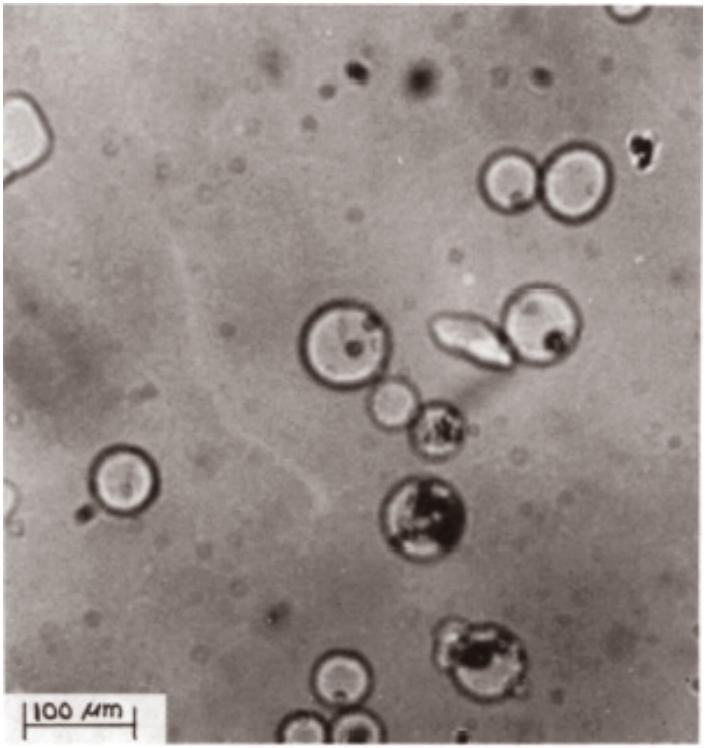

FIG. 5—*Becke line inside particles with raised focus showing that particles have a higher refractive index than liquid.*

of a particle. With normal transmitted illumination on the microscope these color fringes are very faint and hard to see. By blocking the divergent beam, the inner color fringe is intensified, although because it is against a white background it is still not easy to see. If we block the central beam, the annular light will show against a black background. The divergent beam will show the complimentary color of the central beam. For example, if sodium chloride is mounted in Cargille R. I. liquid 1.544 RI the annular stop will show a yellow outline against a white background, while the central stop will show a blue outline on a black background. If we mount the sodium chloride in 1.540 RI the annular stop color is blue-green, and the central stop is orange. Figure 10 is a diagram showing the annular stop blocking the divergent beam and the central stop blocking the central beam.

If the refractive indices of the solid and liquid are plotted against wavelength, the color of the wavelength they intersect is shown in the central beam and the complimentary color in the divergent beam (Fig. 11). This technique is called dispersion staining. A dispersion staining device that has annular and central

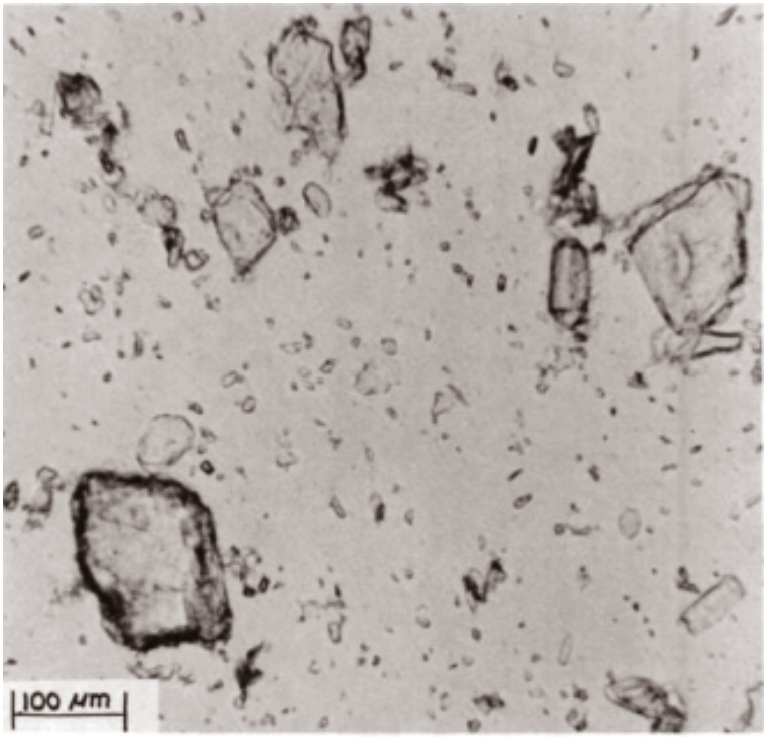

FIG. 6—*Gypsum with impurities mounted in 1.600.*

stops built in is available from McCrone Associates[3] along with a volume containing hundreds of dispersion curves. Here you can see the central stop in position (Fig. 12).

Birefringence

Birefringent particles (of which gypsum is one) include all the crystalline forms except cubic. They have more than one refractive index and when light is passed through a polarizing filter, through a birefringent crystal, and through another polarizing filter (called an analyzer), consecutively, the background will be black and the particles bright (Fig. 13). The particles may be grey, white, or any color of the rainbow. The smaller particles of gypsum are grey or white, while the larger particle is colored. From this we can deduct that the colors depend on the thickness of the particle.

But some small crystals have more color than the big gypsum crystals. Natural

[3]Obtained from McCrone Associates, Inc., 2820 S. Michigan Ave., Chicago, IL 60616.

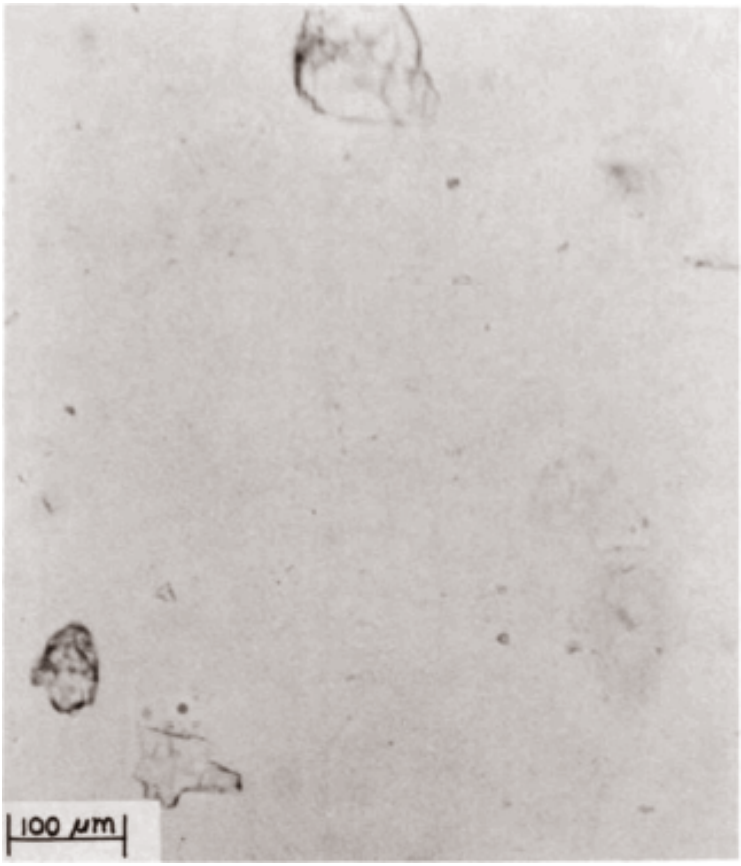

FIG. 7—*Gypsum with impurities mounted in 1.528.*

anhydrite is much more birefringent than gypsum. The amount of birefringence is the difference between the highest and lowest refractive index. Gypsum has a birefringence of 0.01 whereas anhydrite has a birefringence of 0.04.

Polarizing colors are then dependent on two variables: the birefringence of the substance and the thickness of the particle. There is a chart showing polarizing colors versus thickness and birefringences called a Michel-Levy chart [*2,3*]. Thickness is plotted on the ordinate, while polarizing colors are plotted along the abscissa.

Gypsum has a birefringence of 0.009, so that a particle 60 μm thick shows first order red. A particle of anhydrite having a birefringence of 0.044, and also showing first order red, will be only 10 μm thick. Polarizing colors give other clues too. If the particle is black with crossed polars it is either glass or a cubic system crystal (Fig. 14).

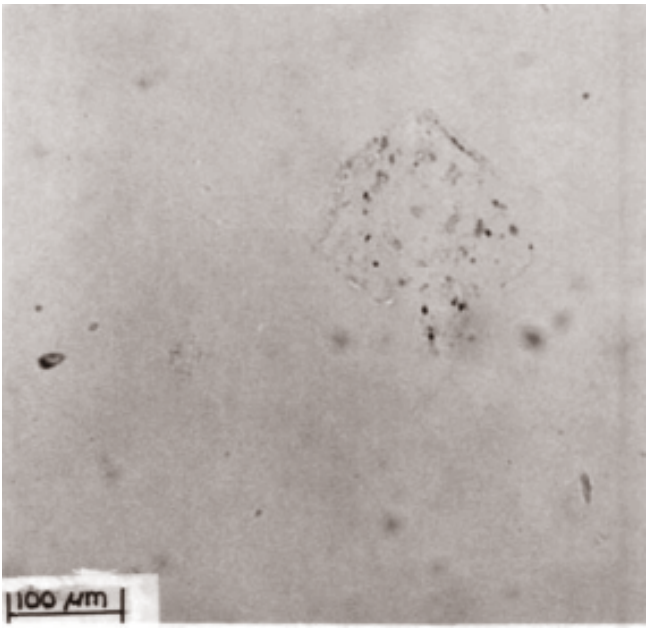

FIG. 8—*Quartz mounted in 1.544.*

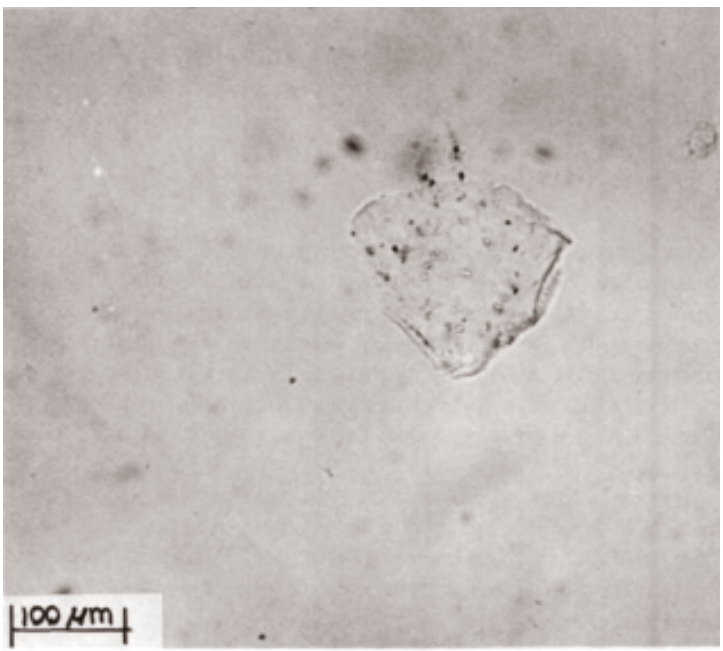

FIG. 9—*Same field as Fig. 8 rotated 45°.*

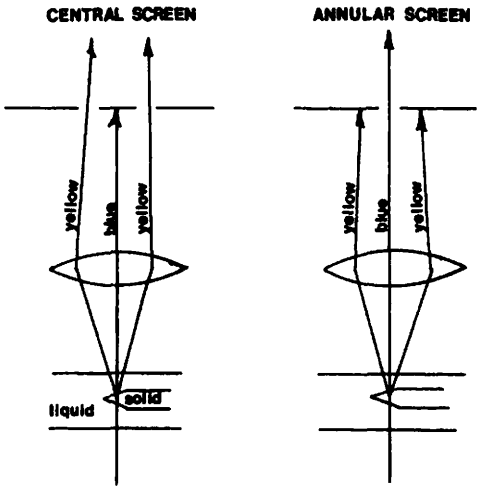

FIG. 10—*Dispersion staining.*

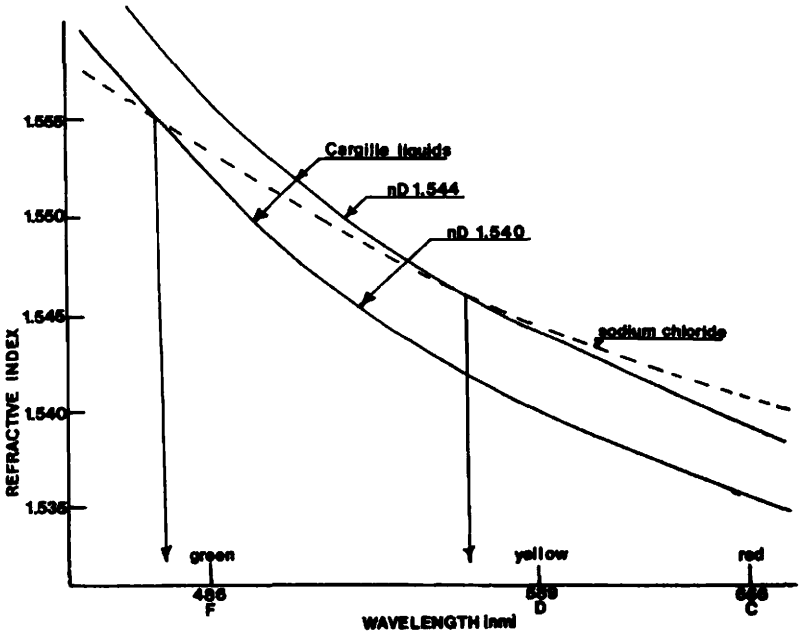

FIG. 11—*Refractive index versus wave length.*

FIG. 12—*Dispersion staining devise showing central stop.*

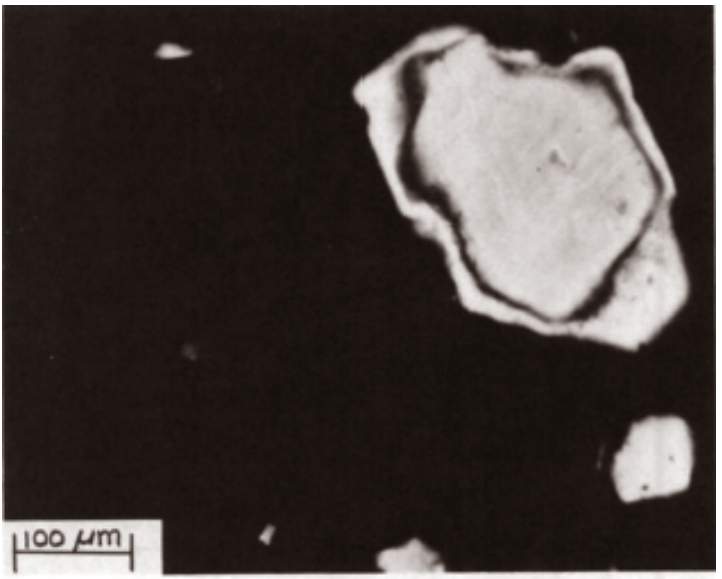

FIG. 13—*Birefringent gypsum particles with crossed polars.*

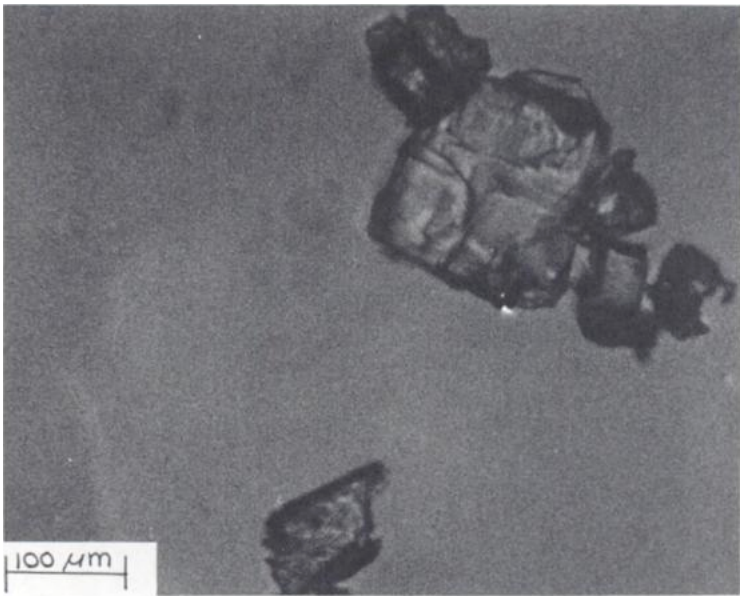

FIG. 14—*Cubic crystals with crossed polars.*

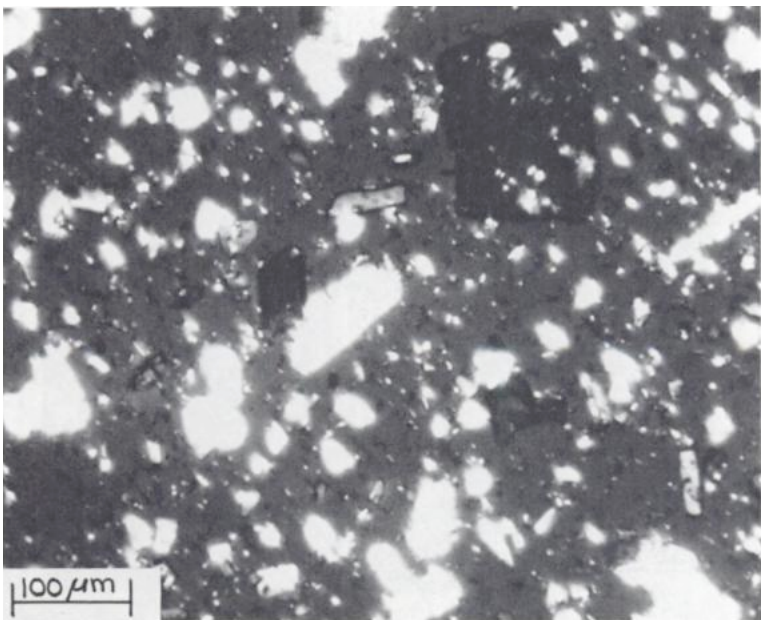

FIG. 15—*Natural anhydrite with parallel extinction.*

Angle of Extinction

Birefringent crystals will turn dark every 90° as the stage is rotated. The angle at which they turn dark is called the extinction angle and may be paralled (Fig. 15), oblique (Fig. 16), or symmetrical (Fig. 17) and is typical of the substance.

So now we have five clues to help us identify a particle. Let us see how we can use these clues to help us identify gypsum and impurities.

Qualitative Analysis

Gypsum

Gypsum powder ground from rocks usually looks like ground rocks (Fig. 18) while selinite or satinspar shows the crystalline form of gypsum, which is monoclinic (Fig. 19). Since by-product gypsum is precipitated from solution, it often shows a crystalline form. One type of by-product gypsum is shown in Fig. 20. The refractive indices of gypsum are 1.521 and 1.530, so if it is placed in 1.528, it is virtually invisible (Fig. 21). The difference between 1.530 and 1.521 is 0.009, which is the birefringence of gypsum. This means that a particle showing first order red will be 60 μm thick.

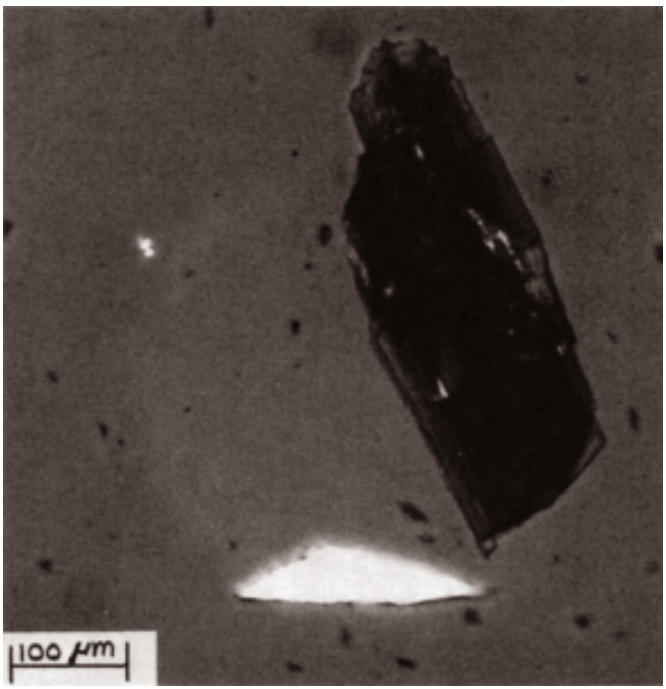

FIG. 16—*Gypsum crystals with oblique extinction.*

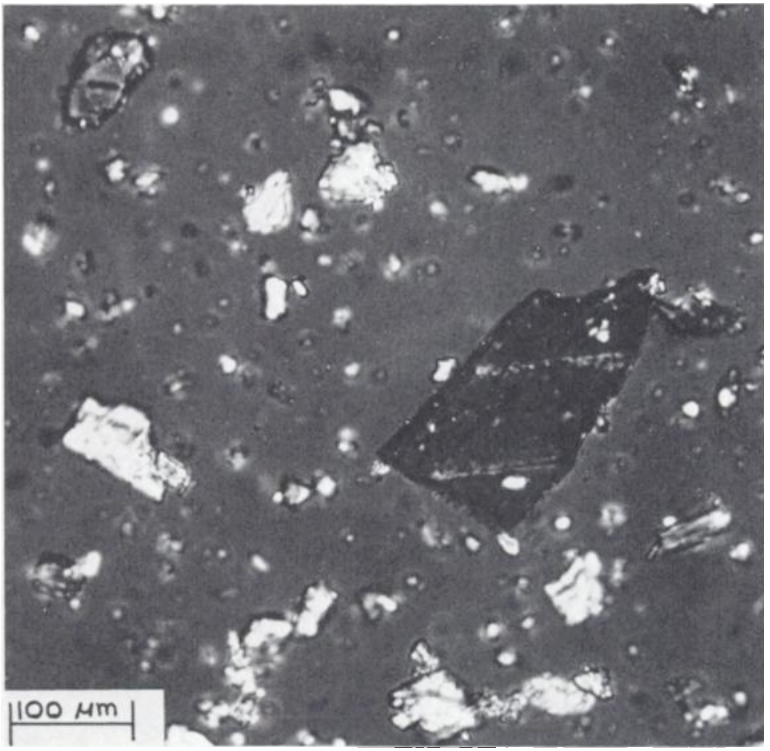

FIG. 17—*Calcite crystals with symmetrical extinction.*

The extinction position is oblique. This may be hard to see in many rock specimens, but in selinite it is apparent (Fig. 22).

When mounted in Cargille liquid, 1.528 RI gypsum has a blue outline with central screening on the dispersion screening device. This is a good method for finding small amounts of raw gypsum in stucco.

Natural Anhydrite

Natural anhydrite is orthorhombic with good cleavage. It is almost always seen as blocky crystals with 90° corners. The refractive index is 1.570 to 1.614, which is much higher than gypsum, so it stands out when we mount the specimen in 1.528 RI to make the gypsum disappear (Fig. 23). The birefringence is 0.044 RI, which means that particles as small as 10 μm will show some color. As a matter of fact anhydrite is very colorful in the sizes we ordinarily encounter and is easy to recognize. It has parallel extinction that helps to confirm our identification (Fig. 15).

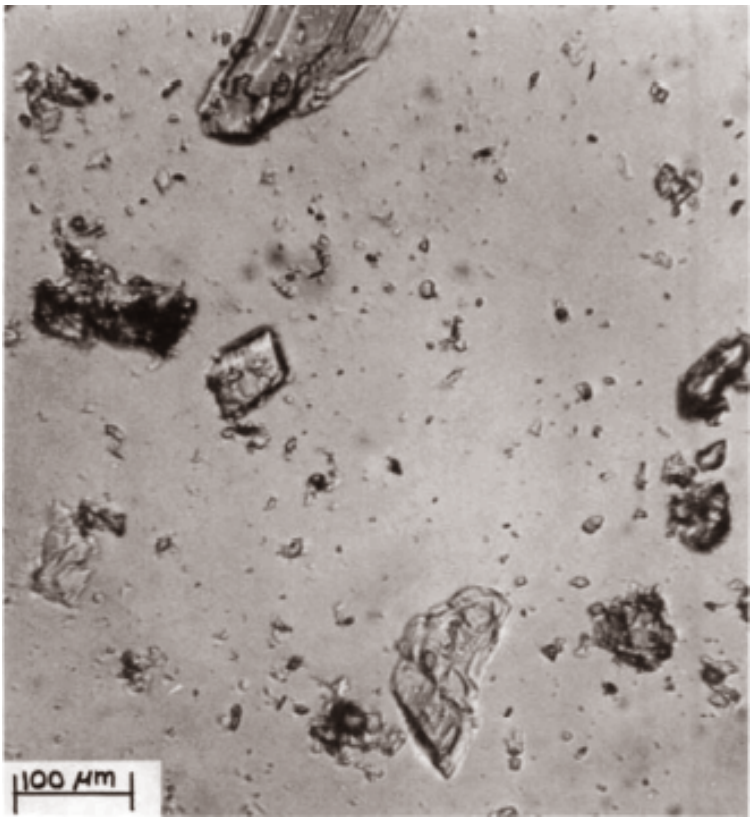

FIG. 18—*Ground rock gypsum.*

Silica

The silica in gypsum is usually quartz and often looks a lot like gypsum except that it does not disappear when mounted in 1.528 RI (Fig. 24). Its birefringence is the same, so in polarized light it looks like gypsum (Fig. 25), but with dispersion staining the gypsum of course turns blue while the quartz will be light yellow-orange.

Limestone

Limestone in gypsum may be either calcite or dolomite. The refractive indices for calcite are 1.486 and 1.658, which make it stand out when we make the gypsum disappear (Fig. 26). Limestone is distinguished mainly by its high bi-

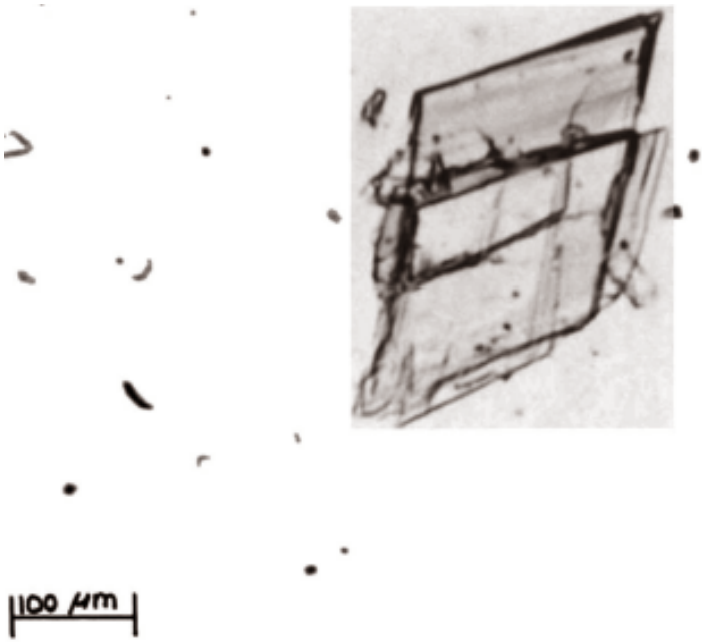

FIG. 19—*Selinite.*

refringence, 0.172, which means even very fine particles have polarizing colors. Larger particles will have such high order colors that they are white.

Now you might ask, How can we tell high order white from low order white? Well we can. They look different, and if you look close you can see color fringes around the edges of a high order white particle. If you still are not certain whether it is high or low order white a first order red plate can be used. A first order red plate is made from a single crystal of selenite that is 60 µm thick (another use of gypsum). It will produce a red background. First order grey or white particles will either add or subtract from it depending on their orientation. This will make the low order white particle either yellow or blue, whereas the high order white will be virtually unaffected.

Sometimes we may want to know whether the limestone is dolomite or calcite. This is very easy using dispersion staining. When mounted in Cargille liquid 1.660 with the central stop in place, each dolomite particle will turn yellow or orange at one point as the stage is revolved while each calcite particle will turn blue.

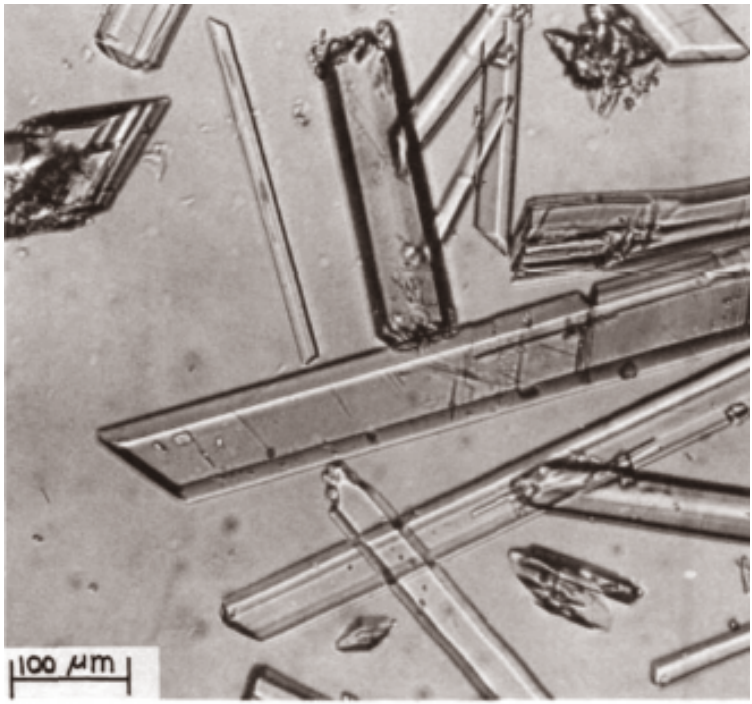

FIG. 20—*By-product gypsum.*

Phase Analysis

Dihydrate Gypsum

We have already talked enough about gypsum to be able to recognize it when we see it, so we will move to hemihydrate.

Hemihydrate

Beta hemihydrate is called stucco, kettle stucco, or plaster. It is made by calcining gypsum in air at atmospheric pressure. The particles retain the same shape as the gypsum particles from which they were made, but they are no longer clear or solid. They are porous and translucent (Fig. 27). Winchell and Winchell [*1*] say they have a refractive index of 1.586 with a birefringence of 0.021. I find that for kettle stucco the refractive index is somewhat variable and usually closer to 1.540. In any case we can not make the particles disappear because of the porosity, but that porosity is usually enough to distinguish it from other phases of gypsum.

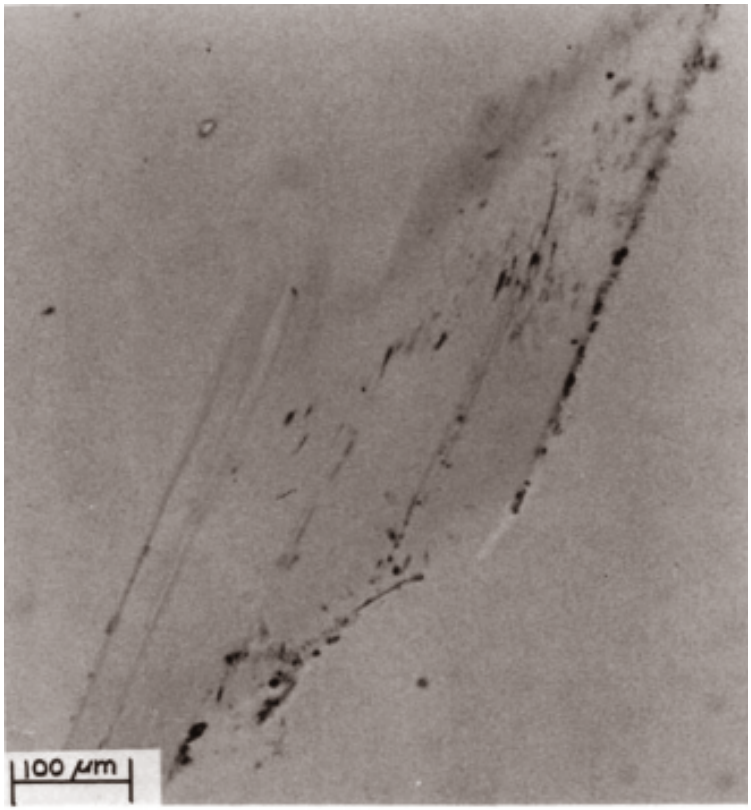

FIG. 21—*Gypsum crystal in 1.528 RI.*

Alpha Hemihydrate

Alpha hemihydrate is made by calcining gypsum in an autoclave under pressure or in a salt solution. It has different forms depending on the conditions under which it is made. The crystals may be blocky (Fig. 28) or very acicular (Fig. 29), or anything in between. The refractive indices are near the book values of 1.558 and 1.586. The birefringence is 0.028, which is in between gypsum and anhydrite, and has parallel extinction. The dispersion staining clue can be used for confirmation. When mounted in 1.564 RI, the hemihydrate crystals will change from orange to blue as the stage is rotated.

Soluble Anhydrite

Soluble anhydrite, because it is unstable, is hard to study. The refractive index and other optical data vary considerably, not only from specimen to specimen but from particle to particle in the same sample. It looks just like hemihydrate

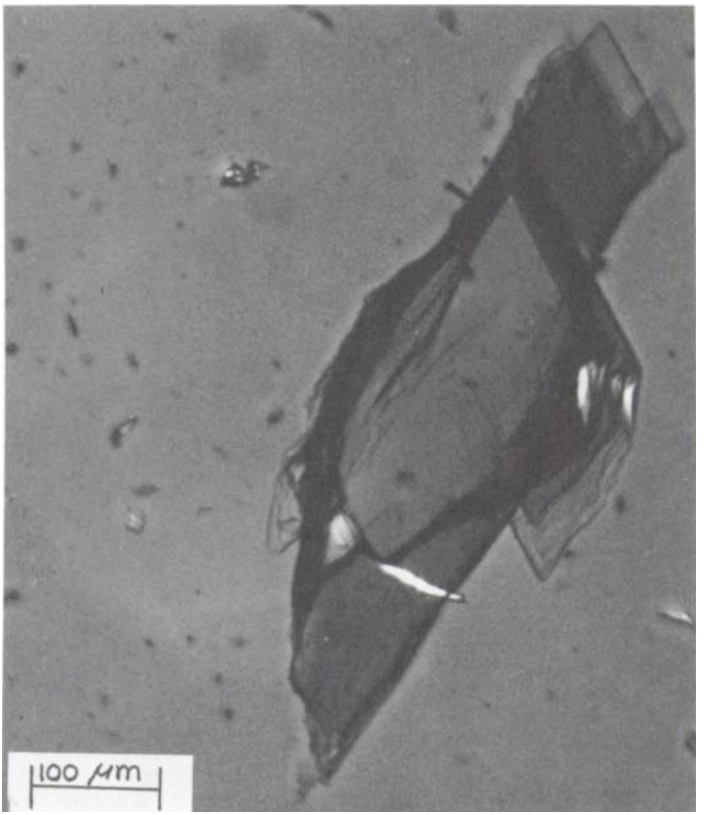

FIG. 22—*Selinitic gypsum showing oblique extinction.*

with polarizing colors, but when mounted in 1.564 RI using dispersion staining, the soluble anhydrite is not blue and orange like the hemihydrate but is white.

Deadburned Gypsum

If the soluble anhydrite is further heated to over 538°C (1000°F) a stable anhydrite is formed that is sometimes referred to as "dead-burned." It has a refractive index similar to natural anhydrite, and the dispersion colors in 1.596 RI are blue and red.

Quantitative Analysis of Natural Anhydrite

Estimation by Inspection

The fastest method of analyzing a specimen on the microscope is to merely look at it and make an estimate of the percentage of natural anhydrite present.

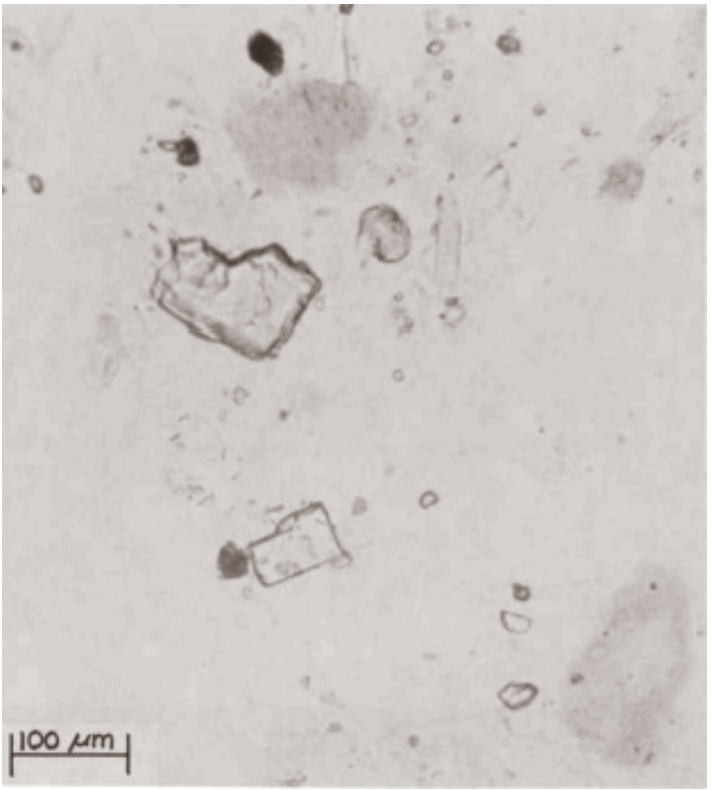

FIG. 23—*Gypsum with natural anhydrite mounted in 1.528 RI.*

The accuracy of this method depends a great deal on the amount of practice one has had. The accuracy can be increased by making a series of standard specimens and comparing the unknown specimens to the standard. To increase the accuracy still further, make individual estimates of a number of fields on the slide and average these. This is the method I use on a routine basis.

I have made up a series of known standard specimens containing from 0.5 to 10% natural anhydrite. I did a lot of practicing on these until I could get them to within ± 0.5%. It is a good idea to go back to these standards occasionally to recalibrate your eyeballs.

If a constant volume is used it will also cut down on the error. A small scoop was fashioned by flattening the end of a length of brass rod and drilling a small depression. Two scoopfuls make a specimen, which is then dispersed in a drop of 1.528 Cargille liquid. A field is examined with plain light, and of course all the impurities stand out from the almost invisible gypsum. When a likely particle

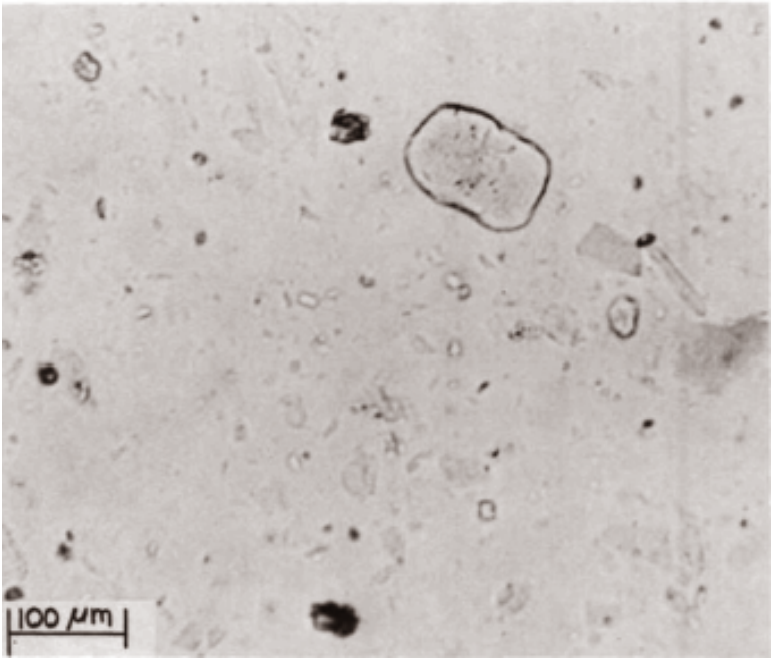

FIG. 24—*Quartz in gypsum mounted in 1.528 RI.*

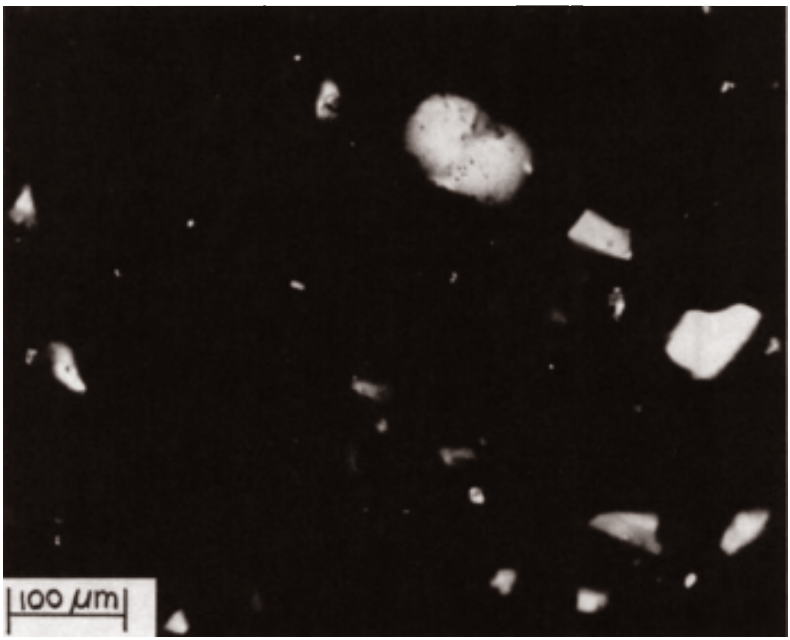

FIG. 25—*Same field as Fig. 24 with crossed polars.*

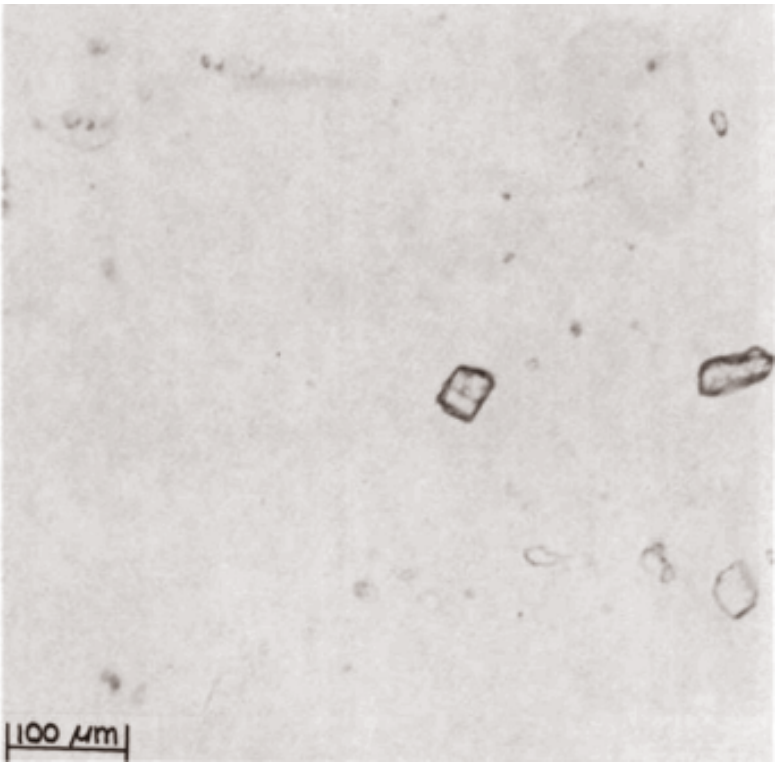

FIG. 26—*Limestone with gypsum mounted in 1.528 RI.*

is found, the analyzer is slid into position and the particle is examined for birefringence and extinction angle. If it is confirmed to be natural anhydrite a judgement is made as to its percentage of that particular field taking into account the size and number of particles. Also taken into account is the difference in density between gypsum and anhydrite.

After at least 20 fields are estimated, they are averaged. At this point a judgement is made as to whether additional fields need to be counted. If the percentage in each field is fairly uniform, 20 fields are enough, but if one large particle in one field is found and nothing in the other fields, make another mount and check at least 20 more fields.

This procedure is not the most accurate method, but it only takes a few minutes per specimen and is reliable enough for routine work.

While I am doing this I am making a judgement on the amount of limestone, sand, shale, and other impurities present and the total purity of the gypsum as a check on the chemical analysis. This is not as precise as the chemical analysis, but if there is a large discrepancy, the specimen is rerun.

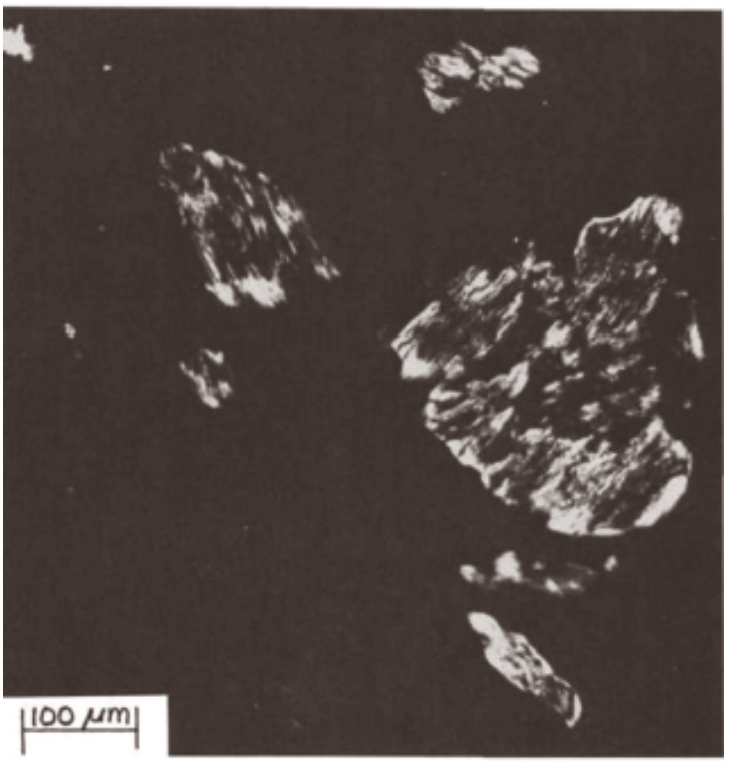

FIG. 27—*Beta hemihydrate (kettle stucco), crossed polars.*

By Counting

If more accuracy is needed there are counting methods that can be used. The best and by far most tedious method is to count and measure all the particles in each field and group them by compound, then calculate the weight percent of each by

$$\text{weight } \%\ A = [\rho_A \cdot \Sigma n_A d_A^3 / (\rho_A \cdot \Sigma n_A d_A^3 + \rho_B \cdot \Sigma n_B d_B^3, \text{ etc.})] \times 100 \quad (1)$$

To get an accurate count, at least 200 particles should be measured and counted. From this data in addition to an analysis you can also calculate a particle size distribution of each component.

If all the particles are the same size then the measurement of diameter is not necessary. The method used by Gardner, a predecessor at Bestwall Gypsum Company, was to count the particles passing a 63-μm (230-mesh) screen and retained on a 60-μm (240-mesh) screen [*4*].

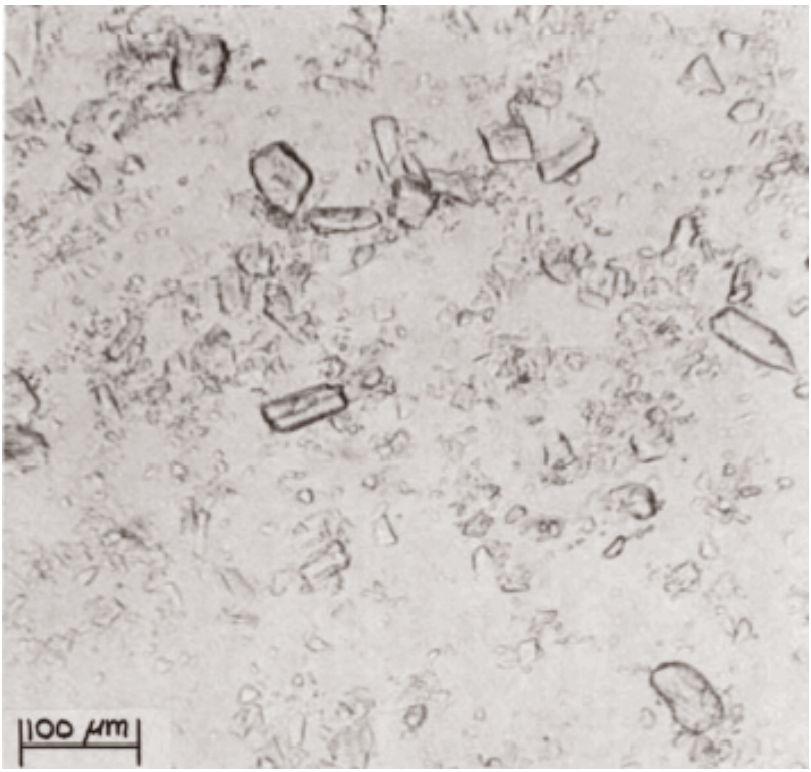

FIG. 28—*Alpha hemihydrate, blocky crystals.*

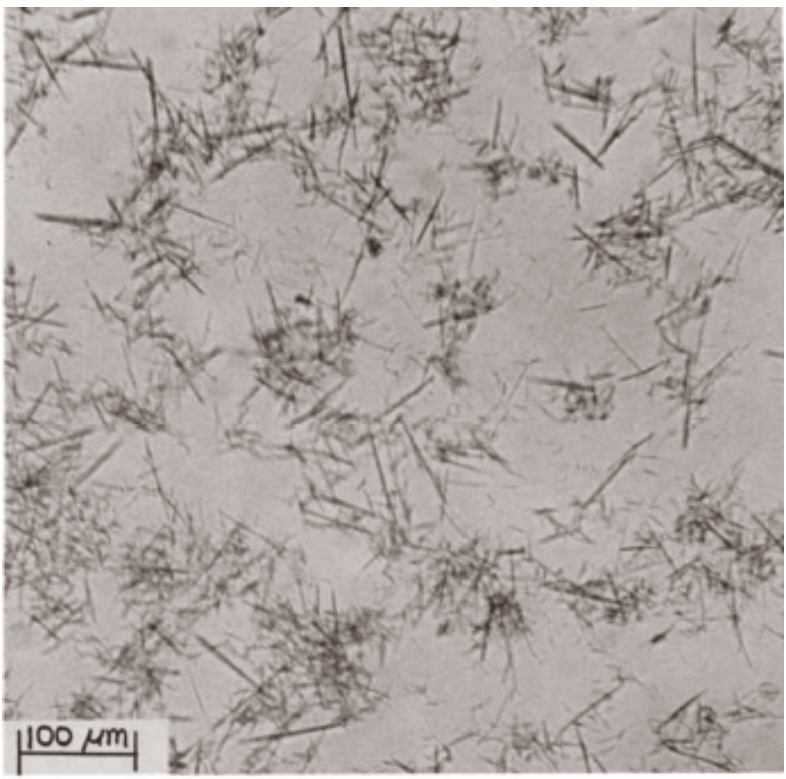

FIG. 29—*Alpha hemihydrate, acicular crystals.*

Further if a known weight or volume of sample is counted, then it is not necessary to count the gypsum particles but only the anhydrite or other components of interest. The microscope can then be quite useful in analyses of natural anhydrite in gypsum.

References

[1] Winchell, A. N. and Winchell, H., *The Microscopical Characters of Artificial Inorganic Solid Substances*, Academic Press, New York, 1964.

[2] Chamot, E. N. and Mason, C. W., *Handbook of Chemical Microscopy, Vol. I*, Wiley, New York, 1958.

[3] Rogers and Kerr, *Optical Mineralogy*, McGraw Hill, New York.

[4] Gardner, H. F., "Notes on the Chemical and Microscopic Determinations of Gypsum and Anhydrite," *Proceedings 26, Vol. 1*, American Society for Testing and Materials, Philadelphia, 1926, pp. 296.

Danica H. Turk[1] *and Larbi Bounini*[1]

The Effect of Sorbed Water on the Determination of Phase Composition of $CaSO_4 \cdot H_2O$ Systems by Various Methods

REFERENCE: Turk, D. H. and Bounini, L., **"The Effect of Sorbed Water on the Determination of Phase Composition of $CaSO_4 \cdot H_2O$ Systems by Various Methods,"** *The Chemistry and Technology of Gypsum, ASTM STP 861*, R. A. Kuntze, Ed., American Society for Testing and Materials, 1984, pp. 48–56.

ABSTRACT: The efficiency of calcination processes is monitored by careful phase analysis of $CaSO_4 \cdot H_2O$ systems. The usual method of determining a small amount of gypsum in such systems involves the determination of sorbed (free) water, water of crystallization (combined water), and Ca^{++}/SO_4^{--} ratio. The removal of free water from $CaSO_4 \cdot \frac{1}{2}H_2O$ and active orthorhombic calcium sulfate occurs at about the same temperature range as the decomposition of $CaSO_4 \cdot 2H_2O$, which then becomes a most critical stage in the phase analysis of these systems. This paper discusses (1) relative merits of various methods utilized in removing free water, which includes several thermal methods and microwave drying, and (2) the state of the sorbed water as it develops from exposure to radically varying relative humidity conditions.

KEY WORDS: gypsum, drying, anhydrite, α-hemihydrate, β-hemihydrate, phase analysis, drying curves, water sorption

The operation and optimization of the various gypsum manufacturing processes require that the composition of the products and raw materials be accurately known. The analysis mainly involves quantitative determination of the different phases of calcium sulfate. Various methods for phase analysis have been developed [*1*] and accepted by appropriate regional or national standard setting organizations as listed in Table 1. Despite the long history of the gypsum industry and the widespread use of gypsum, none of these methods became universally accepted.

Although the test conditions and procedure may differ, the gypsum phase analysis methods consist of two basic steps:

[1]Research associates, United States Gypsum Company, Graham J. Morgan Research Center, 700 North Highway 45, Libertyville, IL 60048.

TABLE 1—*Removal of free water by oven drying.*

Country	Source [1]	Sample Weight, g	Drying Temperature, °C	Drying Time, h
United States	ASTM C 471[a]	50	45	2
Germany	DIN 1168-1955	4000	35 to 40	24
Spain	UNE 7065	50	45	2
	F. Paris and C. Lopez	. . .	45	8
	EXCO	100	45 ± 5	constant weight
Portugal	VP-319/1963	100	50 ± 5	constant weight
France	NF-B-12-401	10	50	constant weight
Italy	UNI 5371-64(G)[b]	100	50 ± 2	constant weight
	UNI 6782-71(H)[c]	100	40	1
International	ISO 3052-1074	100	40 ± 4	constant weight
Switzerland	Piece 1952	5	40	24
Rilem	GP 23	100	50 (silica gel)	24

[a]ASTM Chemical Analysis of Gypsum and Gypsum Products (C 471).
[b](G) = gypsum.
[c](H) = calcium sulfate hemihydrate.

(1) free water removal from sample and
(2) submission of "dried" sample to chemical analysis.

The dry weight of the sample is the basis in the calculations involved in the reconstruction of the sample composition. Any error in the dry weight would affect the proper ratios of the different gypsum phases since an error in free water is actually credited to or against water of hydration. Table 2 shows the manner in which an error in percent free water affects the hemihydrate content in a calcined gypsum sample.

The free water removal step is usually carried out in a heated oven without regard to convection. As can be seen from Table 1, the sample weight, the oven temperature, and the criterion for proper drying vary widely. Although the drying temperature appears to be empirically determined, it was selected to avoid possible decomposition of the hydrates. Except for the International Union of Testing and Research Laboratories for Materials and Structures (RILEM) procedure, no mention is made of the humidity conditions in the oven. The type of air convection must be specified for it affects the drying rate especially when drying time is fixed and sample weight varies. Improper handling of the sample after oven

TABLE 2—*The effect of drying on changes in composition of* β *calcium sulfate hemihydrate.*

Percent	Underdried	Actual	Overdried
Free water	0.74	0.82	0.90
Combined water	5.92	5.82	5.74
Hemihydrate	95.33	93.72	92.43

drying and before weighing could result in free moisture pickup, thus introducing an error in the dry weight.

The complete removal of free water from gypsum samples without affecting the chemically bound water, or water of hydration, requires special care and complete understanding of the factors affecting the moisture-solid equilibrium.

This work represents an attempt to elucidate the complex nature of proper drying and its effect on the composition of gypsum containing various calcium sulfate phases.

Factors Affecting Free Water Removal

The factors affecting the process of free water removal from calcium sulfate and its hydrates are

(1) the chemical and physical characteristics of the sample and
(2) the conditions under which the water is driven off.

Characteristics of the Samples

Although the chemical composition of the calcium sulfate compounds is relatively well known, the physical characteristics of these compounds received little attention despite their great influence on the manufacturing processes and uses of the gypsum products. Table 3 illustrates the diverse nature of the physical characteristics of the known phases of calcium sulfate as indicated by their widely varying crystal modification, aggregation state, and internal structure.

Each calcium sulfate phase could exist in several forms with widely varying physical characteristics depending on the manufacturing process. A good example is provided by the hemihydrate that may be manufactured in three different forms, including α-hemihydrate, β-hemihydrate, and aged β-hemihydrate, each with a characteristic crystalline structure, surface area, and porosity (Table 3). The interaction of the compounds with the environmental conditions (adsorption of water and heat transfer) depends on the character of the surface and the magnitude of the area. Consequently, the affinity for water and the resistance to its removal vary with the type of material as shown in Fig. 1. Samples of commercial origin containing different phases of calcium sulfate were "dried" at 24°C and 0.1% relative humidity in a closed chamber containing magnesium perchlorate as a drying agent. The weight loss data (Fig. 1) show that the rate and amount of water loss, as represented by the slope and the relative position of the drying curve, respectively, vary not only with the hydration level but also with the aggregation state. Unlike β-hemihydrate, α-hemihydrate with its lower surface area and no porosity exhibits lower initial water uptake and lower rate of drying. Calcium sulfate dihydrate also shows different drying behavior for natural gypsum and gypsum obtained by hydration of hemihydrate. It seems evident that the compounds with higher state of hydration have a tendency to lose higher amounts of water when exposed to conditions of low humidity even

TABLE 3—*Chemical and physical characteristics of hydrated and anhydrous calcium sulfates.*

Composition	Crystal Structure	Aggregation State	Surface Properties	
			SA, cm^2/g[a]	Porosity[b]
$CaSO_4 \cdot 2H_2O$	monoclinic	natural rock		
		ground	7 000 to 10 000	low
		rehydrated		
		β-hemihydrate	24 000	low
$CaSO_4$ ½H_2O	hexagonal	α-hemihydrate	5 000	low
		β-hemihydrate	75 000 to 80 000	high
		Aged β-hemihydrate	≈25 000	low
$CaSO_4$III	hexagonal	Dehydrated α- or β-hemihydrate	≈150 000	high
$CaSO_4$	orthorhombic	natural	5 000	low
		"deadburnt"	60 000	high

[a] SA is surface area by nitrogen adsorption using, the Brunauer, Emmett, and Teller (BET) method [2].

[b] Porosity indicated by the presence and shape of the hysteresis loop of the nitrogen adsorption isotherm.

at room temperature. In an industrial environment where the product is often a mixture of several calcium sulfate phases, it makes the design of the drying procedure for such material difficult.

Drying Conditions

The conditions under which the free water is removed are as important to proper drying as the physical and chemical properties of the sample. These two factors must be considered simultaneously when designing a drying procedure. Drying by controlling the temperature alone would not be reliable because of the effect the relative humidity (RH) has on the amount of water desorbed from the solid surface. However, drying under controlled conditions of temperature and relative humidity may be effective in free water removal only when a pure calcium sulfate is present.

In a mixture of phases, each component would retain a characteristic amount of water when allowed to come to equilibrium with the environmental conditions. Drying curves obtained by the oven drying method at temperatures ranging from 35 to 55°C normally exhibit a plateau at equilibrium (at constant weight); however, the height of the plateau for a sample with given characteristics depends on the temperature and prevailing relative humidity. Decreasing the relative humidity has the same effect on drying as raising the temperature and may eventually decompose the calcium sulfate hydrates as shown in Fig. 1 by the absence of plateaus in the weight loss curves. Table 4 compares the sample weight loss for oven drying at 45°C and exposure to low humidity and room temperature. In the case of oven drying, the sample actually reached constant

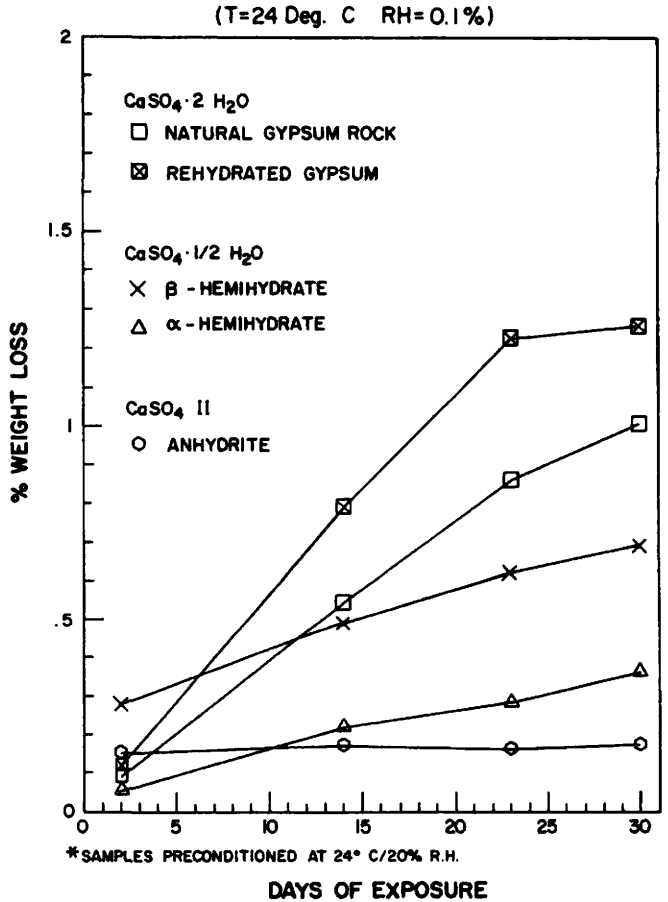

FIG. 1—*Samples dried over magnesium perchlorate.*

weight after 22 h. When dried in a closed container in the presence of magnesium perchlorate, the sample lost more weight in 24 h than in the oven and continued to lose weight for the entire test period even though the temperature was only 24°C. Since the initial weight loss of the sample during drying, by any method, is due mainly to free water removal, then it seems reasonable that use of microwave energy could be an effective method of drying.

Microwave drying was studied using CEM corporation moisture/solids/analyzer, Model AVC™-80, equipped with a built-in electronic balance having a maximum load of 8 g and a sensitivity of 0.2 mg. The microwave had a frequency of 2450 MHz and variable power from 0 to 600 W. Power of 600 W was used in this experiment.

TABLE 4—*Water removal under different conditions.*

	Weight Loss, %		
		MG $(ClO_4)_2$	
$CaSo_4 \cdot \frac{1}{2}H_2O$	Oven at 45°C for 16 h	2 Days	30 Days
β-hemihydrate	0.16	0.26	0.72
β-hemihydrate/Aged	0.14	0.18	0.75
α-hemihydrate	0.05	0.06	0.33
Rehydrated α-hemihydrate	0.03	0.12	1.28

Figure 2 shows typical drying curves for commercial β-hemihydrate that was preconditioned in three different environments to prepare samples with different amounts of free moisture. The curves exhibit a definite plateau after only a few minutes of exposure to microwaves, which is a strong indication that the weight loss is due to free water removal only.

Table 5 shows weight loss of different materials by microwave drying after exposure to 98 and 75% RH and 24°C for different lengths of time. The percent combined water was determined for all the cases shown in Table 5 and was found to be essentially constant for each sample regardless of the weight loss by microwave treatment (Fig. 3). This indicates that complete drying was achieved and that the chemically bound water was not affected by microwave at any level of free water.

Conclusions

In trying to develop an accurate method for gypsum phase analysis based on energy or mass balance or both, the mechanism of free water uptake must be understood. It was established that the amount of free moisture uptake depends on the physical structure of the sample as indicated by the adsorption and thermodynamic equilibria. The drying process becomes a shift in equilibrium when the temperature and relative humidity are intentionally changed to promote drying.

When a drying temperature is selected, the relative humidity should not be too low so as to initiate calcination, or too high so as to promote surface adsorption and capillary condensation. In addition the drying conditions of temperature and relative humidity must not affect the chemical equilibrium. However, since each calcium sulfate compound has its own stability region in the phase diagram, the drying conditions must be in a region where all the phases present in the sample remain stable.

Exposure of a sample to microwave does not affect the chemical equilibrium because of the selective absorption of microwave radiation energy. As can be seen from the shape of drying curves in Fig. 2, most of the microwave energy goes toward evaporating the free water. Table 5 shows that microwave drying resulted in a higher free moisture content than oven drying, especially for the

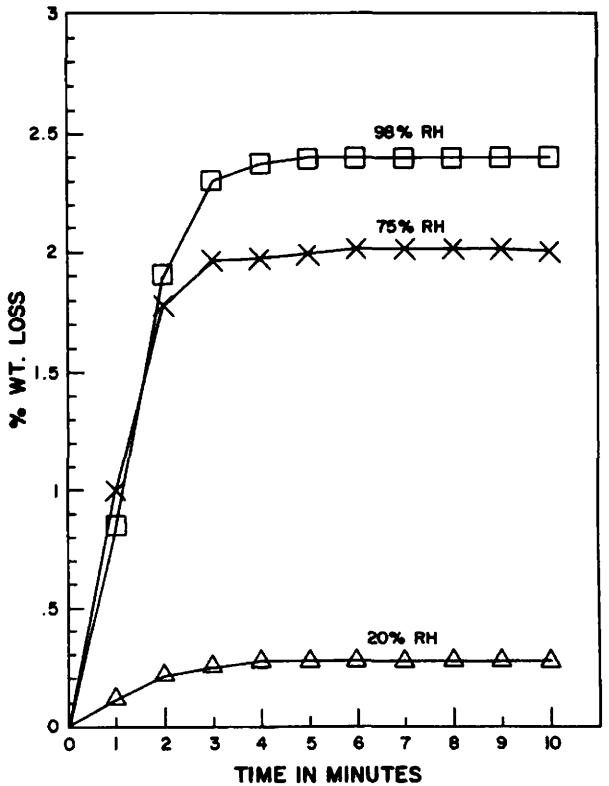

FIG. 2—*Microwave drying curves for calcium sulfate hemihydrates.*

TABLE 5—*Microwave drying of different calcium sulfate compounds after the exposure to 75% and 98% RH.*

$CaSO_4{\cdot}½H_2O$	Weight Loss, %[a]					
	0h	3h	6h	12h	24h	48h
		98% RH				
β-hemihydrate	0.25	0.91	1.47	1.98	2.40	2.84
β-hemihydrate/Aged	0.24	0.79	1.22	1.66	2.27	2.57
α-hemihydrate	0.04	0.35	0.52	0.66	0.97	1.17
$CaSO_4$II "Deadburnt"	0.05	0.14	0.16	0.20	0.28	0.41
		75% RH				
β-hemihydrate	0.25	0.82	. . .	1.42	2.01	. . .
β-hemihydrate	0.24	0.64	. . .	1.34	1.71	. . .
α-hemihydrate	0.04	0.17	. . .	0.59	0.82	. . .
$CaSO_4$II	0.05	0.10	. . .	0.10	0.18	. . .

[a] Exposure to relative humidity.

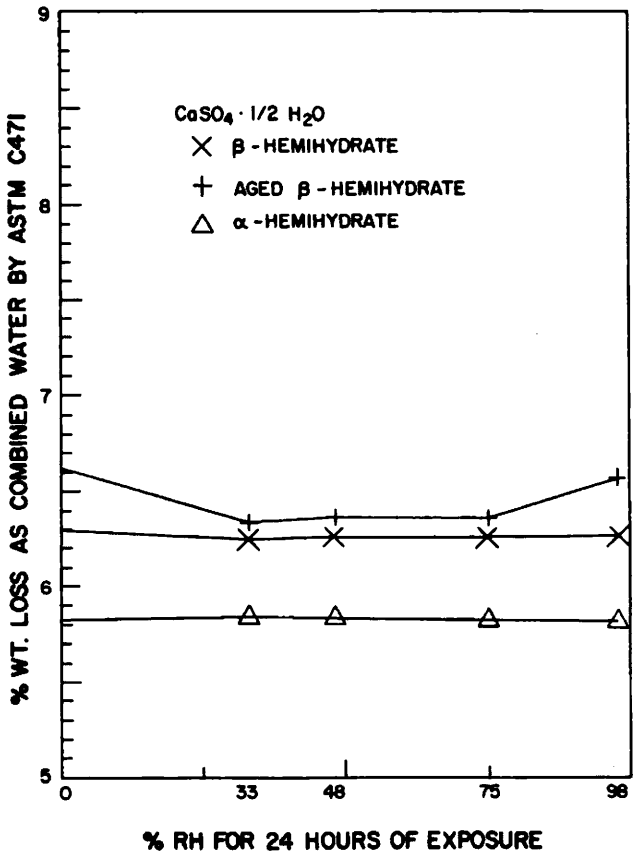

FIG. 3—*Effect of microwave drying on combined water.*

β-hemihydrate samples. This is due to the highly porous nature of the atmospheric calcined gypsum. The microwaves tend to evaporate condensed water from all pores, whereas a portion remains filled when oven dried depending on the temperature and relative humidity.

In summary, it was shown that

(1) improper drying results in erroneous composition,

(2) the physical and chemical characteristics of the samples must be taken into account when designing a drying procedure,

(3) the drying conditions must match the character of the sample, and

(4) use of microwave drying seems to overcome the difficulties in matching the properties of the sample and the drying conditions.

Acknowledgments

The authors wish to thank the United States Gypsum Company for permission to present this paper, which is one of the series of papers on phase analysis.

Thanks also go to David A. Adamski for obtaining microwave drying data and to J. M. Summerfield and R. F. Stone for helpful discussions and encouragement.

References

[1] Murat, M., "Report of RILEM Technical Committee 23-GP," *RILEM Materials and Structures*, Vol. 15, No. 85, Jan. 1982, p. 63.

[2] Brunauer, S., Emmett, P. H., Teller, E., *Journal of American Chemical Society*, Vol. 60, 1938, p. 309.

Etienne Karmazsin[1]

A Simple Apparatus for Measurement of the Hydration Ratio of Plasters and Plaster Rocks

REFERENCE: Karmazsin, E., **"A Simple Apparatus for Measurement of the Hydration Ratio of Plasters and Plaster Rocks,"** *The Chemistry and Technology of Gypsum, ASTM STP 861*, R. A. Kuntze, Ed., American Society for Testing and Materials, 1984, pp. 57–66.

ABSTRACT: In the frame of calcium sulfate β-hemihydrate hydration kinetical studies, a simple experimental set up has been developed to determine the rate of hydration for different species of incompletely hydrated plaster specimens. This apparatus may also be used to determine with accuracy the amount of gypsum contained in plaster rocks, and acquire simultaneously quantitative analysis for six specimens. The apparatus is described, and the effect of vapor pressure is studied.

Experimental results on incompletely hydrated plaster specimens show that either the weight loss or the integration curves allow the determination of the hydration ratio of the specimen with high accuracy. It has been experimentally shown that the amount of heat involved in the hydration reaction is proportional all along the reaction to the conversion rate.

KEY WORDS: plaster, gypsum, anhydrite, vapor pressure, humidity, measure and integration, hydration ratio, plaster rocks, calcium sulfate β-hemihydrate, calcium sulfate dihydrate, reactor, water vapor molar fraction, isothermal calorimeter, thermoelectric captor

Properties and reactivity of a calcium sulfate β-hemihydrate are widely dependant on the preparation procedure. Although kinetical studies on the hydration reaction are done by a number of researchers, there is no standard procedure to elaborate a stable, reproducible calcium β-hemihydrate specimen. This paper presents a very simple apparatus and an experimental procedure setup to elaborate a specimen that is stable and allows kinetical studies even after a long time of conservation. This apparatus also allows the simultaneous determination of the hydration rate for six different species of incompletely hydrated plasters and demonstrates experimentally that the amount of heat involved in the hydration

[1]Associate professor, Department of Applied Chemistry and Chemical Engineering, University Claude Bernard Lyon I, 43 Boulevard du 11 Novembre 1918, 69622 VILLEURBANNE Cedex, France.

reaction is proportional all along the reaction to the conversion rate, which may be determined with a very high accuracy either from the weight loss or by means of the thermal flow integration curves.

The Reactor

The reactor is a cylinder made of stainless steel (Fig. 1) (its length is 36 cm and its inner diameter is 10 cm). At the upper part it is connected to a vapor pressure reserve (4.5 L) containing a small amount of an ammonium sulfate supersaturated aqueous solution. This solution provides an 81% relative humidity atmosphere between the temperature of 293 and 303 K. The vapor pressure reserve, connected to an exhaust valve, allows control of vapor pressure in the reacting area. The reactor, the temperature of which is regulated at 398 K or 423 ± 1 K, contains a sample holder with six specimens symmetrically disposed around the axis. The sample holder is composed by two stainless steel disks (92

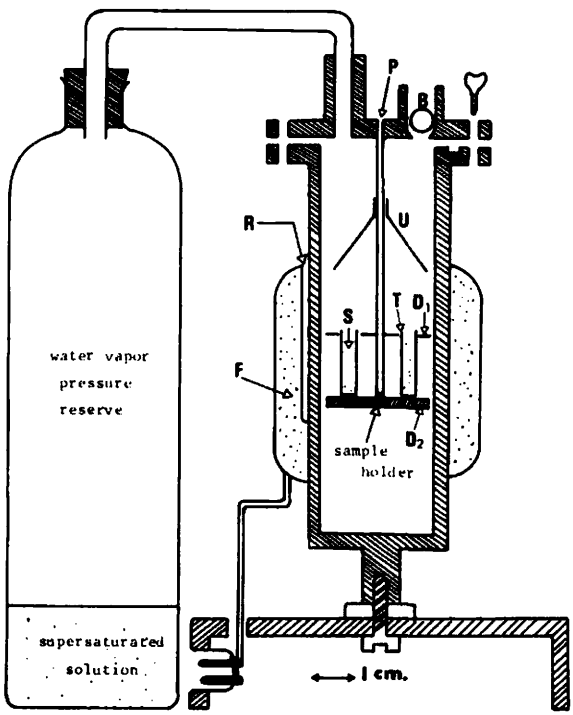

FIG. 1—*Cross view of the reactor and water pressure reserve.* B: *exhaust valve,* S: *specimen,* U: *umbrella* D_1, D_2: *stainless steel disks;* P: *pipe sustaining the sample holder, it is a pipe that contains the temperature measurement thermocouple;* T: *cylinder containing a specimen;* F: *isolated heating resistor; and* R: *furnace control thermocouple.*

mm in diameter). The upper disk D_1 has six round holes symmetrically disposed around the axis (Fig. 1). In each hole a stainless steel cylinder *T* contains a specimen (generally 2 g). Temperature is measured by a thermocouple placed at the level of the specimens in the pipe P that sustains the disks D_1 and D_2.

An isolated electrical resistor F is wound around the reactor to realize a furnace of 600 W, which is controlled by a thermocouple R. A sort of umbrella protects the specimen against possible water drops. The upper part of the reactor contains a Teflon® ball used as an exhaust valve to control vapor pressure in the reactor.

The Calorimetric Set

A simple isothermal calorimeter has been set up to follow the hydration reaction. Figures 2 and 3 show different views of the calorimeter. The laboratory cell D (Fig. 2) made of polyester resin is placed in an expanded polystyrene block B; it has two gilded copper sides E and F that direct the heat flow through two thermoelectric captors H (Fig. 4). These captors (Cambridge Thermoionic Corporation) are soldered to a 3-cm thick copper block G. Dissipation of the heat flow is made by means of a black aluminium radiator L (Fig. 3). The calorimeter is locked by two permanent magnets and opened by screwing the rod N (Figs. 3 and 4). The necessary quantity of water is put in a detachable medical syringe O, which is guided to enter the female cone A (Fig. 2) of the needle C that is bent to arrive at the top of the laboratory cell.

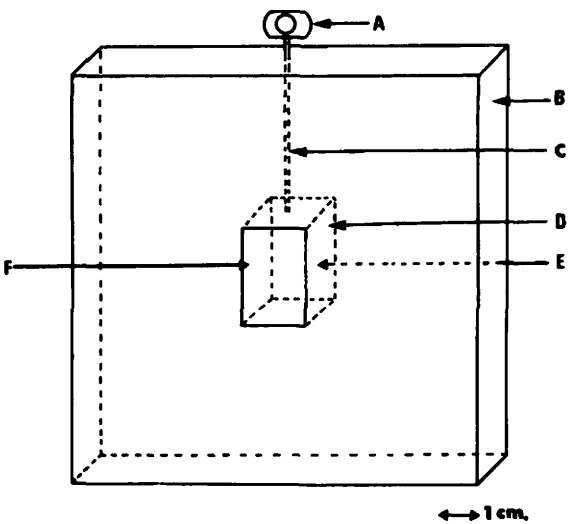

FIG. 2—*Cross view of the calorimeter.* A: *female cone of the needle,* B: *expanded polystyrene,* C: *injection needle,* D: *laboratory cell, and* E, F: *gilded copper sides.*

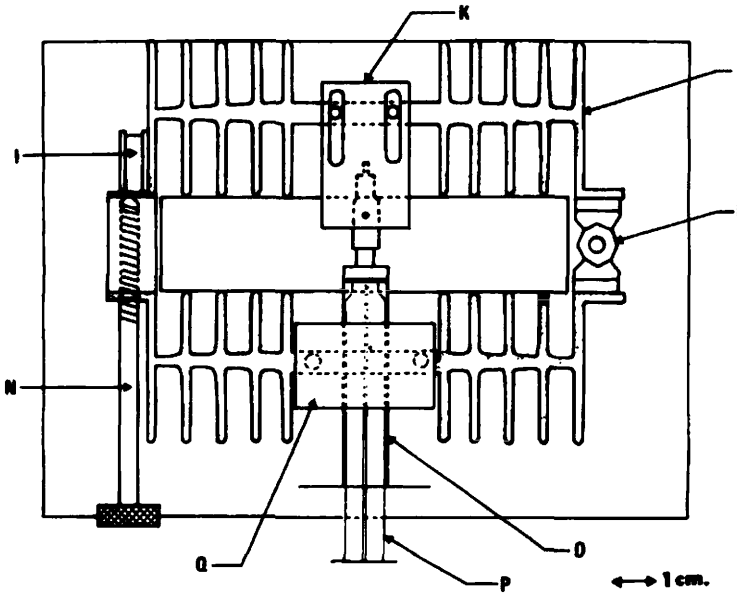

FIG. 3—*Upper view of the calorimeter.* I: *permanent magnet,* K: *positioning guide for the needle female conus,* L: *black radiator,* M: *hinge to open the calorimeter,* N: *stem of the screw opening the calorimeter,* O: *medical syringe,* P: *piston of the syringe, and* Q: *guide for positioning the syringe.*

The calorimeter is put in a thermoregulated metallic box. After temperature equilibrium of the system is reached, water is injected without opening the box, by turning the stem of a screw that pushes the piston rod of the medical syringe.

A high precision electronic integrator is directly connected to the thermoelectric captors so as to record simultaneously the thermal flow and its integral curve versus time. Figure 5 shows the thermograms given by this apparatus.

Heat Treatment Temperature Determination

Determination of the optimal heat treatment temperature in the reactor is done by differential thermal analysis (DTA) and thermogravimetric analysis (TG); it appears (Fig. 2) that in our experimental procedure, for all the studied granulometries (<25 to 250 μm), a specimen fired at 398 K for 3 h contains no more gypsum, and a specimen fired at 423 K still contains almost only hemihydrate. Above this temperature anhydrite III appears. The very small amount of anhydrite III contained in a specimen fired at 423 K is different from a gypsum variety, but quite stable and characteristic for a variety of gypsum (Fig. 6) [*1*].

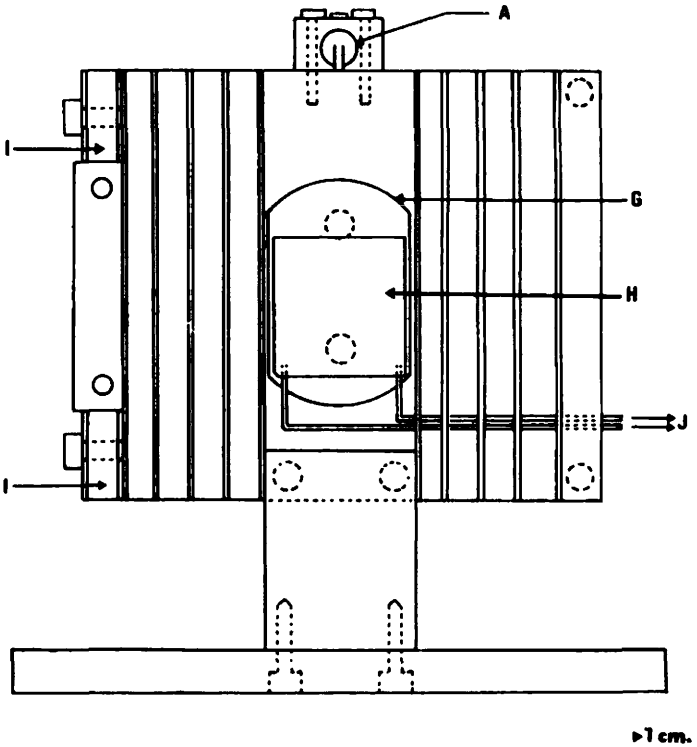

FIG. 4—*Front view of the calorimeter.* A: *female conus of the injection needle,* G: *copper block,* H: *thermoelectric captor,* I: *permanent magnet for locking, and* J: *output of the calorimeter signal.*

Importance of Water Pressure Regulation

By changing the initial water vapor molar fraction in the reactor (varying the vapor pressure reserve temperature), an important variation of t_m appears (t_m is the time of the maximum in the hydration isothermal calorimetric thermogram); t_m increases with the initial water vapor molar fraction. As the initial water molar fraction increases, water diffusion through the specimen is slower during dehydration: the state of crystallization is higher, getting a higher t_m.

Another way to increase water vapor pressure in the reactor is to increase, without any exhaust valve, the amount of specimen. Table 1 shows that if all the six sample holders are filled, t_m is considerably longer. The use of an exhaust valve appears necessary to get a constant t_m, independent of the amount of the specimen [2].

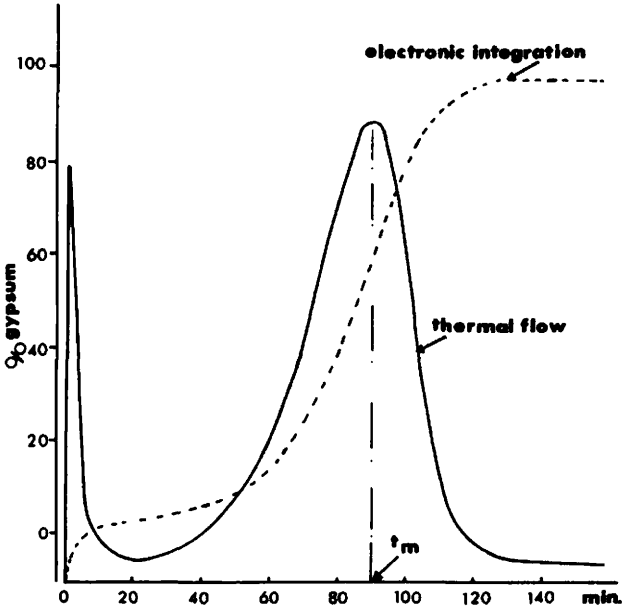

FIG. 5—*Experimental thermograms given by the calorimetric set.*

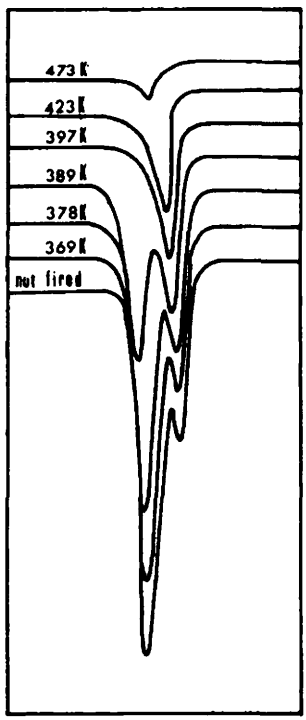

FIG. 6—*DTA curves of a Merck gypsum fired at various temperatures.*

TABLE 1—*Obviousness of an exhaust valve necessity.*

Gypsum	t_m (1 Specimen), min	t_m (6 Specimens), min	Δt_m, min	Exhaust Valve
B-24, 398 K	51	64	13	without
Merck, 398 K	62	73	11	
Merck, 398 K	80	80	0	
Merck, 423 K	91	95	4	with
B-24, 398 K	69	70	1	
B-24, 423 K	91	91	0	

Stabilization Procedure

It is usual, in β-hemihydrate preparation by gypsum dehydration, to do a reversion because the fired products may contain some anhydrite III. Dehydration products after a certain amount of time are placed in a wet atmosphere. Figure 7 shows variations of t_m as a function of conservation time in a wet atmosphere (81% relative humidity) for a β-hemihydrate, without any previous drying of the products.

If the fired products are dried (24 h on a silica-gel dryer), before being put in the wet atmosphere, the evolution of t_m is quite different, as seen in Fig. 8.

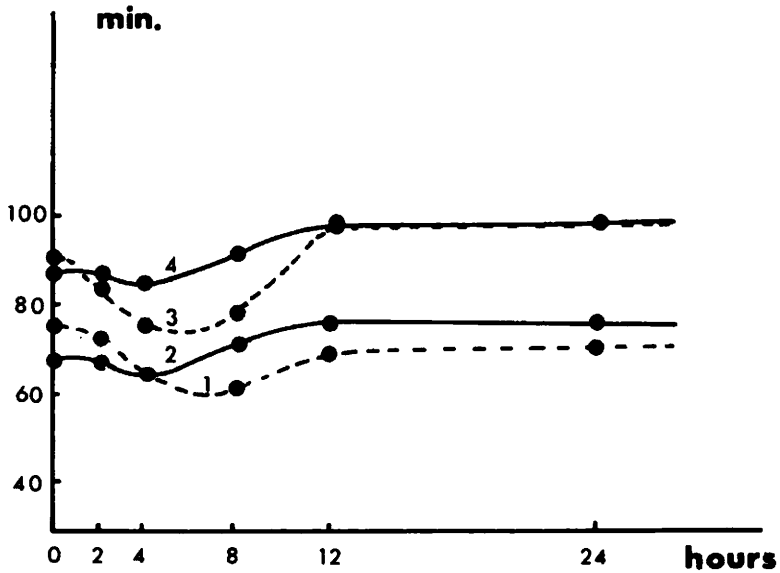

FIG. 7—*Variations of t_m versus conservation time in a wet atmosphere without previous drying. Curve 1: Merck gypsum fired at 398 K; Curve 2: Natural B 24 gypsum fired at 398 K; Curve 3: Merck gypsum fired at 423 K; and Curve 4: Natural B 24 gypsum fired at 423 K.*

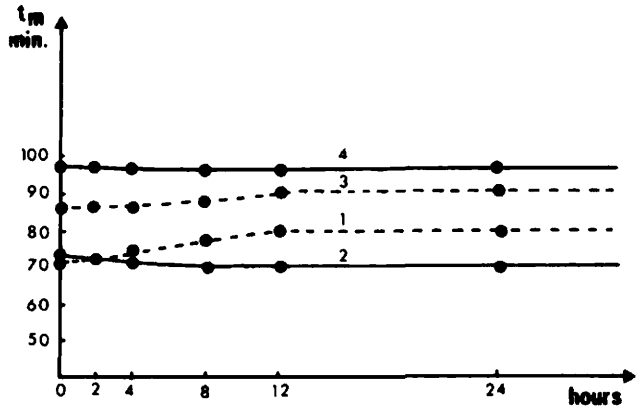

FIG. 8—*Variations of t_m versus conservation time in a wet atmosphere after drying fired products. Curve 1: Merck gypsum fired at 398 K; Curve 2: Natural B 24 gypsum fired at 398 K; Curve 3: Merck gypsum fired at 423 K; and Curve 4: Natural B 24 gypsum fired at 423 K.*

The following procedure was adopted:

(1) drying fired products 24 h on silica gel,
(2) a stay of 15 h in 81% relative humidity at 293 K, and
(3) back to silica-gel dryer for 24 h and then conserved any time on silica-gel dryer.

Use of the Reactor for Hydration Ratio Determination

As gypsum dehydration is realized in quite reproducible conditions, the reactor may be used to determine with accuracy, the amount of gypsum contained in a plaster rock or an incompletely hydrated plaster.

Six specimens are put in the specimen holder; one is a well known reference. Each specimen, after drying, is weighed before and after firing. The percentage of gypsum is given by the classical formula

$$G\% = 100\,\Delta m/m[1 - (145.15/172.27)] = 100\,\Delta m/0.1569$$

where m = the specimen weight after drying and before firing and
Δm = the difference between m and the weight after firing.

Determination of the hydration ratio for a plaster specimen hydrated during various spaces of time demonstrates experimentally that the amount of heat involved in the hydration reaction is strictly proportional to the conversion rate, even when hydration occurs with setting modificators.

The electronic integrator, associated to the isothermal calorimeter [*3–5*] gets

TABLE 2—*Comparison of conversion rates obtained from weight loss calculations and from thermal flow integration curves, for a pure Merck hemihydrate.*

Time, min	Gypsum, % from Weight Loss	Gypsum, % from Integration Curve
20	2.75	3.30
40	6.61	7.01
60	14.05	14.9
80	39.51	40.29
100	78.78	77.23
120	97.36	97.76
140	97.42	97.80

simultaneously thermal flow curves and integration curves of thermal flow versus time and thermal flow curves versus conversion rate. Hydration reaction is stopped after various spaces of time, and the conversion rate is calculated from weight loss and from the thermal flow integration curve. Table 2 shows experimental results obtained for a Merck hemihydrate. These values may be plotted versus time and compared. Figure 8 shows a very good agreement between experimental and calculated points.

Results obtained with an industrial hemihydrate, hydrated with setting additives, are shown in Table 3. Conversion rate values, calculated from weight loss, are in a good agreement with those given by thermal flow integration (Fig. 9).

Conclusion

With a very simple apparatus and experimental procedure it is possible to elaborate a stable, reproducible standard specimen for kinetic studies. With this apparatus, the hydration ratio of incompletely hydrated plasters or plaster rocks can be determined with accuracy. Finally this apparatus demonstrates experi-

TABLE 3—*Comparison of conversion rates obtained from weight loss calculations and from thermal flow integration curves an industrial hemihydrate, hydrated with setting additives.*

Time, min	Gypsum, % from Weight Loss	Gypsum, % from Integration Curve
10	5.93	6.00
20	11.02	11.74
30	21.92	22.06
40	38.81	37.74
50	52.97	51.40
60	60.10	59.81
75	66.83	67.65
90	69.84	70.90
112	73.80	73.46
140	73.99	73.75

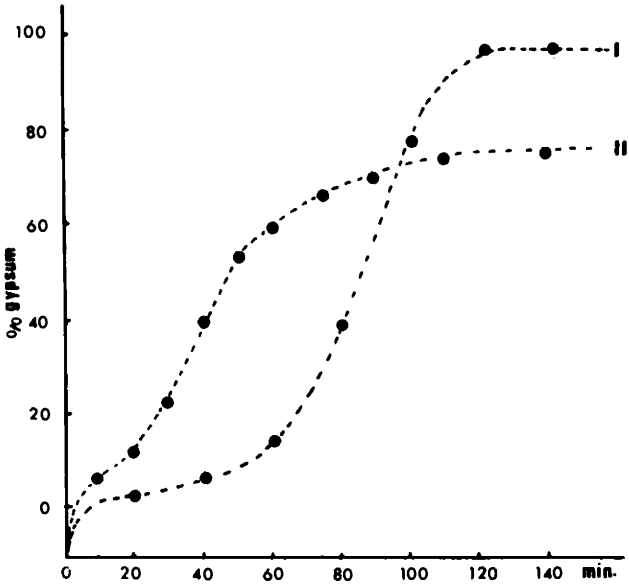

FIG. 9—*Comparison of conversion rates obtained from weight loss and thermal flow electronic integration for a pure Merck hemihydrate (Curve I) and for an industrial product (Curve II).* ----- *is thermal flow electronic integration and* ● ● *is experimental points given by weight loss.*

mentally that all along the hydration process, the amount of involved heat is strictly proportional to the conversion rate, even when hydration occurs with setting additives.

References

[1] Murat, M., Karmazsin, E., and Charbonnier, M., "Evolution Topochimique des Poudres de Semihydrate $CaSO_4$, $\frac{1}{2}H_2O\beta$ Lors de Leur Conservation en Atmosphere Humide," *C. R. Acad. Sc.*, Paris, France, 1974, t. 278, pp. 167–169.

[2] Karmazsin, E., "Cinetique et Mecanisme D'Hydratation des Sulfates de Calcium Semihydrates. Etude Par Calorimetrie en Regime Isotherme," Thèse de doctorat, Université Claude Bernard—LYON I et Institut National des Sciences Appliquées de Lyon, Lyon, France, 1978.

[3] Murat, M. and Karmazsin, E., "Cinetique D'Hydration des sulfates de Calcium Semihydrates, Essai D'interpretation des Courbes: Vitesse Degre D'Avancement," *C. R. Colloque Internationaux de la RILEM*, M. Murat and M. Foucault, Lyon, France, 1977, pp. 217–236.

[4] Murat, M. and Karmazsin, E., "Influence de L'origine du Gypse sur La Vitesse D'hydration du Semihydrate. Etude par Calorimetrie Isotherme," *Proceedings of Eurogypsum*, Barcelona, Spain, 1977.

[5] Triollier, M., Hydration de Sulfate de Calcium Semihydrate, "Thèse de doctorat, Universite Scientifique et Médicale et Institut National Polytechnique de Grenoble, Grenoble, France, 1979.

S. Goswami[1] *and D. Chandra*[2]

Determination of Sulfur Trioxide in Gypsum

REFERENCE: Goswami, S. and Chandra, D., **"Determination of Sulfur Trioxide in Gypsum,"** *The Chemistry and Technology of Gypsum, ASTM STP 861*, R. A. Kuntze, Ed., American Society for Testing and Materials, 1984, pp. 67–71.

ABSTRACT: This paper deals with the various sources of error in different steps of the procedure for determination of sulfur trioxide in gypsum samples, using hydrochloric acid as solvent for gypsum and barium chloride to precipitate barium sulfate. The paper suggests reduction in the amount of acid and barium chloride used in order to minimize errors. Thus, it justifies the need for the revision of Section 12 of ASTM, Chemical Analysis of Gypsum and Gypsum Products (C 471).

ASTM C 471 recommends use of 50 mL of 1 + 5 hydrochloric acid (sp gr 1.19) as solvent for a 0.5-g gypsum sample and 20 mL of 10% barium chloride as precipitant. This results in too high a concentration of acid and chloride ions in reaction solution before and after precipitation, justifiable only for dissolution of impure gypsum samples and formation of coarse barium sulfate crystals to give rapid filtering. The method is silent about the final volume to be made of reaction solution, which determines the acidity before precipitation. It is also silent about the use of and the type of filtering crucibles.

The greatest source of error is the occlusion of chloride ions caused by both hydrochloric acid and barium chloride in addition to adsorption of H^+, coprecipitation of barium chloride and Ca^{++} ions, and increased solubility of barium sulfate in acidic solution.

Therefore, the following suggestions have been made (1) reduce the initial amount of hydrochloric acid used as solvent to 25 mL of 1 + 5 hydrochloric acid for the 0.5-g test sample, (2) use 20 mL of 6% barium chloride solution (preferably old), (3) make the volume of the reaction solution up to 400 to 500 mL before precipitation of barium sulfate, and (4) use filtering crucibles. These changes will increase the accuracy of the sulfate determination by minimizing error caused by high acid and chloride concentration and by maintaining quick dissolution and filtering. Analyses performed with these changes have been found to be consistent and accurate.

KEY WORDS: gypsum, sulfur, chemical analysis, precipitation (chemistry)

Section 12 of ASTM Chemical Analysis of Gypsum and Gypsum Products (C 471) deals with the determination of sulfur trioxide in gypsum gravimetrically. Basically, gypsum is dissolved in dilute hydrochloric acid, and sulfate is precipitated as barium sulfate by addition of hot/boiling barium chloride solution.

[1] Chemist, Rajasthan State Mines and Minerals Ltd., Sadul Club Building, Bikaner-334001, Rajasthan, India.

[2] Lecturer, Department of Chemistry, Dungar College, Bikaner-334001, Rajasthan, India.

The white crystalline precipitate of barium sulfate is filtered, washed with water, ignited, and weighed.

Section 12 of ASTM C 471 reads:

> Dissolve 0.5 g of the sample in 50 mL of HCl (1 + 5). Boil. Add 100 mL of boiling water, and continue boiling for 5 min. Filter immediately and wash thoroughly with hot water. Boil, and while boiling add slowly 20 mL of boiling $BaCl_2$ solution. Digest hot for 1 h or until the precipitate settles. Filter and wash. Dry carefully. Ignite over a bunsen burner at lowest heat possible until the filter paper is burned off. Ignite at bright red heat for 15 min, and weigh. Multiply this weight by 0.34297 to determine the weight of sulfur trioxide (SO_3).

Discussion

There are many sources of potential error in the gravimetric determination of sulfate as barium sulfate. The greatest source of error concerns the tendency of barium sulfate to carry down and retain the constituents of solvent and precipitant. The most significant source is caused by the adsorption of extraneous (mainly chloride) ions by barium sulfate.

Acidity—Hydrochloric Acid Solvent

Both hydrochloric acid and barium chloride cause occlusion of chloride. Hydrochloric acid is worse than barium chloride in this respect. Therefore the sulfate solution before the precipitant is added should not contain more than 0.1% of hydrochloric acid by volume [*1,3*]. A further complication caused by excess acidity is adsorption of H^+ ions, which causes liberation of sulfuric acid when barium sulfate is ignited [*2,3*]. In addition to this, high acidity of reaction solution will cause error because of the solubility of barium sulfate in hydrochloric acid. The solubility of barium sulfate in water, though small, is not negligible (4 mg/L at 20°C). The presence of mineral acid increases the solubility to a considerable extent, that is, in 0.1*N* hydrochloric acid the solubility of barium sulfate is about 10 mg/L at 20°C [*4*]. This limits the amount of hydrochloric acid that can be used. A concentration of 0.05*N* with respect to hydrochloric acid before precipitation has been found to be most suitable [*4,5*].

The amount of hydrochloric acid 50 mL of 1 + 5 hydrochloric acid [sp gr 1.16, 32% weight by weight (w/w) as per Indian Standard (IS) of hydrochloric acid] is 1.68N for a 0.5-g test sample of gypsum is too high for any purpose except the quick dissolution of gypsum and other impurities such as carbonate and so forth. This high acidity of the resulting solution before and after barium sulfate precipitation is very likely to introduce errors that affect the results. Reduction of final acidity is therefore necessary for accurate determination of sulfate.

The method is silent about the final volume of reaction solution, which should be specified because it also determines the effective acidity before the precipitation of barium sulfate. Some of the acid is consumed in dissolution and evap-

oration, but the final acidity under the procedure currently followed is very high. Provided the final volume before precipitation is considered to be 450 mL, the resulting acidity of the reaction solution comes to be 0.1 to 0.18*N* if 32% w/w hydrochloric acid of 1.16 sp gr is used, and will be more if hydrochloric acid of sp gr 1.19 (as per ASTM C 471) is used. This much acidity at the point of precipitation is still too high as compared to the suggested suitable concentration of 0.05*N* acid. The solution need be only slightly acidic to reduce occlusion and coprecipitation of barium chloride with barium sulfate, which is greater in neutral solution than in acidic solution. A high concentration of chloride ions also increases the occlusion of barium chloride.

The amount of acid used initially must be reduced to 25 mL of 1 + 5 hydrochloric acid for 0.5 g of gypsum sample, and the final volume made up to 400 to 450 mL. This acidity will allow the quick dissolution of pure as well as low grade gypsum samples and bring the final acidity to the level of 0.05 to 0.1*N*, which is most suitable for accuracy. This will also minimize the errors because of occlusion of chloride ions and barium chloride, adsorption of H^+ and coprecipitation of barium chloride and Ca^{++} ions, and solubility of barium sulfate in acidic solutions.

Barium Chloride Precipitant

The amount of barium chloride occluded increases with the concentration of sulfate solution, as well as with the concentration of chloride ions and barium chloride, and with the rate of addition of barium chloride precipitant. The amount of occlusion is less with slow, dropwise addition of hot/boiling barium chloride to continuously stirring reaction solution than with rapid addition [*4*].

Because of the error caused by occlusion of barium chloride in the presence of hydrochloric acid, the amount of excess barium chloride should be limited. The method provides for the use of 20 mL of 10% barium chloride weight by volume (w/v), that is, 2 g of barium chloride for 0.5 g of test sample of gypsum, while the theoretical amount of barium chloride for complete precipitation of sulfate (on a 100% purity basis of gypsum) is only 0.71 g. An excess of 1.29 g of barium chloride (that is, more than 180% excess) does not appear justified except for the reasons that excess addition of barium chloride facilitates increase in size of barium sulfate crystals with rapid settling and filtering, for which only 30 to 50% excess has been suggested in literature [*6,7*]. Therefore, for achieving the beneficial effects of excess barium chloride and at the same time minimizing the possibility of barium chloride occlusion and coprecipitation, the excess barium chloride should be limited to 20 mL of 6% barium chloride for a 0.5 g of sample, which would be about 70% excess.

Experiments conducted initially with the use of 25 mL of 1 + 5 hydrochloric acid (sp gr 1.16, 32% w/w as per IS) as solvent and 20 mL of 6% barium chloride as precipitant for 0.5 g of sample, and making the volume of reaction solution before precipitation up to 400 to 450 mL, do not show discrepancy in

results for sulfur trioxide determination in gypsum samples. Therefore, the amount of hydrochloric acid used initially and the precipitant barium chloride should be reduced to the suggested levels to give greater accuracy.

Other Details

Old solutions of barium chloride or fresh solutions filtered through fine filter paper are reported to be more effective than the fresh solutions in promoting the formation of large crystals of barium sulfate precipitate [*4,8*]. For the purpose of rapid filtering and for avoiding transfer of barium sulfate precipitate and ignition of filter paper, the use and type of filtering crucibles should be specified.

Conclusions

The determination of sulfur trioxide by barium sulfate precipitation is beset with potential errors at every step of the procedure. The details of the procedure must be clear and strictly followed for accurate results. Therefore, in the light of this discussion, the following recommendations are submitted for revision of the ASTM C 471.

1. Use 25 mL of 1 + 5 hydrochloric acid for 0.5 g of gypsum sample weighed accurately to nearest milligram. Only for exceptionally impure and hard to dissolve samples should any higher concentrations of acid be used.
2. Use a 250-mL beaker for the test sample. Boil until dissolution or for 3 to 4 min. Add about 100-mL of boiling water and continue boiling for about 5 min.
3. Filter immediately through a 41 Whatman or equivalent filter paper or through filter crucibles, wash thoroughly with hot water, and make the solution up to 400 to 450 mL in a 600-mL beaker. Bring it to boiling.
4. Add boiling/hot 20 mL of 6% barium chloride solution preferably with the help of pipette, drop by drop with stirring. Barium chloride solution should be prepared at least one day before use. Freshly prepared barium chloride solution should be filtered through fine filter paper.
5. Digest hot for 1 h or until the precipitate settles. Filter through 42 Whatman® filter paper or equivalent and wash with hot water to make it chloride free. Alternatively, filter crucibles (Gooch, Coors, Sintered glass crucibles) may be used for quick filtering and to avoid the ignition of filter paper.
6. Dry the sulfate precipitate and ignite over a bunsen burner at the lowest heat until the filter paper is burned off in free access of air.
7. Ignite at bright red heat for 15 min, and then cool and weigh.

References

[*1*] Chatterjee, *Zeitschrift Fuer Anorganische Chemie*, Vol. 121, 1922, p. 128.
[2] Hahn, F. L. and Kein, R., *Zeitschrift Fuer Anorganische Chemie*, Vol. 206, 1932, p. 398.

[3] *Gravimetric Determination of Sulphate in Comprehensive Analytical Chemistry*, C. Willson, and D. Willson, Eds., Vol. 1C, Elsevier Publishing Company, Amsterdam, Netherlands, 1962, p. 282.
[4] Belcher and Nutten, "Determination of Sulphate," *Quantitative Inorganic Analysis*, 2nd ed., Butterworths Scientific Publications, London, England, 1960, pp. 70–75.
[5] Vogel, A. I., *A Textbook Quantitative Inorganic Analysis*, 3rd ed., ELBS, pp. 462–463.
[6] Diehl and Smith, "Procedure for Determination of Sulphate," *Quantitative Analysis*, John Wiley and Sons Inc., New York, and Chapman and Hall Ltd., London, England, 1953, p. 108.
[7] Chalmers, R. A., *Quantitative Chemical Analysis*, Oliver Boyd, London, England, 1956, pp. 260–261.
[8] Bogen and Moyer, *Analytical Chemistry*, Vol. 26, No. 1481, 1956, p. 473.

Vladimir Kocman[1]

Rapid Multielement Analysis of Gypsum and Gypsum Products by X-Ray Fluorescence Spectroscopy

REFERENCE: Kocman, V., **"Rapid Multielement Analysis of Gypsum and Gypsum Products by X-Ray Fluorescence Spectroscopy,"** *The Chemistry and Technology of Gypsum, ASTM STP 861*, R. A. Kuntze, Ed., American Society for Testing and Materials, 1984, pp. 72–83.

ABSTRACT: A rapid and precise X-ray fluorescence method has been developed for the multielement analysis of gypsum and gypsum products. Gypsum specimens are calcined at 1000°C and then fused with sodium tetraborate flux into flat and transparent disks. The choice of a suitable flux system for the specimen preparation is critical because of a rapid decomposition of anhydrite, $CaSO_4$, in lithium based fluxes at temperatures above 950°C. This decomposition causes not only visible imperfections in the disk surface but also alters considerably the concentrations of the major elements, calcium and sulfur. The procedure used for a fast setup of ten element analysis of gypsum on the Philips PW-1400 spectrometer utilizing synthetic standards and off-line calculated alpha coefficients is presented. Calibrations carried out with chemically analyzed specimens and their mixtures are compared to those performed with synthetic standards prepared by blending pure chemicals and anhydrite into the flux.

KEY WORDS: gypsum, X-ray fluorescence, thermogravimetry, analysis of gypsum, borates, Claisse fluxer, synthetic standards, matrix corrections

While X-ray fluorescence methodology has been well developed for the multielement analyses of silicates, rocks, ores, cements, metals, alloys, and various other compounds, its use in the analysis of gypsum and gypsum products has been somewhat neglected. This may have been due to the lack of well analyzed or certified gypsum standards available commercially or possibly because of the difficulties experienced in specimen preparation.

During the course of setting up a rapid and precise analytical method, we examined several approaches to this problem with the objective of selecting one that would give the most reliable results in the shortest possible time.

The first part of this paper examines several aspects of preparation of suitable specimens for X-ray fluorescence spectroscopy analysis with respect to their

[1] Research scientist, Domtar Research Centre, P.O. Box 300, Senneville, Quebec, Canada H9X3L7.

chemical stability and the reproducibility of the analytical results. The question of specimen decomposition during fusion is examined for various flux systems by thermogravimetry and differential thermal analysis.

The second part of this paper is devoted to the procedure used for a quick setup of ten element analysis of gypsum and gypsum products on the Philips PW-1400 X-ray fluorescence spectrometer, utilizing alpha coefficients. Calibration data obtained with chemically analyzed specimens and their mixtures are compared with those based on synthetic standards prepared by blending pure chemicals with anhydrite.

Experimental Procedure

Specimen Preparation, Pressed Powders

Since gypsums are quite easily pulverized to powders of -150 mesh, the first experiments were carried out with disks pressed from pulverized and dried (45°C) gypsum. Excellent results were obtained by pressing approximately 8 g of gypsum into 32-mm diameter aluminum cups at 25 tons. The resulting pellets were of very high quality with extremely flat and shiny surfaces. The pellets did not however survive even the low vacuum of the X-ray fluorescence spectrometer required for the determination of elements below atomic number 20 (calcium). The hydrogen bonded water was rapidly removed from the surface of the gypsum and caused a slow but steady change in the chemical composition of the top layers of the pellet. This greatly influenced the stability of the specimen and the reproducibility of the countrates. The technique of pressing gypsum powders into pellets was therefore not suitable and had to be abandoned.

More promising results were obtained with gypsum calcined at 1000°C. The resulting anhydrite pressed well into 32-mm diameter aluminum cups when mixed with a small amount of methylmethacrylate binder. These pellets were relatively stable in vacuum, but rehydrated and recarbonated quite rapidly in air. They were therefore unsuitable for repetitive analyses or long-term storage. The recarbonation was mainly caused by the presence of calcium and magnesium oxides in the specimen. These resulted from calcination of calcite or dolomite impurities present in most industrial gypsums. Particle size effects and the relative roughness of the pellet surface also had a negative effect on the obtained countrates and consequently the analytical results.

Fusion Techniques

The most popular and elegant specimen preparation technique introduced by Claisse [*1*] is based on fusion of solid specimens with lithium tetraborate. The method was used with great success in our laboratory for the rapid quantitative X-ray fluorescence analysis of silicates, bricks, refractories, limes, iron, and manganese ores. The use of lithium tetraborate and lithium fluoride flux systems was therefore examined first.

A small amount, 2.5 to 3.0 g of representative gypsum specimen, was calcined for 1 h at 1000°C in a platinum crucible, and the loss on ignition was recorded. A portion of 1.0000 g of the calcined specimen was mixed with 6.000 g of dense lithium tetraborate (Spectroflux 100®, Johnson and Matthey Co.) and 0.3000 g of lithium fluoride. Approximately 3 mg of lithium bromide was added to the mixture as a release (nonsticking) agent. Fusions were carried out on a propane flame, using a Claisse fluxer [2] equipped with crucibles and molds made from 95% platinum-5% gold alloy. The volume of molten flux was adequate to fill the 32-mm diameter mold to a sufficient height and produce a disk approximately 4 mm thick.

The disks prepared in this fashion were not perfect. Often they adhered to the molds and cracked unpredictably on cooling. Most of the disks contained trapped gas bubbles, which caused porosity of the disk surface. Some disks crystallized on the edges. Although various ratios of lithium tetraborate to lithium fluoride were tried and higher proportions of the flux mixture to the specimen were used, the gas entrapment problem and the unpredictable cracking of the disks on cooling were never rectified. Consequently, cracked and porous disks had to be remelted and recast, sometimes several times, resulting in prolonged specimen preparation times.

Sodium tetraborate (Spectroflux 200®, Johnson and Matthey Co.) was tried with much greater success. Disks produced by fusion of 0.5000 g of calcined gypsum and 6.00 g of sodium tetraborate (Table 1) produced absolutely clear and transparent disks with perfect surfaces. The use of a higher specimen to flux ratio was dictated by the lower solubility of anhydrite in molten borax.

The use of sodium tetraborate means that one has to sacrifice the determination of the element sodium in gypsums. Most gypsums, however, contain low levels of sodium, typically below 0.3% sodium oxide. If necessary, sodium can be determined in gypsum by atomic absorption spectrophotometry.

The advantages of using sodium tetraborate for the fusions outweigh the loss of sodium as an analyzed element. Times required for the fusion and swirling of the flux on flame (Table 1) were quite short. The use of lithium fluoride and lithium bromide was eliminated completely. The disks prepared from sodium tetraborate release easily from the molds each time, without any sign of sticking, cracking, or crystallization.

Thermal Behavior of Anhydrite in Lithium and Sodium Fluxes

Because of the suspected decomposition of anhydrite, $CaSO_4$, in lithium-based tetraborate flux systems at elevated temperatures, it was decided to study their behavior by means of thermal analysis (TGA, DTA). Thermal scans were performed on the Mettler TA-2 thermoanalyzer equipped with a DTA-20 macroholder. Platinum crucibles were filled with 200 mg of specimen flux mixtures and balanced by equal portions of alumina as the reference material. All specimens were heated at a rate of 10°C/min in an oxidation atmosphere (stream of air).

TABLE 1—*Fusion technique used for disk preparation.*

Step	Description
1	Determine the loss on ignition in a muffle furnace at 1000°C using pulverized (− 150 mesh) specimen dried at 45°C.
2	Weigh 0.5000 g of the freshly calcined specimen into a Claisse crucible containing 6.00 g of dense sodium tetraborate ($Na_2B_4O_7$, Spectroflux − 200). The latter (borax) was previously dried for several hours at 350°C and kept in an air-tight container.
3	Mix the specimen with the flux using stainless steel microspatula.
4	Fuse for 4 min on a Claisse fluxer (stationary heat) and swirl for 3 min on the flame.
5	Wait 1 min (no swirling) to increase the temperature of the melt and pour into 32-mm molds.
6	Six disks can be produced and cooled simultaneously in about 15 min. The minimum thickness of the disk should be 4 mm.

After reaching the upper temperature set limit, the temperature was held constant (isothermal hold) for several hours. The weight-loss curves (TG) are shown in Fig. 1. The weight losses recorded on lithium and sodium fluxes alone (Spectroflux 100 and 200) caused by thermal decomposition above 1000°C were negligible. Similar results were obtained with mixtures of anhydrite and sodium tetraborate. The latter showed a weight loss of less than 0.1% when heated at 1000°C for 1 h.

When lithium tetraborate and lithium fluoride are used as a flux, or when

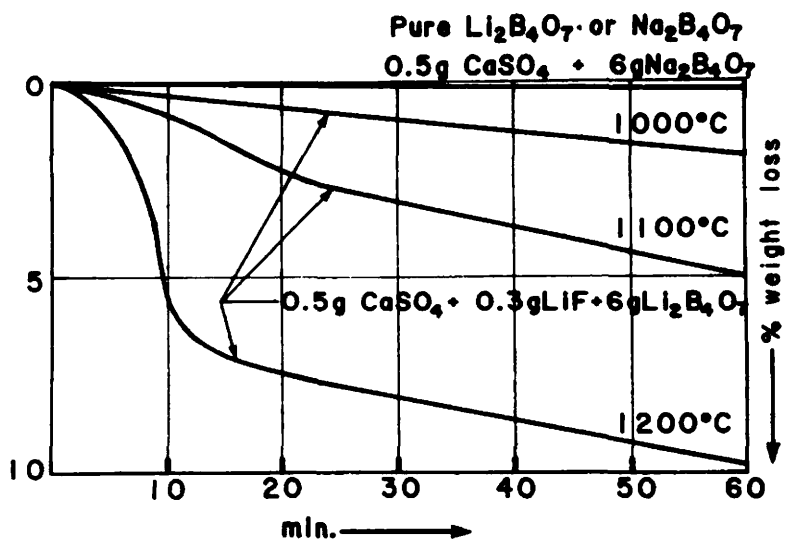

FIG. 1—*Isothermal heating of mixtures of anhydrite ($CaSO_4$) with various fluxes. Weight of mixture—0.200 g, crucible material—platinum atmosphere—air, instrument—Mettler thermoanalyzer.*

lithium fluoride is added to sodium tetraborate, significant weight losses are recorded. The rates of decomposition of anhydrite in lithium-based fluxes increase drastically with temperature. As the operator could easily set the temperature on the Claisse fluxer, such that overheating of the flux mixture occurs (the maximum temperature reached by the propane flame can be as high as 1200°C), the use of lithium-based fluxes is not recommended for the analysis of gypsum specimens. Errors have been observed caused by losses as high as ±0.4% for the major elements, calcium and sulfur. These values were obtained on a number of lithium tetraborate fusions carried out on an identical anhydrite specimen. On the other hand the maximum errors obtained on replicates fused with sodium tetraborate flux were on the order of ±0.07% for calcium and ±0.12% for sulfur. Obviously the change in the composition of the specimen in lithium-based fluxes is a significant factor that has a negative effect on the precision of the calibration procedures and the analysis of unknown specimens.

Calibration of X-Ray Fluorescence Spectrometer

A Philips PW-1400 wavelength dispersive spectrometer equipped with four crystals (LiF, Ge, PET, and TlAP) was used for the analysis. The rhodium target tube was operated at 2.5 kW (50 kV and 50 mA). The sample holders were 32 mm in diameter with a copper mask. The elements determined and their respective peak and background times are shown in Table 2. The intensity ratio method was employed using a synthetic monitor specimen.

Calibrations with Chemically Analyzed Standards

As certified gypsum standards were not available commercially, the calibrations were carried out on a set of "round-robin" analyzed specimens and their mixtures. Three other well analyzed gypsum specimens were supplied by the U.S. Gypsum Co., IL. In addition, several of these had to be spiked with additives in order to expand their calibration ranges on calcium and minor elements. Disks were prepared from calcined gypsums according to the conditions given in Table 1.

Calibration with Synthetic Standards

This set of standards was prepared from one very well analyzed and relatively pure gypsum specimen. The specimen was calcined and spiked with pure oxides and chemicals (Table 3) to alter its composition. The choice of the additives used for the spiking is critical. The compounds must be thermally stable under the fusion conditions and dissolve well in the molten borate flux. The oxygen balance of the specimen should also be maintained.

The required composition of the standard specimens was precalculated with the help of the VISICALC® program [*3*]. Portions of freshly calcined spiking compounds and anhydrite were weighed directly into the platinum crucible,

TABLE 2—*Fixed peak and background times used for the measurement of individual elements and mean counting errors.*

Parameters	Element									
	Ca	S	Mg	Sr	Al	Fe	Si	K	P	Cl
Peak, s	20	40	80	20	40	20	40	20	40	40
Background, s	. . .	. . .	40	10	. . .	10	. . .	. . .	. . .	. . .
Error, %[a]	0.12	0.12	1.03	0.70	0.70	0.21	0.57	0.31	0.51	0.71

[a]Defined as $100/\sqrt{\text{count}}$.

TABLE 3—*Spiking compounds used for the preparation of synthetic calibration standards.*

Element	Spiking Compound
Ca	CaO
S	. . .
Mg	MgO
Sr	$SrSO_4$, SrO
Si	SiO_2
Al	Al_2O_3
Fe	Fe_2O_3
K, P	$K_4P_2O_7$
Cl	NaCl

utilizing a digital semi-microbalance. The exact weight of each additive was recorded and reentered into VISICALC to obtain the true concentrations. The balance of added anhydrite varied between 0.35 to 0.5 g and was high enough to permit a quick and exact weighing. Predried (350°C) sodium tetraborate (Spectroflux 200®) was added and mixed with the spiking compounds and anhydrite. Such a mixture was fused, thoroughly mixed on flame, and cast into disks, using the Claisse fluxer.

Calibration Ranges

The calibration ranges covered by the set of 16 synthetic standards are given in Table 4. The calibration ranges for the chemically analyzed standards were identical.

Matrix Corrections

Because of the high specimen to flux ratio (1:12) the resulting matrix effects are small, but not negligible. The alpha-influence coefficients used successfully in this procedure were calculated by Dr. Richard Rousseau of the Geological

TABLE 4—*Calibration ranges of synthetic standards.*

Element Calculated as	Range, %
CaO	30 to 44
SO_3	35 to 58
MgO	0 to 11
SrO	0 to 2
Al_2O_3	0 to 6
Fe_2O_3	0 to 6
SiO_2	0 to 10
K_2O	0 to 6
P_2O_5	0 to 5
Cl	0 to 1

Survey of Canada in Ottawa [4]. The matrix correction model used in this work was that described by DeJongh [5]

$$C_i = (D_i + E_i R_i)(1 + \Sigma \alpha_{ij} C_j / 100)$$

where

C_i = concentration of element i,
D_i = intercept of the calibration line,
E_i = slope of the calibration line.
R_i = countrate ratio for element i,
α_{ij} = precalculated alpha coefficients for element i, and
C_j = concentrations of other elements in the specimen.

The DeJongh model is similar to the Lachance-Trail model [6], but includes correction for self-absorption effects. The alpha coefficients shown in Table 5 were used as starting values for the straight line regression procedure executed by the PW-1400 software package.

Experimental Results and Discussion

Table 6 compares the standard deviations of the calibration line and relative errors calculated for the medium ranges of the individual elements for both sets of standards. Examination of the sigmas clearly revealed a higher precision of calibrations obtained with synthetic standards. The differences are most pronounced for the major elements, expressed as CaO and SO_3. These two elements comprise on average 80 to 98% of the total sum of the analyzed elements in anhydrite; therefore the precision of their determination is a key factor in obtaining good analytical totals. Precision of the determination of the minor elements varies and is poorest for the low atomic number elements as expected. The reproducibility of the results obtained by repeat analyses of identical disks was better than ±0.04% on CaO and ±0.08% SO_3 owing to the excellent stability of the PW-1400 spectrometer. Differences in analytical results obtained on several disks fused from one gypsum specimen were influenced mainly by weighing errors caused by recarbonation and rehydration of the calcined gypsum specimen. These errors are minimized by weighing only freshly calcined specimens to ±0.0001 g and flux to ±0.01 g. Recent work of Houseknecht [7] discusses in detail the effect of errors in the specimen preparation and their impact on the final analytical results.

Results obtained on a calcined (water, carbon dioxide) free basis are recalculated, with respect to loss on ignition to the original dried (45°C) specimen. Thermoanalytical data (DTA and TGA) can provide more detail on the proportion of water, organic impurity, carbon dioxide, and so forth present in the specimen, and the use of this technique is highly recommended for more complex analyses.

TABLE 5—*Alpha-influence coefficients used in the matrix correction procedure (Courtesy of Dr. R. Rousseau, Geological Survey of Canada in Ottawa).*[a]

Element Measured	Contributions of Other Elements in the Matrix									
	MgO	Al_2O_3	SiO_2	P_2O_5	SO_3	Cl_2O	K_2O	CaO	Fe_2O_3	SrO
Mg	0.0000	0.0033	0.0082	0.0119	0.0156	0.0076	0.0200	0.0293	0.1004	0.4410
Al	0.0975	0.0000	0.0008	0.0049	0.0085	0.0007	0.0091	0.0182	0.0893	0.4309
Si	0.0840	0.0998	0.0000	−0.0017	0.0021	−0.0059	−0.0029	0.0061	0.0768	0.4186
P	0.0686	0.0843	0.0991	0.0000	−0.0048	−0.0128	−0.0166	−0.0079	0.0623	0.4031
S	0.0521	0.0678	0.0825	0.1038	0.0000	−0.0177	−0.0311	−0.0228	0.0461	0.3849
Cl	−0.0004	0.0146	0.0288	0.0491	0.0643	0.0000	−0.0804	−0.0736	−0.0106	0.3162
K	0.0184	0.0341	0.0489	0.0697	0.0858	0.2971	0.0000	−0.0572	−0.0191	0.3281
Ca	0.0066	0.0222	0.0371	0.0577	0.0738	0.2839	0.4246	0.0000	−0.0295	0.3122
Fe	−0.1365	−0.1224	−0.1089	−0.0909	−0.0761	0.1095	0.2361	0.2300	0.0000	0.0932
Sr	−0.4949	−0.4861	−0.4775	−0.4668	−0.4571	−0.3441	−0.2648	−0.2664	0.0092	0.0000

[a]Values calculated for 0.5-g specimen + 6 g of $Na_2B_4O_7$, rhodium target tube at 45 kV, Philips geometry (64/35°), Lachance-Trail algorithm.

TABLE 6—*Comparison of the mean standard deviations of the calibration line and the relative errors on individual elements.*

Element Calculated as % Oxide	CaO	SO_3	MgO	SrO	Al_2O_3	Fe_2O_3	SiO_2	K_2O	P_2O_5	Cl
Sigma chemical, ± %	0.25	0.31	0.08	0.06	0.14	0.04	0.06	0.02	0.02	0.02
Sigma synthetic, ± %	0.07	0.15	0.05	0.01	0.03	0.01	0.03	0.01	0.01	0.01
Mean concentration, %	37	47	5.5	1	3	3	5	3	2.5	0.5
Relative error chemical, %[a]	0.60	0.60	1.5	6.0	5.0	1.3	1.2	0.6	0.8	4.0
Relative error synthetic, %[b]	0.21	0.31	0.9	0.8	1.0	0.3	0.6	0.3	0.4	2.0

[a]Chemically analyzed standards.
[b]Synthetic standards.

The method described is suitable for the analysis of gypsum rock, hemihydrate, anhydrite, wallboard cores, gypsum bricks, gypsum plasters, quickset fillers, speciality gypsums, gypsum-based flooring cements, and other gypsum products. The use of synthetic standards not only increased the precision of the determination of the individual elements but also allowed for the extension of the calibration ranges. Examination of various specimen preparation procedures indicated that the anhydrite-sodium tetraborate system for the fusion of the disks is superior to lithium-based flux systems and to other pressed powder techniques.

Although the method was developed for a wavelength-dispersive spectrometer, it is also suitable for use on energy-dispersive systems. The choice of the algorithm for the correction of inter-element (matrix) effects will depend mainly on the available software. Our experience has shown that the use of off-line calculated matrix coefficients as starting parameters in the regression procedure is mathematically more sound than simply accepting those empirically calculated from a set of standards. The latter often have incorrect signs or magnitudes and are valid only within a particular narrow calibration range.

The question of the thermal stability of a sulfur-bearing mineral or compound often arises when ashing or calcination is involved at higher temperatures (in our case 1000°C for the gypsum specimens). West and Sutton [*8*] reported the first sign of dissociation in $CaSO_4$ above the 1225°C inversion temperature of α to β anhydrite. We have verified their results on the Mettler thermoanalyzer, which allows for simultaneous recording of both DTA curve and the TG weight loss curve and found anhydrite stable up to 1200°C. The only sulfur losses incurred during the calcination of the gypsum to anhydrite may originate from pyrite (FeS_2) present as a trace mineral in some gypsum. The same sulfur loss will however result during the determination of sulfate by ASTM Chemical Analysis of Gypsum and Gypsum Products (C 471) [*9*]. In this procedure the gypsum specimen is dissolved and boiled in diluted hydrochloric acid and any sulfur present as sulfides will be inevitably lost as hydrogen sulfide.

Acknowledgments

We would like to thank Dr. Bruce A. Hudgens of the U.S. Gypsum Co. Research Center, IL, for the help with the round-robin analyses of several gypsum specimens and stimulating discussions on the subject. We are also grateful to Dr. Richard Rousseau and Mr. G. R. Lachance of the Canadian Geological Survey in Ottawa, who calculated the alpha coefficients used in the matrix corrections procedure and provided many valuable suggestions.

References

[*1*] Claisse, F., "Accurate X-Ray Fluorescence Analysis Without Internal Standard." *Norelco Reporter 4*, 1957, p. 95.

[*2*] "Claisse Fluxer for Preparation of Glass Discs," Corporation Scientifique Claisse, Ste Foy, Quebec, Canada.

[3] "VISICALC,"® Instant Calculating Electronic Worksheet Software, Visicorp, San Jose, CA, 1982.
[4] Rousseau, R., "A Computer Program for Calculating Alpha-Coefficients," Geological Survey of Canada, Ottawa, Canada, 1980, unpublished.
[5] DeJongh, W. K., "X-Ray Fluorescence Analysis Applying Theoretical Matrix Corrections," *X-Ray Spectrometry*, Vol. 2, 1973, pp. 151–158.
[6] Lachance, G. R. and Trail, R. J., "A Practical Solution to the Matrix Problem in X-Ray Analysis," *Canadian Spectroscopy*, Vol. 11, No. 43, 1966, pp. 43–47.
[7] Houseknecht, T. M., "Fusion Techniques for Sample Preparation in X-Ray Fluorescence Analysis," Pit And Quarry, Vol. 72, Jan. 1983, pp. 72–75.
[8] West, R. R. and Sutton, W. J., *Journal of the American Ceramic Society*, Vol. 37, 1954, pp. 221–224.

Lydia M. Luckevich[1] *and Richard A. Kuntze*[1]

The Relationship Between Water Demand and Particle Size Distribution of Stucco

REFERENCE: Luckevich, L. M. and Kuntze, R. A., **"The Relationship Between Water Demand and Particle Size Distribution of Stucco,"** *The Chemistry and Technology of Gypsum, ASTM STP 861*, R. A. Kuntze, Ed., American Society for Testing and Materials, 1984, pp. 84–96.

ABSTRACT: In gypsum board production, the amount of water required for a stucco slurry with a suitable fluidity is considerably greater than the amount necessary for hydration of the stucco. Since excess water must be removed by drying, it is advantageous, from an energy point of view, to reduce the consistency or water demand of stucco. Constant board density is maintained thereby through increased addition of foam.

The high water demand of stucco produced by conventional calcination methods is due largely to the ability of the stucco to disintegrate, a process during which larger stucco particles break down into smaller particles upon contact and subsequent mixing with water. The water demand of stucco may be reduced by aging, that is, the exposure of stucco to water vapor over a period of time, which reduces the ability of the stucco to disintegrate. However, aging also has a negative effect on both setting characteristics of the stucco and, as a result, on the strength of the gypsum formed.

The objective of the work described in this paper was to study the relationships between water demand and particle size distribution as affected by changes in disintegration during aging. Particle size analysis and several methods of consistency measurement were used for this purpose. It was found that a direct relationship exists between water demand of stucco and particle size distribution as defined by percent disintegration, with minor deviations at initial stages of aging. In contrast, nonlinear relationships were found, with preliminary experiments, for stuccos containing aridizing agents or surfactants, which indicates that the water demand of stucco is also affected by surface properties. The water demand of stucco is not a function of the surface area of the stucco, that is, other properties, such as particle shape and surface characteristics, play a significant role. Similarly, the magnitude of the differences in water demand of various types of stucco indicates that particle size distribution, although the major factor, is not the only one influencing this property.

KEY WORDS: gypsum, stucco, disintegration, water demand, consistency

Modern gypsum board production is a complex process that involves the preparation of an aqueous slurry by mixing calcined gypsum (stucco) with water

[1] Associate research scientist and director, special programs, respectively, Ontario Research Foundation, Sheridan Park, Mississauga, Ontario, Canada L5K 1B3.

and a variety of additives such as foam, starch, surfactants, fibers, and set control agents. The slurry is cast between two layers of paper, and the board is formed by molding both paper and slurry into the desired shape and dimension and allowing the stucco to harden by hydration. The formed board consists of a wet gypsum core, lined front and back, and at both edges by paper. The core at this stage contains excess water because more water is required for slurry preparation than is necessary for hydration of the stucco. This excess water must be removed by drying through the paper, an energy intensive process. From the point of view of energy conservation, it is obvious that it would be advantageous to reduce the consistency or water demand of stucco, that is, the amount of water that must be added to the stucco to produce a slurry that can be poured. The amount of water reduced would be replaced by increased addition of foam to maintain the required core density and board weight.

Methods of reducing the water demand of stucco exist, including aging, that is, exposure of the stucco to water vapor over a period of time [*1,2*], spraying liquid water into the stucco immediately after calcination [*3,4*], introducing deliquescent salts into the calcination kettle [*5*], and the use of surface active agents. However, these methods generally have deleterious effects on other aspects of the board-making process. For instance, an aged stucco yields a gypsum with a lower strength than gypsum obtained from fresh stucco, and aridizing salts may cause deterioration of the bond between board core and paper.

A fresh stucco, in addition to having a high water demand also has the characteristics of high disintegration, that is, upon contact with water, large stucco particles are broken down into smaller particles [*6,7*]. The degree of disintegration that a stucco undergoes is increased by mechanical mixing. Also, the ability of the stucco to disintegrate is progressively lost with aging. Thus, aging affects both water demand and disintegration in a similar fashion, that is, both decrease. For this reason, it has been suggested that a relationship exists between the two [*8*].

The nature of this relationship is the focus of this paper. Particle size distribution data were used to determine disintegration as a function of mechanical mixing and of aging. Similarly, several methods of consistency measurement, employing various types of mixing, were used to determine water demand as a function of aging.

Experiments

A relatively pure form of natural gypsum (Terra Alba) consisting of 98.6% $CaSO_4 \cdot 2H_2O$ was used for this study. The gypsum was ground to pass a 150-μm (No. 100) sieve and calcined in a laboratory kettle designed for both continuous and batch operation. In this manner, three 15-kg lots of stucco were prepared by continuous calcination, and three 5-kg lots of stucco were calcined by the batch process. To two lots of the latter, either calcium chloride or surfactants were added.

TABLE 1—*Time required to reach limiting values (average of three calcinations).*

Consistency Measurement	Time Required for Consistency to Reach Limiting Value, approximate days	Time Required for Disintegration to Reach Limiting Value, approximate days
DIN	6	4
Pouring	15	10
7 s	10	10
60 s	21	15

After calcination, the stuccos were cooled to room temperature with constant stirring to remove all entrained water vapor. The residual gypsum content and soluble anhydrite content as determined by phase analysis [9] were always less than 4.0 and 2.0%, respectively.

The stuccos prepared in the laboratory were aged at 21°C and 65% relative humidity for various periods of time. Two stucco properties, that is, consistency and disintegration, were determined immediately after calcining and after various periods of aging. These tests were continued until equilibrium values had been reached; the times required to reach these values are given in Table 1. The consistency test methods and the techniques to obtain particle size data, as well as the treatment of these data, are described briefly below.

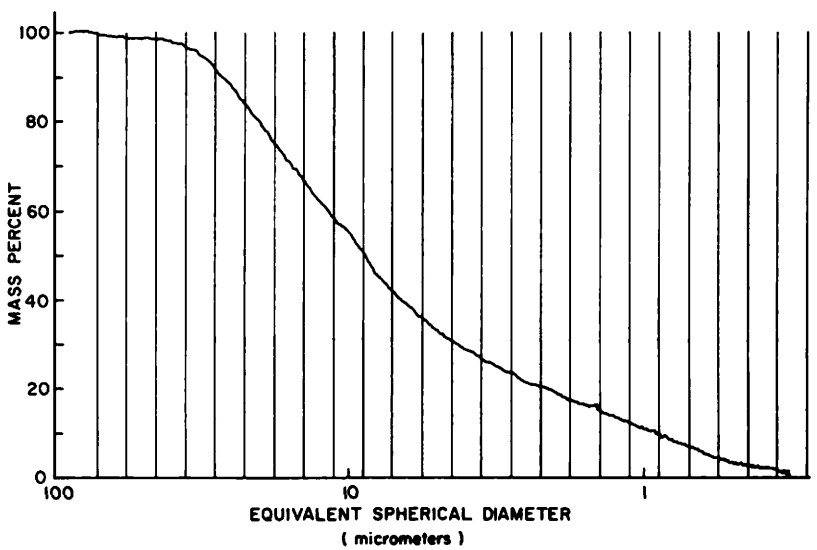

FIG. 1—*Particle size distribution curve.*

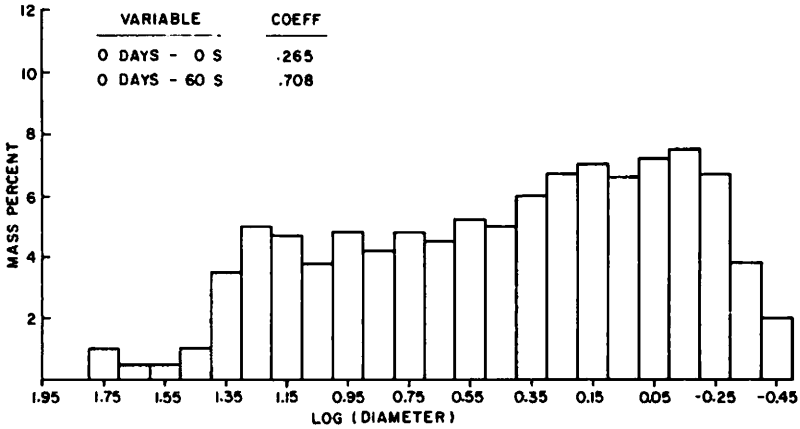

FIG. 2—*Particle size distribution: no aging, 7-s dispersion.*

Consistency Procedures

All consistency measurements were conducted by adding 0.2-g sodium citrate to 100 mL of gaging water to prevent premature stiffening caused by hydration of the stucco.

DIN Consistency

This type of measurement is widely used in Europe [West German Industrial Standard (DIN) Test Methods for Gypsum Plaster (DIN 1168)] to determine the so-called water:stucco factor, that is, the amount of stucco in grams that can be wetted by 100 mL water. The method consists of sprinkling stucco into the water at a specific rate without mechanical mixing. Therefore, it differs from other consistency measurements in that only spontaneous disintegration occurs.

Pouring Consistency

It is common practice in North America to carry out consistency measurements based on the fluidity of water:stucco slurries. The method used for the present work consisted of adding a specified amount of stucco to water and mixing both by hand for 30 s after a brief soaking period. The resulting slurry is poured onto a glass plate to form a patty. The water:solid ratio producing a patty with a specified dimension is taken as the pouring consistency. In this measurement, both spontaneous disintegration and a minimal amount of induced disintegration occur.

7-s Consistency

This consistency measurement is also commonly used in North America. Stucco:water slurries are mixed for 7 s in a high-shear Waring® Blendor to simulate

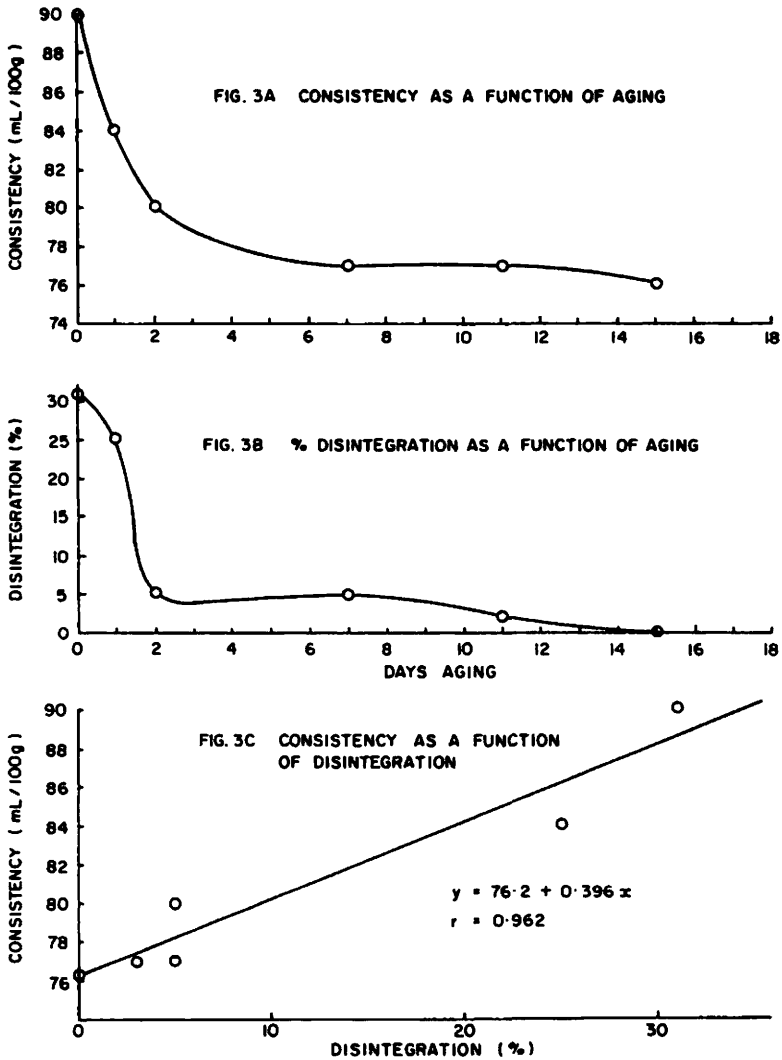

FIG. 3—*Terra Alba DIN consistency.*

the mixing that occurs in a pin mixer during gypsum board production. The correct consistency is expressed as the water:solid ratio that produces a slurry with a specified penetration as determined by the modified Vicat apparatus [apparatus used in ASTM Physical Testing of Gypsum Plasters and Gypsum Concrete (C 472)]. Because of the high mechanical energy involved, a significant amount of induced disintegration is obtained in addition to spontaneous disintegration.

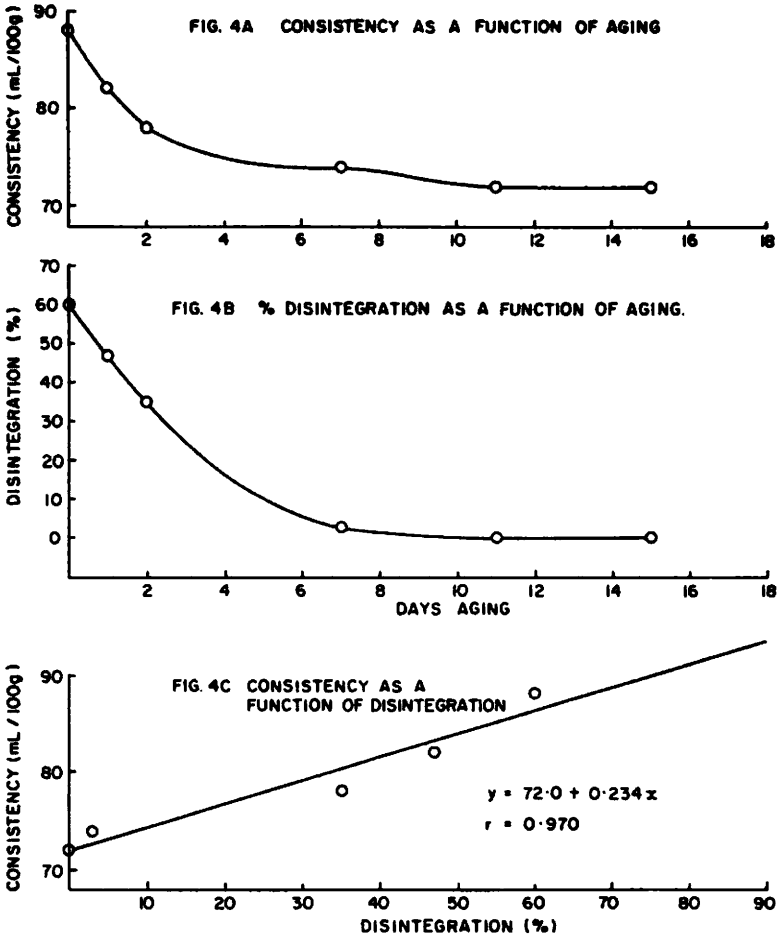

FIG. 4—*Terra Alba pouring consistency.*

60-s Consistency

The mixing procedure used in this test, that is, 60 s in a high-shear Waring Blendor, is intended to produce maximum disintegration of the stucco particles [*6*]. The viscosity of a slurry mixed by this method if measured by a Ford® cup viscometer, and the water:solid ratio with which a specified flow time is obtained is taken as the consistency.

Disintegration Measurements

To determine the degree of disintegration occurring during the consistency procedure, the stucco slurry was mixed immediately after the test with at least

six times its volume of methanol. After mixing, the stucco solids were filtered, washed with acetone, dried, and stored in a sealed container. Control specimens, that is, stucco not subjected to disintegration, were also collected after each calcination and each aging period and stored after drying in sealed containers before particle size analysis.

Particle Size Analysis

The particle size distribution of the dry stucco was measured using a Sedigraph® 5000D particle size analyzer. Specimens were prepared by dispersing the stucco in Sedisperse® A-11 and placing the suspension in an ultrasonic bath for 2 min. Data were acquired in the form of a cumulative mass percent versus equivalent spherical diameter curve. As demonstrated in Fig. 1, this analysis included particles with an equivalent spherical diameter as small as 0.325 μm. For all specimens tested, the particles had equivalent spherical diameters smaller than 90 μm.

Particle Size Data Treatment

Determination of Percent Disintegration—For unaged stucco that had not been subjected to the disintegration procedure, the majority of the particles were in the larger size range (5 to 70 μm). After disintegration to the greatest possible degree, that is, without aging and with 60 s mixing in the Waring Blendor, the majority of the particles were in the smaller size range (0 to 5 μm). Both were taken as having a particle size distribution representative of 0% disintegration or 100% disintegration, respectively. Specimens that had been subjected to aging or less than total disintegration or both had a particle size distribution in between these two limits, representing a specific percentage of disintegration. To calculate this percentage, a regression analysis was performed. For example, Fig. 2 represents a histogram for a specimen that had not been aged but had been mixed for 7 s. The regression analysis shows the degree of disintegration of this specimen as 72.8%. This method of regression analysis was performed on all specimens whereby the correlation coefficients obtained ranged from 0.7 to 0.9.

Results and Discussion

Figures 3 through 6 illustrate the effect of aging time on consistency and disintegration, as well as the relationship between consistency and disintegration for continuously calcined Terra Alba. These data show that both consistency and disintegration decrease with time and suggest a linear relationship exists between these properties. Regression analysis of the data yields slopes, intercepts, and correlation coefficients of these curves as given in Table 2. Similar data for batch calcined stucco are summarized in Table 3.

There is a slight deviation from a linear behavior at early aging periods. For instance, Fig. 7 shows the particle size distribution for continuously calcined Terra Alba dispersed for 7 s at zero- versus one-day aging. The particle size

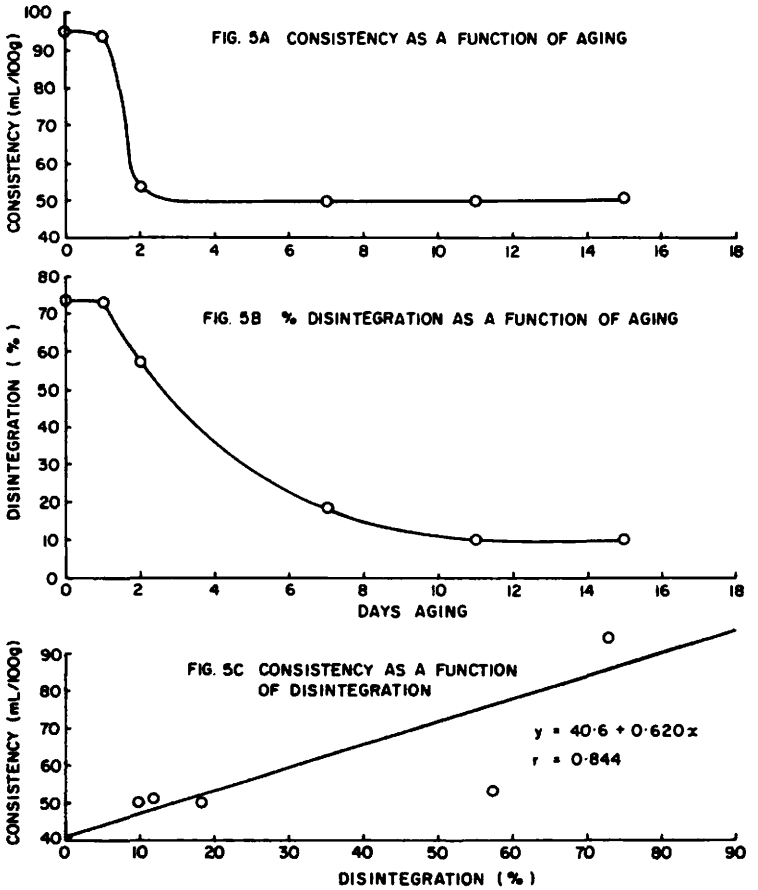

FIG. 5—*Terra Alba 7-s consistency.*

distribution at one-day aging shows a higher mass percentage in the 1 to 2 μm range and a lower mass percentage in the 0 to 1 μm range. Thus, even though one-day aging decreases the mass percentage of submicrometre particles, the stucco still disintegrates to a large degree. Therefore, at low periods of aging, almost complete disintegration may be achieved simultaneously with a lowered consistency.

The intercept is an indication of slurry viscosity. The 60-s consistency slurries are most fluid and consequently have the greatest intercept. The DIN and pouring consistency slurries are of comparable fluidity, and both are less viscous than 7-s consistency slurries. The intercept of the latter has the lowest value.

The fact that the consistency is a direct function of the disintegration suggests that at a given fluidity, the thickness of the water layer around each particle is

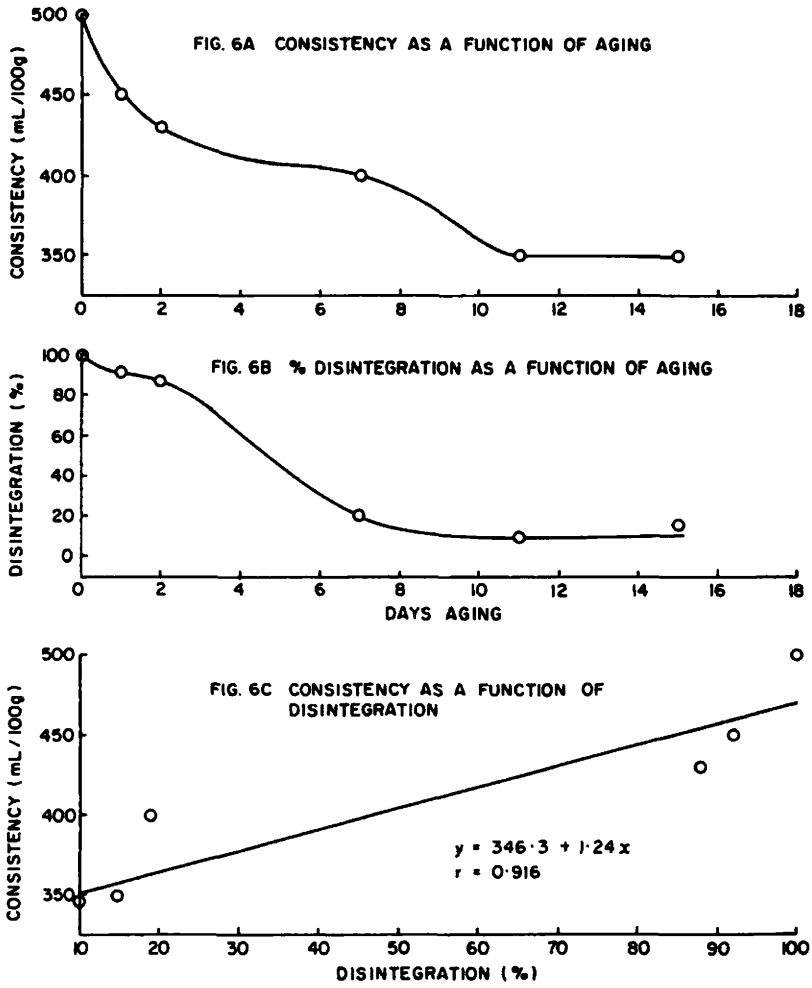

FIG. 6—*Terra Alba 60-s consistency.*

constant, that is, the volume of water required to achieve a certain fluidity is proportional to the surface area of the particles. If this is true, then the thickness of the water layer around each particle can be estimated by dividing the volume of water consumed by the total surface area of the particles. However, as shown in Tables 4 and 5, the thicknesses of the water layer are not constant but range is from 3.9 to 24.7 μm for completely disintegrated stucco and from 9.2 to 90.8 μm for undisintegrated stucco at various fluidities. The water layer thickness in slurries of continuous calcined stucco is smaller than that of batch calcined material.

TABLE 2—*Terra Alba continuously calcined consistency/disintegration regression data.*

Consistency Measurement	Slope, mL/100 g	Intercept, mL/100 g	Correlation
DIN	0.396	76.2	0.962
Pouring	0.234	72.0	0.970
7 s	0.620	40.6	0.844
60 s	1.24	346.3	0.916

The magnitude of the water layer corresponds to between 700 and 15 000 water molecules and suggests that in all slurries the particles are widely separated by a water layer of the same thickness as the particles themselves, thus isolating the particles from each other.

The fact that the water thickness is not constant may be partially explained by changes in particle size, size distribution, and shape. For example, a decrease in particle size upon disintegration may result in closer packing of the particles with a corresponding reduction of the water thickness required around each particle to yield a given slurry fluidity. Similarly, if undisintegrated particles have an irregular shape, their surface area will be greater than that of spherical particles, requiring a thicker water layer to maintain the same slurry fluidity.

The addition of calcium chloride or surfactants during the calcination appears to modify the relationship between consistency and disintegration. Preliminary data suggest that the consistency of stucco containing these admixtures is no longer a direct function of disintegration, but that surface properties play a significant role.

In considering other factors that may influence water demand, many intrinsic stucco properties must be taken into account such as purity, particle size and morphology of the gypsum, calcination methods, and stucco surface properties. In addition, the water demand of stucco is dependent on its history such as aging time and conditions, aridization, and presence of surface active agents.

For example, most stucco specimens contain a significant proportion of insoluble impurities, usually inorganic salts such as anhydrite, calcite, and dolomite. These salts do not disintegrate spontaneously upon dispersion in water and therefore do not increase the water demand. Consequently, the water demand of a given stucco will decrease as the impurity increases.

During the calcination process, the gypsum undergoes comminution caused

TABLE 3—*Terra Alba batch calcined consistency/disintegration regression data.*

Consistency Measurement	Slope, mL/100 g	Intercept, mL/100 g	Correlation
DIN	0.334	74.1	1.000
Pouring	0.681	69.6	0.989
60 s	1.41	363	0.882

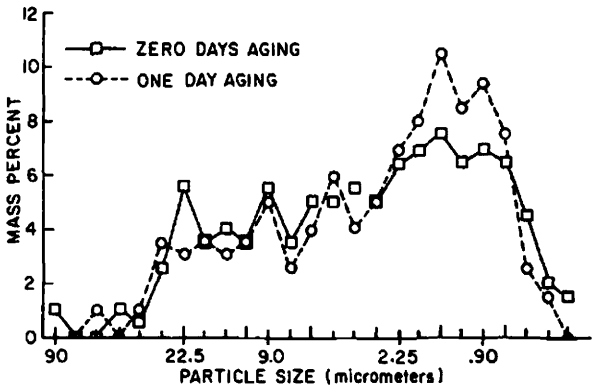

FIG. 7—*Comparison of 7-s dispersion zero- and one-day aging.*

by both dehydration and stirring/fluidization. With decreasing particle size of the gypsum, the dehydration proceeds more uniformly and generates a more constant water vapor pressure in the kettle. Stucco prepared under these conditions will not disintegrate to the same degree as stucco prepared from larger gypsum particles calcined more rapidly in a less homogeneous environment, and consequently, will tend to have a lower water demand.

The method by which gypsum is calcined may have a profound effect on the water demand of stucco because it dictates the local conditions at the calcining surface. For example, in an autoclave, the gypsum is dehydrated through a solution process. This prevents the formation of soluble anhydrite and yields a stable solid, which has undergone little or no lattice disruption. As a result, the particles have low surface energy. In a tray calcination, the gypsum is rapidly dehydrated in a low water vapor environment. The formation of soluble anhydrite is promoted and lattice disruption and particulate surface energy are increased, resulting in a relatively unstable product. The intermediate case is a continuous

TABLE 4—*Terra Alba continuously calcined consistency/surface area data.*

Consistency Measurement	Disintegration, %	Consistency, mL/100 g	Surface Area, cm^2/g	Water Thickness, 10^{-6} m
DIN	0	76.2	4 400	17.3
	100	115.8	24 700	4.7
Pouring	0	72.0	4 400	16.4
	100	95.4	24 700	3.9
7 s	0	40.6	4 400	9.2
	100	102.6	24 700	4.2
60 s	0	346	4 400	78.6
	100	470	24 700	19.0

TABLE 5—*Terra Alba batch calcined consistency/surface area data.*

Consistency Measurement	Disintegration, %	Consistency, mL/100 g	Surface Area, cm^2/g	Water Thickness, 10^{-6} m
DIN	0	74.1	4 000	18.5
	100	107.5	20 400	5.3
Pouring	0	69.6	4 000	17.4
	100	137.7	20 400	6.8
60 s	0	363	4 000	90.8
	100	504	20 400	24.7

kettle in which the gypsum particles are being dehydrated with constant stirring in a nearly saturated steam atmosphere. The formation of soluble anhydrite is inhibited and moderate lattice disruption takes place.

The water demand of a stucco can be reduced through the addition of surface active agents into the gaging water. These surface active agents stabilize the interface between the solid and aqueous phase and can reduce inter-particulate adhesion. This in turn yields a slurry of greater fluidity at a given solids concentration.

The physical, chemical, and electrical properties of the stucco particle surface will affect the affinity of the stucco for the aqueous phase and the resilience of the stucco surface when subjected to external influences such as agitation. These in turn affect the thickness of the solid/liquid interface and the amount of particulate disintegration that can occur, thus affecting the fluidity of the slurry at a given solids concentration.

Conclusions

The objective of this study was to examine the relationship between water demand and particle size distribution of stucco as affected by changes in disintegration during aging. The results of this work show that both the water demand of a stucco and its disintegration respond to aging in a similar fashion. The experimental data suggest that when all other factors are kept constant, there is a direct relationship between water demand and particle size distribution, which is linear for all practical purposes, and that particle size distribution is governed by disintegration.

In the presence of aridizing agents or surfactants, the consistency is no longer a direct function of only the disintegration but appears to depend on surface properties and particle morphology. This indicates the possibility of obtaining a stucco with a low water demand without loss of high disintegration which is necessary to maintain desired setting and strength properties. Further work is required to elucidate the influence of surface properties and other factors on the interdependent relationship between water demand and particle size distribution.

Acknowledgments

The authors would like to thank Dr. R. B. Bruce of Westroc Industries for his helpful comments and Mrs. D. Walker for her diligent experimental work.

References

[1] Kuntze, R. A., "Effect of Water Vapour on the Formation of $CaSO_4 \cdot \frac{1}{2}H_2O$ Modifications," *Canadian Journal of Chemistry*, Vol. 43, No. 9, Sept. 1965, pp. 2522–2529.

[2] Kuntze, R. A., "The Aging of Gypsum Plaster," *Materials Research and Standards*, Vol. 7, No. 8, Aug. 1967, pp. 350–353.

[3] O'Neill, E. E., "Process for Preparing Calcined Gypsum," U.S. Patent 4,114,070, 26 Sept. 1978.

[4] O'Neill, E. E., "Process for Preparing Calcined Gypsum and Gypsum Board," U.S. Patent 4,201,595, 6 May 1980.

[5] Way, S. J., "Influence of Calcium Chloride and Grinding on the Water Requirement of Gypsum Plasters," *Journal of the Australian Ceramic Society*, Vol. 17, No. 2, Feb. 1982, pp. 44–48.

[6] Lane, M. K., "Disintegration of Plaster Particles in Water," *Rock Products*, Vol. 71, No. 3, March 1968, pp. 60–63 and 108.

[7] Lane, M. K., "Disintegration of Plaster Particles in Water, Part 2," *Rock Products*, Vol. 71, No. 4, April 1968, pp. 73–75 and 116–118.

[8] Smith, F. H., "Aging of Calcium Sulphate Hemihydrate," *Nature*, Vol. 198, No. 4885, June 1963, pp. 1055–1056.

[9] Wirsching, F., "Gypsum," *Ullmans Encyklopädie der Technischen Chemie*, Vol. 12, Verlag Chemie, Gmblt, Weinheim, West Germany, English translation, 1978.

Thomas Koslowski[1] *and Udo Ludwig*[2]

Retardation of Gypsum Plasters with Citric Acid: Mechanism and Properties

REFERENCE: Koslowski, T. and Ludwig, U., **"Retardation of Gypsum Plasters with Citric Acid: Mechanism and Properties,"** *The Chemistry and Technology of Gypsum, ASTM STP 861*, R. A. Kuntze, Ed., American Society for Testing and Materials, 1984, pp. 97–104.

ABSTRACT: The object of the investigation was the retardation of gypsum plasters with citric acid. For that purpose measurements were carried out to get information about the mechanism of set retardation and the influence of citric acid on the microstructure and properties of gypsum plasters. Citric acid acts as a retarder by forming citrate. The citrate affects the nucleation and the crystal growth of gypsum by adsorption. That entails the retardation of the hydration period and the habit modification. The influence on the microstructure was investigated by means of the quantitative image analyses and by X-ray methods. Citric acid changes the properties of fresh and hardened mortars. The volume of setting and hardening gypsum plaster passes through a minimum. Increasing citric acid additions raise the minimum and decrease the following expansion. Strength formation was measured by binding and compressive strength tests and by Brinell hardness determination. With increasing citric acid addition, paralleled by higher humidities, a strong decrease in strength can be observed. In addition, the influence of citric acid on the creep behavior of hardened gypsum was examined.

KEY WORDS: citric acid, gypsum, mechanical properties, mechanism of set retardation, microstructure of retarded gypsum mortars, texture index, strength, creep properties

It is of the greatest importance for a given application to adjust a controlled setting and hardening of gypsum mortars. For this purpose retarding and accelerating agents are used in practice.

The one layer wall finish, for instance, requires a retardation of the gypsum plaster.

The object of this research work is the investigation of the mechanism of retardation of gypsum plaster by the addition of citric acid and its influence on the properties of the fresh and hardened mortar. The significance of this work lies in the explanation of the retardation mechanism and its close connection with the microstructure and hence with the mortar properties.

[1] Doctor of engineering, graduate mineralologist, SICOWA, Handerweg 17, 5100 Aachen, West Germany.

[2] Professor of engineering, Institut für Gesteinshüttenkunde, Mauerstrasse 5, 5100 Aachen, West Germany.

Starting Materials

The main physical and technological research work was done with an industrial plaster of paris. Synthetic hemihydrate prepared from dihydrate (MERCK 2161) and autoclaved α-hemihydrate were used for the examination of the retardation mechanism.

Experimental Procedure

The retardation mechanism was investigated by

(1) carrying out precipitation reactions as a function of the saturation,
(2) measuring the calcium and sulfate concentrations of setting plasters,
(3) measuring the adsorption of radioactive citric acid on the surfaces of hemihydrate and dihydrate as a function of time, and
(4) examining the influence of the citrate formation on the retardation.

The microstructure of the hardened paste was investigated as a function of the citric acid addition by

(1) analyzing the grain size distribution with the Endter-counter®,
(2) carrying out quantitative image analysis of pictures from scanning electron microscopy (grain size, circumference, area, and shape factor),
(3) determining the texture index by means of X-ray, and
(4) the determination of the porosity of thin sections (spherical shaped pores) and by means of a mercury pressure porosimeter.

The physical and technological properties were examined as a function of the citric acid addition by the

(1) setting, the workability, and the strength according to German standard Gypsum Building Plasters; Terminology, Types and Application, Delivery and Marking, Requirements, Testing, Control (DIN 1168)
(2) volume changes during setting as described by Ref *1*,
(3) creep of hardened gypsum plasters as a function of the humidity, and
(4) moisture take up and the moisture expansion as a function of relative humidity.

More details of the experimental procedure are described elsewhere [*2*].

Results

Mechanism of Retardation

Citric acid acts as a retarder on hydrating gypsum plasters only together with other cations, mainly calcium ions and by forming citrate. But the needed cations

must be extracted from foreign compounds (for example, calcium carbonate and calcium hydroxide) and not from the calcium sulfates. Normal industrial plasters contain such compounds as impurities. In the case of very pure plasters a corresponding addition must be made. Besides gypsum plasters with a higher degree of acidity in comparison to citric acid must be neutralized first.

If the citrate formation is realized the retardation will run in two steps as shown in Fig. 1.

1. Directly after mixing, the citrate will be adsorbed onto the surface of the hemihydrate and hinder nuclei formation.
2. With an increased content of the citrate an adsorption will take place on the dihydrate nuclei and on the surface of the growing gypsum crystals.

The reduction of the nuclei formation (Step I) leads to fewer but larger dihydrate crystals. Increasing absorption on the surface of the dihydrate crystals (Step II) changes the morphology from needle-like to compact-shaped crystals.

Citric acid and calcium hydroxide cause a higher rate of citrate formation than calcium carbonate does. Bigger grain sizes and higher crystallization, especially of the carbonate, lower the formation rate additionally. These differences in the formation velocity lead to a more Step I type retardation with calcium hydroxide

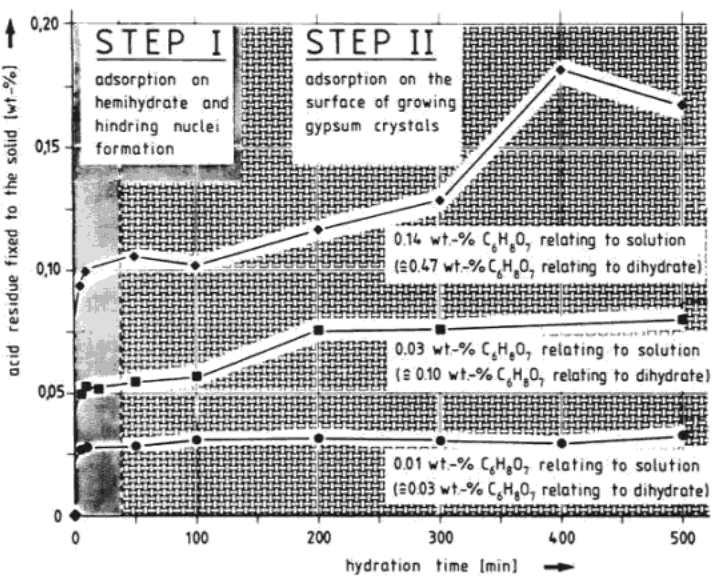

FIG. 1—*Stepwise fixation of citrates on the dehydrated calcium sulfate* (Step I) *and the nuclei or on the growing dihydrate crystals, respectively* (Step II).

and a partly more Step II type retardation with calcium carbonate as a Ca-ion donator.

The increase in the specific surface of the dehydrated calcium sulfates requires a higher amount of retarder addition. This fact is of greater interest with respect to the aging plasters.

In the present research work the addition of citric acid did not cause any change in the solubility of the hemihydrate. But with an equal water/gypsum ratio a decrease of the viscosity was observed with increased citric acid addition.

Influences on the Microstructure of Hardened Mortars

The retardation of the hydration of setting gypsum plasters greatly effects the microstructure of the hardened gypsum. In detail, increased citric additions caused the following alterations.

(1) a linear increase of the average grain size together with a decrease of the quantity of grains per volume unit,

(2) a broader grain size distribution,

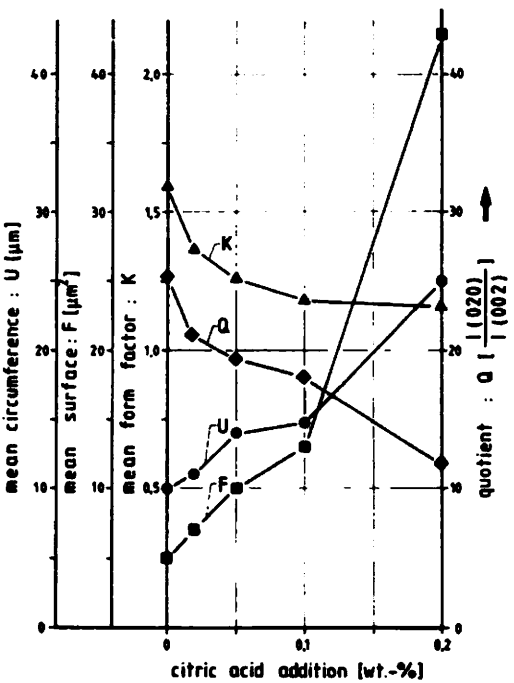

FIG. 2—*Grain structure parameter as a function of citric acid admixture (addition in weight % of hemihydrate).*

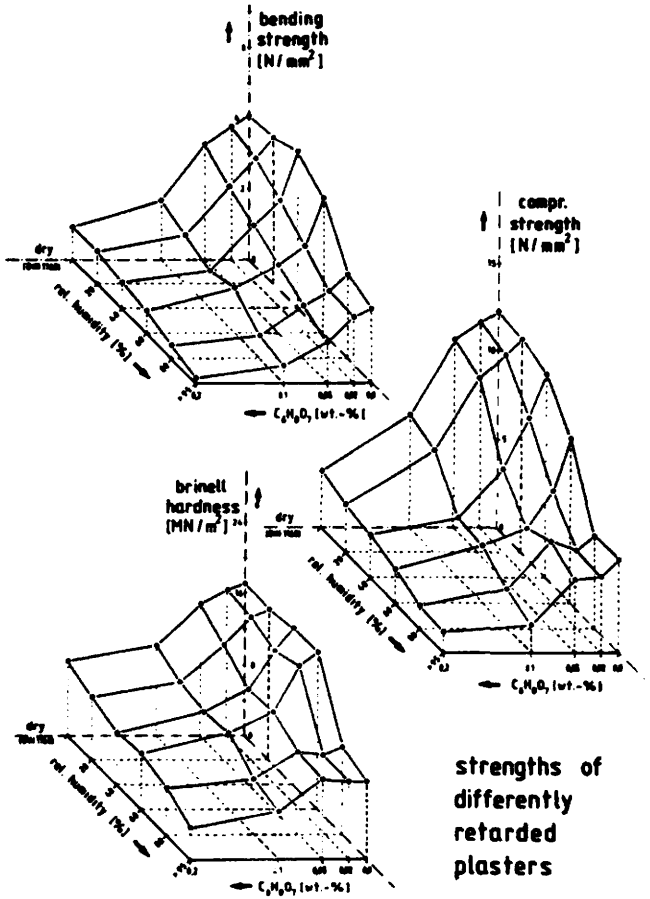

FIG. 3—*Strength formation as a function of citric acid admixture and relative humidity of hardened gypsum mortar.*

(3) a hyperbolic change of the grain shape from long prismatic to compact prismatic,

(4) an increased uniformity of the grain shape, and

(5) a development from sphaerolithic crystal growth to isolated crystals.

The alterations can be partly derived from Fig. 2. The figure shows the measured increase of the average circumferences U and areas F, and the decrease of the shape factor K and of the texture index Q above increased citric acid additions. More details of the experimental data are given elesewhere [2].

A further alteration of the microstructure is caused by the rate of citrate

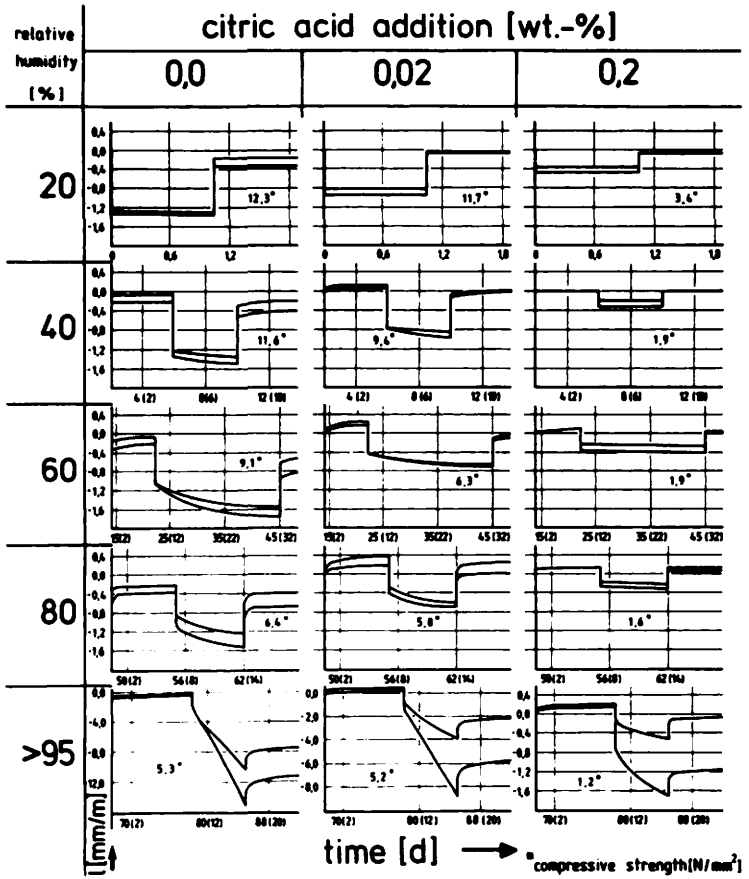

FIG. 4—*Deformation time diagram loaded 20% of the compressive strength at the given humidity (first number: total time of the creep measurement; and in parenthesis: time of a single test cycle).*

lower retardation rates no reduction in strength should occur. On the other hand citrate formed together with calcium hydroxide should also produce better strength.

Additional hardened gypsum was examined with regard to its creep behavior. Figure 4 shows the deformation time diagram of hemihydrate as a function of the citric acid addition and of the equilibrium humidity.

Without load the dihydrate shows an increased expansion with increased humidity. Maximum expansions are in the range of 1 mm/m. Unretarded and less retarded gypsum produced higher rates of expansion than highly retarded gypsum.

At 20% relative humidity the load dependent deformation is only an elastic one, which means the deformation is fully reversible in the deloaded state.

Increasing humidities, especially >80%, result in increasing plastic, that is, irreversible deformation.

Increased retardation produces increased amounts of elastic deformation.

Summary

Calcium-citrate formation and its absorption on the surface of the hemihydrate, on the nuclei and on the growing dihydrate crystals, is the cause of retardation. An increasing citric acid addition leads to an increased grain size and to changes of the shape factor towards one. This change in grain size and in the shape factor results, along with an elongated setting time in

(1) a higher plasticity of the fresh mortar,
(2) less volume expansion during setting,
(3) lower strength,
(4) lower rates of humidity absorption,
(5) lower rates of expansion caused by moisture adsorption, and
(6) lower rates of plastic creep deformation favoring the elastic creep.

But these changes in properties again can be altered by changing the amount and the rate of citrate formation.

Acknowledgment

We thank the Deutsche Forschungsgemeinschaft, Bonn-Bad Godesberg, for the financial support of our experimental works.

References

[1] Kuhlmann, J. and Ludwig, U., "Raumbeständigkeit von Baugipsen," *Zement-Kalk-Gips*, Vol. 30, No. 5, 1977, pp. 214–218.

[2] Koslowski, T., Zitronensäure—ein Verzögerer für Gips, Dissertation, Rheinisch Westfälisch Technische Hochschule, Aachen, West Germany, 1984.

Jean W. Pressler[1]

Byproduct Gypsum

REFERENCE: Pressler, J. W., "**Byproduct Gypsum,**" *The Chemistry and Technology of Gypsum, ASTM STP 861*, R. A. Kuntze, Ed., American Society for Testing and Materials, 1984, pp. 105–115.

ABSTRACT: The United States was the world's leading consumer of crude gypsum in 1982, with a demand of 16 million metric tons in the manufacturing of gypsum wallboard as a set retarder in cement, and some demand for its uses in agriculture. Only about 4% of this was byproduct gypsum sold for agricultural land plaster. Byproduct gypsum is the chemical end product of industrial processing plants, consisting primarily of calcium sulfate dihydrate, $CaSO_4 \cdot 2H_2O$. The oldest byproduct-gypsum-producing industry is that of the phosphate rock chemical processing in Florida. Large sludge ponds and retaining stockpiles are accumulating, and total tonnage may approach 1 billion metric tons by year 2000. The United States has no firm plans for recycling and utilization of this and other forms of byproduct gypsum. Environmental pressures because of solid pollution and the increasing cost of land may influence the United States to develop better utilization within the next ten years. Projected production of byproduct gypsum from coal burning power plant flue-gas desulfurization systems may be equal to the production tonnage of 30 million metric tons per year of phosphogypsum by 1990, thus adding more social and economic pressures for utilization.

Japan phased out natural gypsum production in 1976, and now is recycling 6 million metric tons per year of byproduct gypsum for wallboard, cement, and plaster. She is now leading the world in the technology of utilization of byproduct gypsum, with a balance established between supply and demand. European countries have active research and development projects but are still dumping many million tons per year into the sea.

It is suggested that the United States use more of the increasing tonnages of byproduct gypsum for its traditional uses of wallboard, plaster, and as a set retarder in cement. Other high-tonnage uses are offered, such as cellular gypsum, foamed gypsum for insulation, road construction, gateway supports in coal mines, and its potential as the largest sulfur resource in the world.

KEY WORDS: gypsum, flue gases, sludge disposal, byproduct gypsum, gypsum wallboard, set retarder, land plaster, phosphogypsum, sludge ponds, solid pollution, flue gas desulfurization systems, cellular gypsum, foamed gypsum, gateway supports, sulfur resource

Byproduct gypsum or chemical gypsum or both, synthetic gypsum, phosphogypsum, fluorogypsum, titanogypsum, desulfogypsum, and other names used in recent engineering and scientific literature are synonymous. It is suggested that the definition of byproduct gypsum is the chemical end product of industrial

[1] Physical scientist and commodity specialist, Bureau of Mines, Industrial Minerals Division, 2401 E St., N.W., Washington, DC 20241.

processing plants, consisting primarily of calcium sulfate dihydrate, $CaSO_4 \cdot 2H_2O$.

The U.S. Bureau of Mines first listed domestic byproduct gypsum (BPG) for use as agricultural land plaster in 1972, when three companies in California sold 253 000 metric tons, rising to 520 000 metric tons in 1972. Since that time, no significant change has occurred in the level of consumption or in the end use pattern, with annual shipments varying from 610 000 to 750 000 metric tons, and with California consuming approximately 65% of the total. In 1981, the following companies sold a total of 630 000 metric tons of BPG, valued at $6.6 million, for agricultural purposes: Occidental Petroleum Corp., Allied Chemical Corp., and J. R. Simplot Co., all in CA; Occidental Petroleum Corp., FL; Texasgulf, Inc., NC; and American Cyanamid Co., GA. These companies are mostly chemical processors of phosphate rock with sulfuric acid in the production of phosphoric acid, the first-step basic acid used in the production of superphosphates and multinutrient fertilizers. The one exception is American Cyanamid's titanium dioxide (from ilmenite) paint pigment plant in Savannah, GA. These plants, in the south Atlantic coast states and California, are all located in agricultural areas where the beneficial use of gypsum is recognized by the farmer. Stimulation of leguminous crops, especially peanuts, improvement of fertilizer utilization, softening of clayey soil, and neutralization of alkaline and saline soils are the major applications of gypsum in this area. BPG has had difficulty penetrating other traditional markets including wallboard and set-retarding of cement because of its fine chemical precipitated character and high moisture content, and because of the availability of cheap, high-quality, imported gypsum rock on both coasts. In inland market areas, abundant gypsum deposits are available for integrated mine-plant facilities.

U.S. Gypsum Supply and Demand

Domestic Production and Use

The United States was the world's leading producer of crude gypsum in 1982 with a production of 9.6 million metric tons valued at $89 million (Fig. 1); this accounted for 14% of the total world output. Production decreased 8% compared with that of 1981 and was the lowest since 1975. Leading states were Texas, Oklahoma, Iowa, and California, which together accounted for 52% of the total. Forty-four companies mined crude gypsum at 70 mines in 22 states, and 13 companies calcined gypsum at 69 plants in 29 states. Over 6.1 million metric tons of gypsum rock were imported from Canada, Mexico, and Spain, and only 110 000 metric tons were exported. Including stock changes, apparent consumption was 15.8 million metric tons, and net import reliance, as defined by imports minus exports plus industry stock changes, was 36%.

Of the total supply of crude gypsum, including 630 000 metric tons of BPG, 11.7 million metric tons was calcined for gypsum products, and 4.1 million metric tons was used mainly as a cement retarder or as agricultural land plaster. The calcined gypsum was sold as prefabricated products or as industrial or

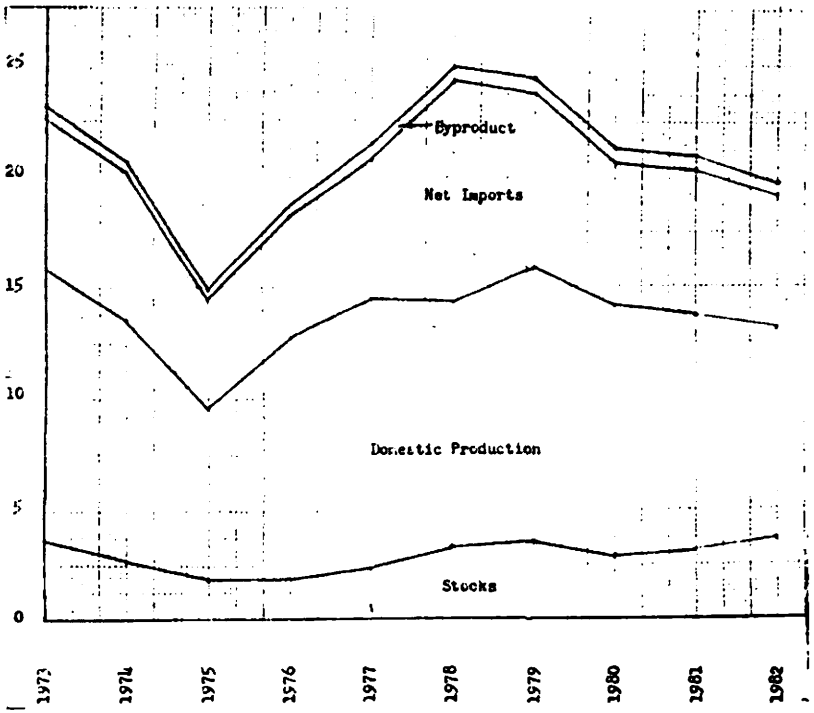

FIG. 1—*U.S. gypsum supply, million metric tons.*

building plaster. Sales of gypsum for use in cement totaled 2.8 million metric tons; for agriculture, 1.2 million metric tons; and for industrial and building plaster, 620 000 metric tons.

Byproduct Gypsum

From the preceding summary of the total gypsum supply-demand relationship in the United States, it is apparent that in the past BPG has played a very small part. However, some interesting technical trends in BPG utilization have been occurring in the United States.

1. American Cyanamid Co. and Lemco, Inc. came to an agreement in 1980 to process and sell BPG produced at Cyanamid's titanium dioxide plant in Savannah, GA. Lemco is building a plant to produce BPG briquets for use as a set retarder in the cement industry in the area.

2. Research-Cottrell, Inc., received a $24 million order from the Board of Water and Light Trustees of Muscatine, IA, for an air pollution control system

that will be the first in the United States to generate commercial-grade gypsum as a byproduct. The system will consist of an electrostatic precipitator and a flue-gas desulfurization (FGD) unit, to be installed on coal-fired 150-MW Unit 9 of Muscatine Power and Water. The double-loop limestone FGD system will treat emissions from the coal-fired system, using coal with a sulfur content of 2.5 to 3.2%. This system, through an oxidation process, will produce a commercial-quality gypsum byproduct suitable for use in building materials, such as wallboard, or for use in the cement industry.

3. In 1982, United States Gypsum Co.'s (USG) wallboard plant in Baltimore, MD, blended over 60 000 metric tons of BPG with its gypsum rock raw material feed. Although high free-moisture content (10 to 20%) and fine size of the BPG presented some problems in materials handling, very satisfactory wallboard was produced. U.S. Gypsum Co. (USG) plans to continue this BPG utilization to demonstrate how improved technology can be used to recycle a solid waste or sludge material.

4. Tampa Electric Co. is installing a limestone-based double loop FGD process in its new 475-MW Big Bend Unit #4 on Tampa Bay, near Ruskin, FL, scheduled for start-up in 1985. The power plant will burn a southern Illinois coal containing 3.5% sulfur and 0.2% chlorine. The project will use pulverized calcium carbonate in the scrubbers, followed by oxidation of the precipitate to gypsum, $CaSO_4 \cdot 2H_2O$. Production of this commercial-quality BPG will be 180 000 metric tons per year, enough to supply about 50% of the raw material required for a medium-size wallboard plant. The major specification problem involves the magnesium (from the calcium carbonate) and the chlorine (from the coal) concentrations in the BPG, which interfere with the physical characteristics of the finished wallboard. Magnesium inhibits crystal growth in the rehydration process, and soluble alkali sulfates and chlorides tend to burn the board at normal drying temperatures and corrodes metal edges and nails after installation.

By the 1985 start-up, Tampa Electric intends to meet the commercial specifications for wallboard use, as well as for briquets for local cement plants. Gypsum rock from Spain is presently imported by the local cement plants. Fully oxidized gypsum, 93+% $CaSO_4 \cdot 2H_2O$, low in chlorides and magnesia, will be produced.

Byproduct Gypsum in the United States

The earliest statistics (Table 1) available in the United States on BPG production, low grade or otherwise, were reflected by the amount of lime used in acid mine water neutralization, principally in Pennsylvania, West Virginia, and Ohio. Some was used in 1970, and lime for this purpose ranged from 40 000 to 73 000 metric tons per year for the next six years. The reaction of lime with effluent mine water produced BPG, which was dumped into the watersheds and river as runoff.

TABLE 2—*Byproduct gypsum produced in the United States (million metric tons).*

Kind	Quantity
Phosphogypsum	30
Fluorogypsum	2
Titanogypsum	1
FGD gypsum (desulfogypsum)	3
Other (from citric acid, boric acid, other organic acid production)	0.7
Total	36.7

adequate for the rest of this country, high-grade low-cost production of phosphate rock from central Florida is projected to decline. Because world and domestic demand for phosphate rock is expected to increase at an annual rate of 2.5% through 1990, additional supplies of domestic rock will be required. Some of Florida's loss in production may be offset by the state's eastern outer continental shelf and dolomitic phosphate rock resources, and from mines in North Carolina. Florida phosphogypsum production may be projected at a similar rate from 1982, indicating an awesome figure of 1 billion metric tons of phosphogypsum sludge stacked in tailings ponds by the year 2000. In addition, another 200 million metric tons will have accumulated in other areas of the United States. By that time, environmental pressures related to solid waste pollution and the high cost of land may force industry to recycle more of this material.

Desulfogypsum

In the United States, conventional lime-limestone FGD processes in coal-fired power plants, in place and projected, account for 88% of total FGD installations. In 1982, combined lime-limestone use for this purpose was approximately 2 million metric tons. If present technology continues, and projected coal-fired utility generating capacity of 450 000 MW is attained by 1990, about 100 million metric tons per year of varying throwaway compositions of byproduct gypsum sludge could be produced by that time. However, this is theoretical. It is probably more practical to consider only the present announced and committed FDG systems, about 30% of total projected coal-fired power plant capacity. This also assumes a conservative estimate of a 2% sulfur coal, and a 90% sulfur dioxide removal from the stack gases. The production rate of BPG by 1990 is projected to be substantially equal to the amount of phosphogypsum production 30 to 35 million metric tons per year, and it is possible that environmental pressures could force the power industry to recycle and utilize this potential commercial desulfogypsum (DGS), which would also provide some financial benefit to the utilities industry. Storage of the sludge will become more critical as the cost of land increases and the public concern for solid pollution intensifies, as occurred in Japan in the 1970s.

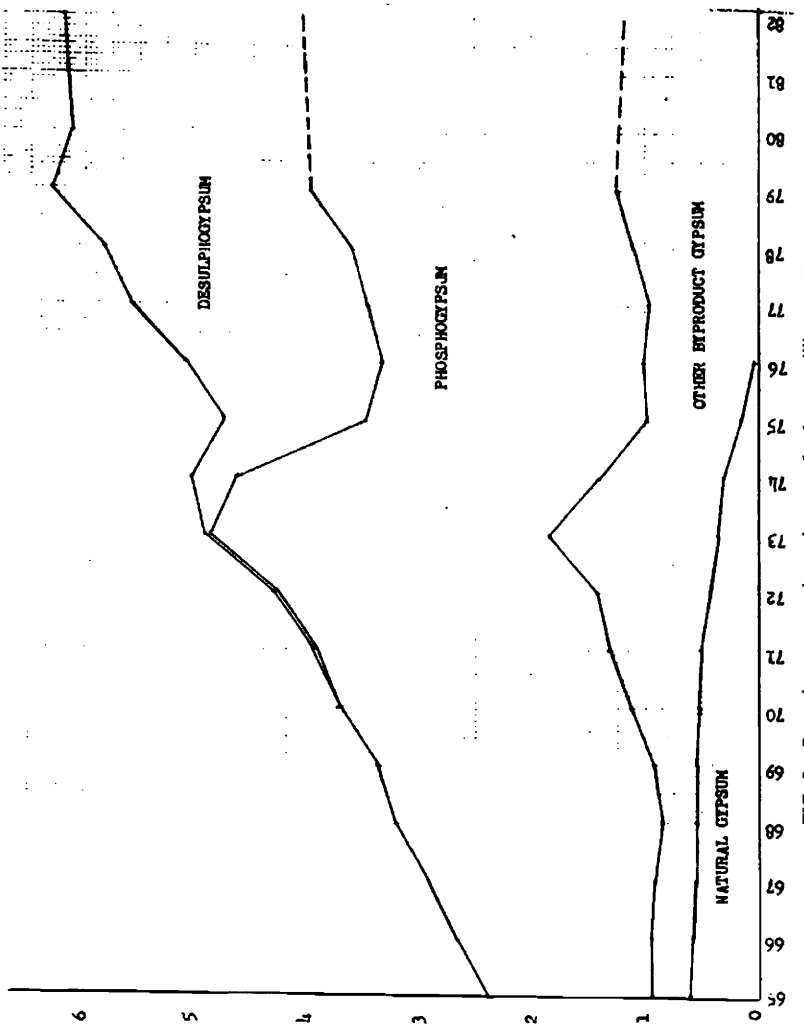

FIG. 2—*Byproduct gypsum demand pattern for Japan, million metric tons.*

Byproduct Gypsum in Japan

Japan produced 400 000 to 600 000 metric tons per year of natural gypsum through the 1960s to 1972, and by 1976 had completely phased out this production (Fig. 2). In place of natural gypsum, BPG came into demand, forced by environmental controls and import restrictions. The technology of utilization developed rapidly, and various types of BPG are now fully accepted for use in cement, wallboard, and plaster. Total demand for cement and wallboard increased at an average growth rate of 7% for the 15-year period ending in 1979, and it is expected to continue to increase at a rate of 5% through 1990 (Fig. 3). By 1981, total consumption was over 6 million metric tons, while supplies of BPG were continuing to increase at a rate slightly higher than 5%.

Linear regression analyses of statistics over the most recent 15-year period indicate growth rates for the following elements of BPG production: Phosphogypsum, 2.5%; desulfogypsum, 83%; titanogypsum, 11%; and fluorogypsum, 15%. It is interesting to note desulfogypsum's rapid growth rate since 1973. Annual production is now over 2.5 million metric tons and is equal to phos-

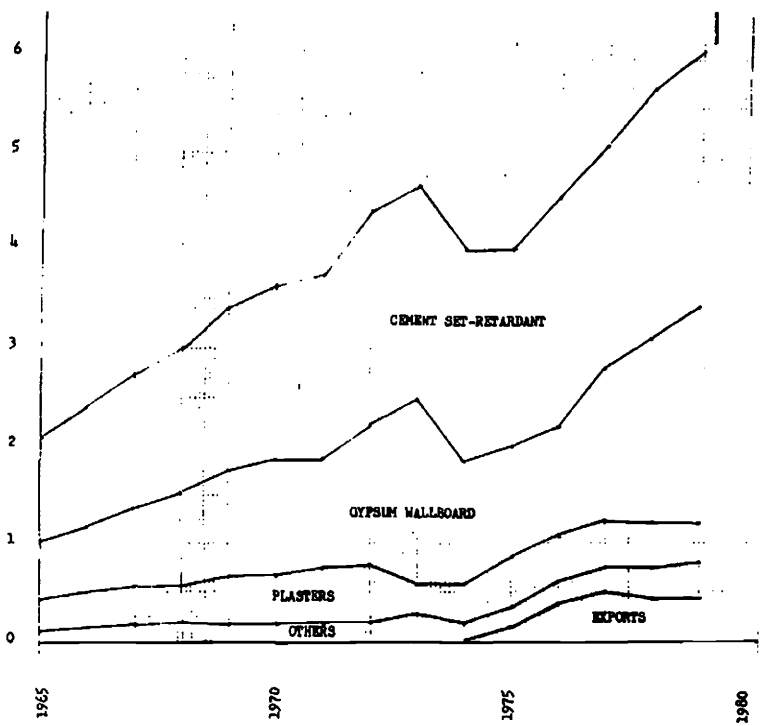

FIG. 3—*Apparent byproduct gypsum supply for Japan, million metric tons.*

prefabricated blocks. APC reported that these products can reduce the construction price for a single unit home by 20%.

The Pregypan (LAFARGE–National Gypsum) plant at Ottmarsheim was recently manufacturing 15 million square metres of premium wallboard per year from phosphogypsum. Using the Japanese NISSAN process for production of phosphoric acid, the phosphogypsum was recrystallized twice in a purifying procedure before being calcined for wallboard production.

It appears that France is somewhat ahead of other Western European countries in the efficient recycling of BPG; however, there is much more to be done to reduce the tonnage dumped into the sea.

Conclusion

It has been previously stated here that U.S. desulfogypsum production by 1990 might be as much as 30 to 35 million metric tons per year, about the same as phosphogypsum for the same year. Referring back to Fig. 2, there is a striking similarity to the projected U.S. BPG supply position in 1990, and Japan's comparable BPG supply relationship in 1982. Here the comparison stops because Japan is recycling substantially all of the BPG for the traditional uses as indicated in Fig. 3, and the United States has no firm plans to develop similar uses by 1990.

Because the total U.S. annual BPG production may be more than 60 million metric tons by 1990, and projected annual natural gypsum consumption may be about 30 million metric tons, it is apparent that the United States has a technical-economic problem regarding the disposal of BPG sludge, combined with impending social and environmental pressures to recycle this material for some economic benefit. It is suggested that U.S. construction materials offer the following high-tonnage possibilities:

1. Cellular Gypsum—France and the low countries (Belgium, Luxembourg, and the Netherlands) are experimenting with this use as previously mentioned. Construction blocks for floor and wall construction and partition blocks for interior use are in common use in North Africa, Mediterranean countries, and the Middle East.
2. Foamed Gypsum—General Electric Co. has a patent for this potentially large use of foamed gypsum for insulation, and a California company has a similar patent. However, only experimental testing has occurred. A West German patent was issued in 1981 to Hoechst AG.
3. Gypsum is the largest resource of sulfur in the world. Most processes for recovering sulfur from gypsum yield sulfuric acid, with a cement raw material high in lime as a coproduct. The Bureau of Mines has done considerable research in the past. Imperial Chemical Industries (ICI), Ltd., of the United Kingdom had operated a commercial plant for several years, but present economics are

unfavorable. Phosphate rock chemical plants might become interested in this sulfuric acid recycling process if the long-term shortfall of sulfur becomes critical. High-calcium tailings could possibly be sold to local cement plants.

4. Gypsum in Road Construction—As an activator in road sections treated with fly ash and lime, a composite of these materials has been used as base layers in France for over eight years. Experiments are being made to increase the amount of gypsum to more than 50%. As an activator in road sections consisting of granulated blast furnace slag and sand, considerable work is being done in France to apply this technique. The Bureau of Mines is experimenting with lime-fly ash-phosphogypsum aggregates as a possible alternative for natural aggregate in asphalt-concrete and in cement-concrete formulations.

5. Anhydrite-II, obtained by heating gypsum to 1000°C, hydrates rather rapidly and obtains high strength by use of accelerators such as potassium and ferrous sulfate. A growing use of this material is in construction of gate side packs in coal mines in Europe and England to give better gateway support with reduced maintenance. It is mixed with water and blown into position by compressed air. Its compressive strength is considerably higher than that of other competitive materials.

A selective bibliography is attached to this paper for those wishing to obtain more technical details.

Bibliography

Allen, M., "Conversion of Byproduct Gypsum to α-Hemihydrate by ICI's Process," *Phosphorus and Potassium*, No. 78, July/Aug. 1975, pp. 42–44.

Dickson, T., "Gypsum—Building from the Depths," *Industrial Minerals (London)*, No. 130, July 1978, pp. 17–31.

"Getting Rid of Phosphogypsum—I. Can Technology Provide the Answer to a Mountainous Waste Problem?" *Phosphorus and Potassium*, No. 87, Jan./Feb. 1977, pp. 37–39.

"Getting Rid of Phosphogypsum—II. Portland Cement and Sulfuric Acid," *Phosphorus and Potassium*, No. 89, May/June 1977, pp. 36–44.

"Getting Rid of Phosphogypsum—III. Conversion to Plaster and Plaster Products," *Phosphorus and Potassium*, No. 94, March/April 1978, pp. 24–39.

"Getting Rid of Phosphogypsum—IV. Uses in the Construction and Agriculture Industries," *Phosphorus and Potassium*, No. 96, July/Aug. 1978, pp. 30–38.

"MASAN: A Versatile New Building Material From Phosphogypsum," *Phosphorus and Potassium*, No. 85, Sept./Oct. 1976, pp. 44–48.

Martin, D. A., Brantley, F. E., and Yergensen, D. M., "Decomposition of Gypsum in a Fluidized-Bed Reactor," BuMines RI 6286, Washington, DC, 1963, 15 pp.

North, O. S., "Processes for Making Portland Cement From Gypsum," *Minerals Processing*, Vol. 10, No. 3, March 1969, pp. 12 14, 28.

Shifler, B. K. and Hove, M. W., "Processes for Recovering Sulfur from Secondary Source Materials," BuMines IC 8076, Washington, DC, 1962, 62 pp.

Alexander May[1] *and John W. Sweeney*[1]

Assessment of Environmental Impacts Associated with Phosphogypsum in Florida

REFERENCE: May, A. and Sweeney, J. W., "**Assessment of Environmental Impacts Associated with Phosphogypsum in Florida,**" *The Chemistry and Technology of Gypsum, ASTM STP 861*, R. A. Kuntze, Ed., American Society for Testing and Materials, 1984, pp. 116–139.

ABSTRACT: In its role to provide technology to prevent or limit adverse environmental impacts associated with mining or minerals processing, the U. S. Bureau of Mines has conducted research at its Tuscaloosa Research Center to assess the environmental impacts of phosphogypsum produced by the Florida phosphate industry. Over the years, stockpiles containing 304 million metric tons of phosphogypsum have accumulated, and the industry continues to generate an additional 30 million metric tons a year. Samples from approximately 300 m of drill core, obtained from nine stockpiles were characterized using chemical, X-ray diffraction, emission spectrographic, radiological, and physical means. The data developed indicated that phosphogypsum is not a corrosive or toxic hazardous waste as defined by the Environmental Protection Agency (EPA) criteria. Radium analyses averaged 21 pCi/g and its content was inversely related to particle sizes. Thirty-nine elements were detected in phosphogypsum; concentrations of these elements did not vary with depth within the stockpiles.

KEY WORDS: gypsum, phosphoric acid, radium, byproduct gypsum, phosphogypsum, hazardous waste, phosphate fertilizer production

In the past 20 years there has been a constant shift in the United States toward using multinutrient and mixed fertilizers in place of single-nutrient fertilizers. This trend has brought about the localization, especially in Florida and along the Gulf Coast, of large raw materials-oriented chemical companies manufacturing wet-process phosphoric acid, which is the basic material needed to produce high analysis multinutrient fertilizers. The manufacture of wet-process phosphoric acid results in the generation of large quantities of waste gypsum. In the fertilizer industry this is usually referred to as phosphogypsum, which distinguishes it from the natural gypsum mineral. As a rule, 5.5 metric tons of phosphogypsum are produced for each metric ton of phosphoric acid produced.

[1]Research chemist and supervisory mining engineer, respectively, U.S. Department of the Interior, Bureau of Mines, Tuscaloosa Research Center, P.O. Box L, University, AL 35486.

In 1978, U.S. production of crude natural gypsum was estimated at 13.5 million metric tons. Annual domestic gypsum consumption in 1978 was at 22.1 million metric tons [*1*], of which 635 000 metric tons were phosphogypsum.

By comparison, the Florida phosphate industry generates 30 million metric tons of phosphogypsum annually with only a small fraction (about 635 000 metric tons) used for agricultural purposes. In addition, there are 304 million metric tons of the material stacked on the ground in Florida. Projections indicate that by the year 2000, over 1 billion metric tons of this phosphogypsum will be available in Florida alone. Figure 1 shows the location of phosphogypsum stacks in Florida.

Phosphogypsum contains radium, and owing to the large tonnages in Florida, is of environmental concern. The Environmental Protection Agency (EPA) proposed in 1978 that phosphogypsum be identified as a potential hazardous waste. On 19 May 1980, the EPA issued its final regulations of toxic and hazardous wastes, but as of July 1981, have deferred regulation of phosphogypsum. A part of the Bureau's Minerals Environmental Technology research program is to assess these types of problems and develop a data base so that, through a continuing

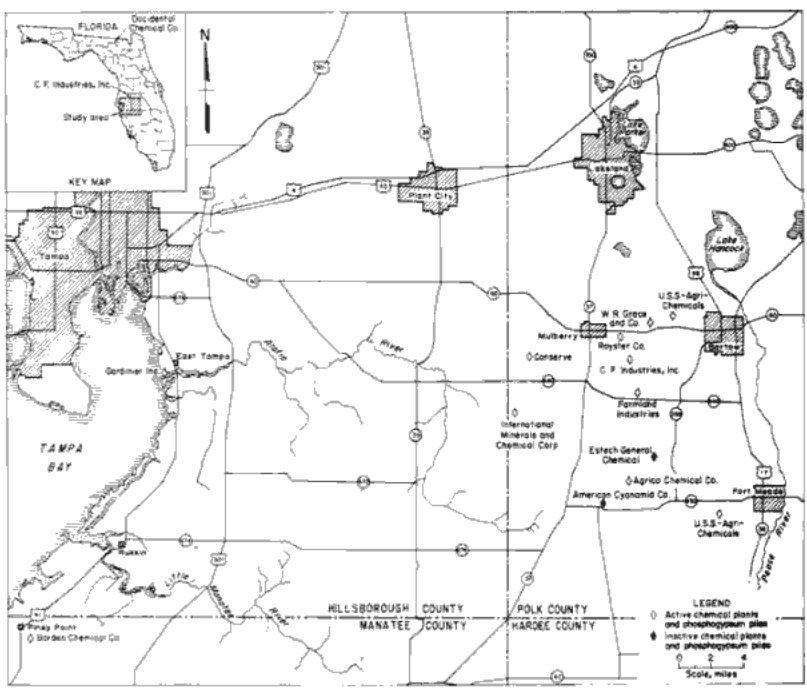

FIG. 1—*Location of phosphogypsum stacks in Florida.*

research effort, potential environmental problems can be mitigated. The Bureau's Tuscaloosa Research Center conducted research to characterize phosphogypsum to determine if it is hazardous or toxic, and if so, to investigate means to mitigate the situation so that the phosphogypsum could be used in a variety of high volume applications.

Criteria for Defining Hazardous/Toxic Waste

The EPA criteria defining hazardous and toxic waste were used as guidelines in this study. The EPA criterion for corrosivity is a pH equal to or less than 2 or equal to or greater than 12.5 [2]. The EPA criterion for toxicity of wastes is based on an extraction procedure to identify toxic wastes likely to leach into the groundwater. The hazardous nature of the waste is judged by the concentrations of specific contaminants in the extract. The contaminants listed by the EPA for toxic consideration are eight metals and six chlorinated organic compounds [2]. There are no probable sources of chlorinated organic compounds in the phosphogypsum or its precursor reactants. Therefore organic compounds were not investigated in this study. The Bureau of Mines considered the total concentrations of trace elements in phosphogypsum, rather than consider only the toxicity caused by leachable elements. Thus, emission spectrographic analyses of the gypsum solids were used to determine trace elements, both toxic and nontoxic. These analyses were correlated with the EPA leaching tests criteria, and also provide information for the assessment of the gypsum under all conditions.

The EPA regulations, proposed 18 Dec. 1978, for the identification of hazardous wastes listed phosphogypsum as a hazardous waste because it was radioactive. To be excluded from the list, the average radium-226 concentration would have to be less than 5 pCi/g of solid waste, or the total quantity of radium-226 would have to be less than 10 μCi for any single discrete source [3]. The final EPA regulations, issued 19 May 1980, still list phosphogypsum as a hazardous waste but defer development of final regulation for phosphogypsum pending congressional action [2].

Phosphogypsum Production

Phosphogypsum is the major byproduct of wet-process phosphoric acid production. Phosphate rock, which is composed of apatite minerals [4], (calcium phosphates containing varying amounts of carbonate and fluoride), is digested with sulfuric acid and water to produce phosphoric acid, phosphogypsum, and minor quantities of hydrofluoric acid.

The reaction of the phosphate rock to produce gypsum, $CaSO_4 \cdot 2H_2O$, may be illustrated by Eq 1

$$Ca_{10}(PO_4)_6F_2 + 10\ H_2SO_4 + 20\ H_2O \rightarrow 10\ CaSO_4 \cdot 2\ H_2O + 6\ H_3PO_4 + 2HF \quad (1)$$

Gypsum forms monoclinic crystals that are tabular and diamond-shaped. Both habits are shown in Fig. 2.

In the Prayon process, commonly used in Florida, the phosphate rock, ground to pass a 150-μm (100-mesh) sieve, is treated with 30 to 46% phosphoric acid and 55 to 60% sulfuric acid. The rock and acid is circulated through reaction tanks to maintain the optimum time and temperature for the reaction and growth of phosphogypsum crystals. The phosphogypsum is filtered, washed with water, and pumped as a slurry to ponds from which the phosphogypsum settles to form the phosphogypsum stacks [5].

The hemihydrate process is similar to the Prayon process but uses higher temperatures and acid concentrations in the reaction tanks. This favors the initial formation of hemihydrate. In subsequent crystallization tanks the hemihydrate is mixed with gypsum suspensions where it recrystallizes as large crystals of the dihydrate, that is, as phosphogypsum.

Figure 3 is an aerial view of a typical active phosphogypsum stack.

Inventory of Phosphogypsum

Seventeen phosphogypsum stacks were identified in Florida. Data regarding the inventory were obtained through the cooperation of the Florida Institute of Phosphate Research and 13 phosphoric acid producing companies. The data

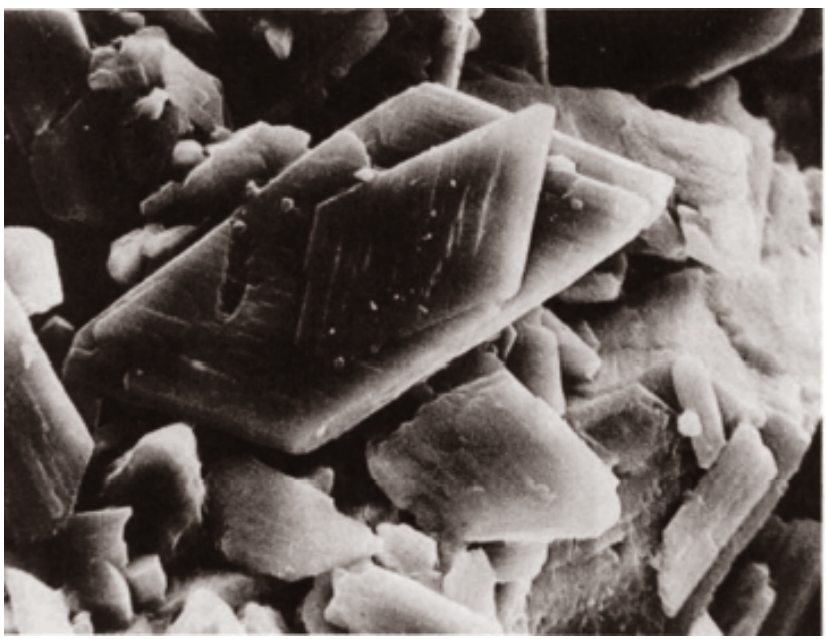

FIG. 2—*Scanning electron microphotograph of phosphogypsum (X1000).*

FIG. 3—*Typical view of a phosphogypsum stack in Florida.*

TABLE I—*Phosphogypsum inventory.*

Gypsum Stack Identification	Year Began	Year Discontinued	Years in Service	Hectare[a]	Annual Production, thousand metric tons per year	Cumulative Total, thousand metric tons
A	1965	active	15	101	2 180	20 000
B	1947	active	33	121	2 720	69 900
C	1956	1971	15	50	inactive	17 100
D	1963	active	17	138	3 360	39 100
E	1948	1980	32	20	inactive	11 000
F	1948	1968	20	40	inactive	4 500
G	1966	active	14	115	3 180	19 300
H	1964	active	15	146	1 000	15 000
I	1975	active	5	121	4 990	15 700
J	1976	1980	4	34	inactive	1 400
K	1961	active	19	81	3 180	16 600
L	1954	1963	9	101	inactive	3 600
M	1973	active	7	24	1 180	5 300
N	1965	active	15	162	2 740	20 600
O	1955	active	25	36	680	5 300
P	1954	active	26	214	4 170	29 200
Q	1965	active	15	57	820	10 000
Total	. . .	. . .	285	1 561	30 200	303 600

[a]1 hectare = 10 km^2.

One chemical analysis was made of each of the 13 core samples and one X-ray diffraction analysis was made of three of the core samples to provide the major chemical and mineralogical components of the stacks.

One spectrographic, pH, and radium-226 analysis was made on each core sample, interval sample, and sized sample to provide minor elements, acidity, and radioactivity data. The analyses indicated differences among the stacks, differences from top to bottom and across the stacks, and differences caused by particle size distributions.

The three core samples obtained from Stack A, their interval samples and sized samples, were analyzed quantitatively for trace quantities of uranium and thorium. The three core samples were also analyzed for radium, uranium, and thorium isotopes. These data were used to indicate the radioactive elements present and their relationships to each other within the stack.

Thirteen core samples were obtained from approximately 300 m of phosphogypsum core. Approximately 800 analyses and tests were performed to yield nearly 2400 individual data points.

Test Procedures

To establish the free water content, samples were dried at room temperature to constant weight and then at 45°C for an additional 2 h. The dried samples were then analyzed for chemical, radiological, and trace elements. The pH measured was that of moist phosphogypsum. Water was added to phosphogypsum to produce very thick slurries into which the pH and standard electrodes were immersed and measurements taken. Except for pH and densities, the chemical and radiological results were then calculated back to the weight basis of the samples as received. The particle size distribution was determined on the dried samples. Emission spectrographic results were reported on the basis of the dried samples.

Chemical analyses were performed in accordance with ASTM Chemical Analysis of Gypsum and Gypsum Products (C 471). Fluoride and phosphorus were determined by the Association of Florida Phosphate Chemists Methods [7]. Uranium was determined by ASTM Tests for Microquantities of Uranium in Water by Fluorometry (D 2907), and thorium was determined by ASTM Test Method for Thorium in Water and Waste Water (D 2333). Radium was determined by the radon emanation method [8], and uranium and thorium isotopes were determined by a chromatographic and radiological technique developed by the EPA.

Test Results

Tables 2 and 3 present the chemical analyses data. Table 4 shows the free water, and Table 5 shows the pH for increment samples. Table 6 gives size distribution data. Tables 7 through 10 address radium, uranium, and thorium results, and Table 11 lists emission spectrographic analyses.

TABLE 2—*Chemical analyses[a] of core samples of phosphogypsum. major components.*

Core Number	Depth of Core, *m*	Samples as Received, weight %					
		Free Water	Combined Water	SiO_2 and HCl Insolubles	Al_2O_3 and Fe_2O_3[b]	CaO[c]	SO_3
A1	21	16.3	15.78	3.46	3.31	24.51	37.30
A2	21	17.2	15.55	4.92	3.48	23.69	36.92
A3	21	18.7	14.66	4.86	3.56	23.15	35.62
B1	30	14.9	13.53	5.34	4.27	22.60	35.30
B2	30	14.8	12.74	13.67	2.49	20.82	31.71
C1	15	16.7	15.24	4.76	3.29	24.44	38.31
C2	24	15.1	9.70	34.15	7.51	14.04	23.48
D	21	14.1	12.02	11.01	6.31	18.66	28.55
E	27	20.7	14.29	6.66	3.41	22.47	35.64
F	9	17.6	15.73	4.48	4.38	23.32	36.17
G	18	18.9	13.19	9.57	4.07	19.22	30.54
H	24	17.2	14.18	8.99	3.74	22.26	34.58
I	9	16.0	10.72	12.90	7.48	15.61	27.55
Average	21	16.8	13.64	9.60	4.41	21.14	33.21

[a]Analyzed by ASTM C 471, Parts 5 through 13 Methods.
[b]Material soluble in hydrochloric acid and insoluble in ammonium hydroxide.
[c]Material soluble in hydrochloric acid, soluble in ammonium hydroxide, and insoluble in oxylate solution = calcium oxide in phosphogypsum.

TABLE 5—*pH of 3-m interval samples of phosphogypsum.*

Depth Interval, m	Sample as Received, weight %													Depth Average, pH
	A1	A2	A3	B1	B2	C1	C2	D	E	F	G	H	I	
0– 3	2.15	2.45	2.45	2.85	3.25	4.35	3.80	2.85	2.55	3.70	2.80	2.65	2.75	2.97
3– 6	2.15	2.35	2.45	2.80	3.40	3.85	3.60	2.75	2.40	3.75	2.90	2.60	2.40	2.88
6– 9	2.25	2.40	2.50	2.95	3.15	2.80	3.85	2.80	2.40	3.50	2.90	2.40	2.65	2.81
9–12	2.10	2.40	2.50	2.60	3.05	2.60	3.40	2.45	2.60	NAp	2.35	2.60	NAp	2.60
12–15	2.20	2.40	2.35	2.80	3.05	2.60	3.65	2.55	2.60	NAp	2.70	2.50	NAp	2.67
15–18	2.20	2.50	2.40	2.75	3.05	NAp	4.40	2.50	2.60	NAp	2.50	2.65	NAp	2.75
18–21	2.25	2.55	2.50	2.80	2.95	NAp	5.15	2.60	2.40	NAp	NAp	3.20	NAp	2.93
21–24	NAp[a]	NAp	NAp	2.70	2.95	NAp	5.50	NAp	2.40	NAp	NAp	4.00	NAp	3.51
24–27	NAp	NAp	NAp	2.80	3.10	NAp	NAp	NAp	2.50	NAp	NAp	NAp	NAp	2.80
27–30	NAp	NAp	NAp	3.00	3.20	NAp	NAp	NAp	NAp	NAp	NAp	NAp	NAp	3.10
Core average	2.19	2.44	2.45	2.80	3.11	3.24	4.17	2.64	2.49	3.65	2.69	2.82	2.60	2.85[b]

[a]NAp = not applicable, no sample.
[b]Grand average, all data.

TABLE 6—*Particle size distribution of sized samples of phosphogypsum.*[a]

Sieve Opening, mm	Sample						
	A1	A2	A3	B1	B2	C2	G
Coarse							
plus 0.710	4.6	10.4	6.6	2.0	1.9	7.2	4.6
minus 0.710 plus 0.500	3.6	9.1	5.3	4.6	5.1	7.5	4.5
minus 0.500 plus 0.250	6.4	12.0	9.1	15.1	35.8	20.1	11.9
total	14.6	31.5	21.0	21.7	42.8	34.8	21.0
Medium							
minus 0.250 plus 0.180	3.6	4.2	5.0	11.9	27.6	8.3	7.8
minus 0.180 plus 0.125	4.9	9.8	6.3	13.0	12.9	25.5	8.9
minus 0.125 plus 0.063	15.6	11.8	15.6	24.2	11.5	12.5	24.9
minus 0.063 plus 0.045	12.0	13.1	13.9	11.0	3.0	8.0	6.7
total	36.1	38.9	40.8	60.1	55.0	54.3	48.3
Fine: minus 0.045	49.3	29.6	38.2	18.2	2.2	10.9	30.7
Cumulative							
plus 0.170	4.6	10.4	6.6	2.0	1.9	7.2	4.6
plus 0.500	8.2	19.5	11.9	6.6	7.0	14.7	9.1
plus 0.250	14.6	31.5	21.0	21.7	42.8	34.8	21.0
plus 0.180	18.2	35.7	26.0	33.6	70.4	43.1	28.8
plus 0.125	23.1	45.5	32.3	46.6	83.3	68.8	37.7
plus 0.063	38.7	57.3	47.9	70.8	94.8	81.1	62.6
plus 0.045	50.7	70.4	61.8	81.8	97.8	89.1	69.3

[a]Dried to constant weight at 45°C.

TABLE 7—*Uranium (U), thorium (Th), and radium (Ra) analyses of sized samples of phosphogypsum, pCi/g.*

Core Number and Size of Sample	U[a]	Th[b]	Ra[c]
Core A1			
coarse[d]	4.3	NA[k]	23
medium[e]	3.4	NA	21
fine[f]	4.3	3.8	27
average[g]	4.0	NA	24
Core A2			
coarse	8.4	NA	19
medium	3.6	NA	22
fine	3.4	NA	30
average	5.0	NA	23
Core A3			
coarse	4.4	3.7	23
medium	4.7	NA	15
fine	6.1	NA	24
average	5.2	NA	20
Core B1			
coarse	5.8	3.9	20
medium	8.7	11.6	26
fine	5.8	3.9	26
average	7.5	8.5	25
Core B2			
coarse	9.5	3.9	15
medium	6.0	3.9	21
fine	6.0	NA	22
average	7.5	NA	18
Core C2			
coarse	5.4	27.0	21
medium	20.7	7.7	16
fine	9.5	NA	30
average	14.2	NA	19
Core G			
coarse	4.7	14.7	8.9
medium	2.5	25.8	6.7
fine	2.5	7.4	10.5
average	3.0	17.8	8.3

[a]Analyses by ASTM D 2907 fluorometric method.
[b]Analyses by ASTM D 2333 colorimetric method.
[c]Analyses by radon emanation method.
[d]Plus 0.250 mm.
[e]Minus 0.250 plus 0.045 mm.
[f]Minus 0.045 mm.
[g]Averages are weighted based on amount in each fraction, in percent, and the amount of the elements in each sample, in picocuries per gram.
[k]NA = not available.

TABLE 8—*Radiological isotopic analyses of core samples of phosphogypsum, pCi/g.*

Isotope	Core		
	A1	A2	A3
Radium	16.10	13.50	13.30
Uranium-234	2.14	1.47	2.44
Uranium-235	0.17	0.13	0.15
Uranium-238	2.13	1.61	2.41
Thorium-227	0.61	0.47	0.59
Thorium-228	0.03	0.03	0.06
Thorium-230	3.30	1.95	3.91
Thorium-232	0.13	0.07	0.11

The X-ray diffraction analyses were performed on core Samples A1, B1, and F. All gave the same results. Only gypsum and alpha-quartz were detected. The limit of detection was about 5% of a mineral present. Fluorides and phosphates were present, as well as compounds of aluminum, magnesium, iron, and other elements. However, these compounds were present at less than 5% and were not detected by the X-ray diffraction.

Discussion

The chemical analyses given in Tables 2 and 3 lists quantities of the major components of phosphogypsum. The analyses in Table 2 and that of sodium chloride in Table 3 were performed by ASTM C 471. Although standard analytical methods were used, phosphogypsum differs sufficiently from gypsum to require scrutiny of the results. In the standard gypsum analysis, iron and aluminum are determined by removing silicon and acid insoluble material and then precipitating the iron and aluminum as hydroxides. The hydroxides are ignited to form oxides, and the iron and aluminum oxides are then weighed. However, phosphogypsum contains phosphates and fluorides that accompany iron and aluminum hydroxides in their analytical determination. These precipitate as calcium phosphates and calcium fluoride. Titanium oxide may also contaminate the iron and aluminum hydroxides. The results for "iron and aluminum oxides," as designated in the ASTM method were thus higher than the actual quantity of iron and aluminum oxides present. Calcium is determined in the filtrate remaining after removing the silicon, acid insoluble material, iron, aluminum, and calcium phosphates, and fluorides. The calcium content determined in this manner represented that which was present in the phosphogypsum. The other analyses were not affected.

A typical phosphogypsum composition is shown in Table 12. The results in Table 12 were from the analyses of the core samples, excluding Samples C2, D, and I. The core for Sample C2 was taken from part of a phosphogypsum stack that had been placed in a phosphate rock mined-out area. The base of

TABLE 9—*Radium analyses of 3-m interval samples of phosphogypsum, pCi/g.*

Depth Interval, m	Sample as Received, weight %													Depth Average, pH
	A1	A2	A3	B1	B2	C1	C2	D	E	F	G	H	I	
0– 3	19	26	28	13	20	19	21	22	18	37	8.9	17	24	21.0
3– 6	25	26	21	18	16	24	26	24	20	45	8.8	20	30	23.4
6– 9	23	27	18	15	17	20	20	34	24	44	9.7	16	23	22.4
9–12	18	19	17	20	20	22	18	22	21	NAp	11.2	24	NAp	19.3
12–15	23	18	16	15	16	25	10	34	26	NAp	8.9	27	NAp	19.9
15–18	19	24	18	19	18	NAp[a]	12	26	20	NAp	10.3	26	NAp	19.2
18–21	18	24	16	24	16	NAp	17	33	24	NAp	NAp	24	NAp	21.8
21–24	NAp	NAp	NAp	14	21	NAp	0.9[b]	NAp	21	NAp	NAp	11	NAp	16.8
24–27	NAp	NAp	NAp	25	19	NAp	NAp	NAp	15	NAp	NAp	NAp	NAp	19.7
27–30	NAp	NAp	NAp	24	24	NAp	NAp	NAp	NAp	NAp	NAp	NAp	NAp	24.0
Core average	20.7	23.4	19.1	18.7	18.7	22.0	17.7	27.9	21.0	42.0	9.6	20.6	25.7	20.91[c]

[a]NAp = *not applicable, no sample obtained.*
[b]Not included in averages.
[c]Grand average, all data.

TABLE 10—*Uranium (U) and thorium (Th) analyses of 3-m interval samples of phosphogypsum, pCi/g.*

	Sample								Depth Average	
	A1		A2		A3		G			
Depth Interval, m	U	Th	U	Th	U	Th	U	Th	U	Th
6– 9	4.0	NA	3.1	NA	4.1	3.7	2.4	14.7	3.4	NA
9–12	4.0	NA	2.9	NA	3.7	NA	3.2	14.7	3.5	NA
12–15	3.7	3.8	3.1	3.7	5.0	3.7	3.9	25.8	3.9	9.2
15–18	4.8	NA	3.1	NA	5.1	3.7	2.3	18.4	3.8	NA
18–21	4.3	NA	3.1	NA	5.9	7.4	NAp	NAp	4.4	NA
Core average	4.2	NA	3.1	NA	4.8	NA	3.0	18.4	3.8	NA

NA—not available because thorium was detected in amounts too small for quantitative results. NAp—not applicable, no sample obtained.

TABLE 11—*Emission spectrographic analyses of phosphogypsum.*

Element Detected	Average, μg/g[a]	Number Detected in	
		Cores	Samples
Aluminum	1 400	13	110
Antimony	100	2	10
Arsenic	40	7	37
Barium	7	2	8
Bismuth	1	2	6
Boron	3	8	37
Beryllium	1	1	1
Cadmium	7	1	1
Cobalt	2	7	33
Copper	8	13	106
Iron	670	13	110
Lead	1	6	6
Magnesium	1 200	13	110
Manganese	15	13	72
Molybdenum	16	3	13
Nickel	2	11	57
Platinum	<1	2	5
Potassium	11	9	56
Rhenium	11	6	23
Silver	<1	4	6
Sodium	250	13	91
Strontium	10	11	79
Tantalum	2	2	5
Tin	4	5	13
Titanium	4 000	13	110
Tungsten	30	3	9
Vanadium	19	13	110
Yttrium	2	3	9
Zinc	9	10	50
Zirconium	10	8	12

[a]Average in cores in which element detected, from analyses of core samples, sized samples, and interval samples.

phosphate mine pits are uneven in elevation and contain overburden spoil. The unusual results for Sample C2 were checked with three different composite samples. Also, the C2 interval from 3 to 6 m and that from 21 to 24 m were analyzed petrographically. These analyses showed that the greater depth had high silica and low gypsum and at shallower depth content was reversed. Results for C2, namely, high silica, iron, aluminum, phosphorus, uranium, and pH, and low calcium, sulfur and combined water, plus petrographic analyses, indicated that the core penetrated overburden spoil. Sample D was from a stack placed below ground level and Sample I from a new stack. The analytical evidence indicates C2, D, and I results were not completely typical of phosphogypsum because of possible contamination by overburden at the gypsum-ground interface.

The bulk densities shown in Table 3 indicated that no significant difference existed between the stacks in compaction of the phosphogypsum. The pH and

TABLE 12—*Typical composition of phosphogypsum from Florida.*[a]

Component	Average	Low	High
Composition of sample, as received, weight %			
moisture	17.30	14.8	20.7
combined water	14.49	12.7	15.8
silicon dioxide and acid insoluble	6.67	3.5	9.6
acid soluble, NH_4OH insoluble	3.60	3.3	4.4
calcium oxide	22.65	19.2	24.5
sulfur trioxide	35.21	30.5	38.3
sodium chloride	0.01	0.01	0.03
sum	99.93	NAp[c]	NAp
HCl soluble, NH_4OH insoluble fraction, weight %			
phosphorus pentoxide	0.61	0.32	0.83
fluorine	0.68	0.38	1.81
aluminum oxide[b]	0.29	0.00	0.50
ferric oxide[b]	0.10	0.00	1.00
titanium dioxide[b]	0.63	0.00	1.00
calcium oxide equivalent of P_2O_5 and F[c]	1.24	0.69	3.00
sum	3.55	1.39	8.14
Density, g/mL	1.51	1.32	1.69
pH	2.57	2.10	3.35
Radium, pCi/g	20.2	8.00	38.00
Gypsum[d]	69.23	60.67	75.48

[a]Calculated quantities from data for Sample A1, A2, A3, B1, B2, C1, E, F, G, and H.
[b]Aluminum, iron, and titanium analyses from emission spectrographic results.
[c]As calcium dihydrogen phosphate and calcium fluoride.
[d]Calculated from percent combined water. For the average, this gives 0.10% calcium oxide and 3.02% sulfur trioxide not in gypsum.
[e]NAp = not applicable.

radium results in Table 3 were those of the core samples. Discussion of pH and radium follows in conjunction with Tables 5 and 9.

Free water, shown in Table 4, represented moisture not bound as water of crystallization. No pattern for the seepage of water through the stacks was apparent from the data. The maximum free water content for each core occurred at depth intervals from 3 to 27 m, but also the minimum occurred at depth intervals from 0 to 27 m. The wettest and driest depth intervals even occurred adjacent to each other. For example, in Core B1, the 18 to 21 m interval was the wettest and the 21 to 24 m interval the driest. In Core B1 the first sample was like mud; the second was like rock. Analysis of variance (ANOVA) of the data showed there was no significant difference in free water among depths and there was a significant difference among cores.

The pH values, shown in Table 5, were all greater than 2.0 and less than 12.5. Every individual pH measurement on all 3-m interval samples and the core samples given in Table 3 were also greater than 2.0 and less than 12.5. This is significant because the EPA defined a hazardous waste by the criterion of corrosivity as one that had a pH equal to or less than 2 or equal to or greater than 12.5. Therefore, all phosphogypsum samples obtained in this investigation were not hazardous wastes by the EPA criterion of corrosivity.

Analysis of variance of the pH data showed that differences among cores and among depths were significant. This was also found when the atypical samples C2, D, and I were excluded. However, when ANOVA was applied to Samples A1, A2, A3 and also separately to B1 and B2, no significant difference was found in pH with depth or with cores. The highest pH values were for Samples C1, C2, and F. All of these are from inactive stacks, the C stack being inactive nine years and the F stack inactive twelve years. The pH values, 4.40, 5.15, and 5.50 for C2 may be due to this core penetrating overburden spoil, as previously mentioned. Excluding these high C2 pH values, the remaining pH values for C2 averaged 3.66, which is still the highest pH value of the cores. The higher pH values for these inactive stacks indicate rainwater may leach hydrogen ions and thus lower the acidity of the stacks.

Particle size distribution is shown in Table 6. Three size distributions were used for uranium, thorium, radium and emission spectrographic analyses. These were the total coarse size (retained on 0.25-mm sieve), total medium size (passes 0.25-mm sieve, retained on 0.045-mm sieve), and fine size (passes 0.045-mm sieve). The coarse, medium, and fine fractions are also convenient summaries of the data. The cumulative percent distribution is a linear function of the logarithm of the sieve opening.

Uranium, thorium, and radium analyses of sized samples are shown in Table 7. The uranium and thorium analyses were for total uranium and total thorium, and the original data were measured in micrograms per gram, μg/g. The micrograms per gram uranium was multiplied by 0.6781 and the micrograms per gram thorium by 4.5423 to convert them to picocuries per gram for comparison to radium data. The factors used in the conversions were based on assuming the natural isotopic abundance of uranium and thorium isotopes. About half of the thorium data were reported as "less than 1 μg/g." Since these data could not be accurately analyzed, they were included in Tables 7 and 10 as not available (NA).

The average concentrations of uranium and radium for the coarse, medium, and fine fractions are shown in Table 13. Radium was most concentrated in the fine fraction, and ANOVA verified that a significant difference existed among the sizes. The results in Table 13 also indicated differences in uranium concentrations with size fractions. However, ANOVA indicates these differences are not significant. Insufficient data were available to statistically analyze thorium data.

Table 8 shows the isotopic analyses of radium, uranium, and thorium in three samples. These results indicated that uranium-238, uranium-234, and thorium-230 were about in equilibrium. Radium was not in equilibrium and was more concentrated in the phosphogypsum than the radiological equilibrium with thorium-230 would allow.

Table 9 shows the analyses of the 3-m interval samples for radium. The average of these data and comparison with the composite samples averages are shown in Table 14.

The EPA proposed regulations of 18 Dec. 1978, stated that 5-pCi radium/g

TABLE 13—*Average uranium (U) and radium (Ra) contents of sized samples of phosphogypsum, pCi/g.*

Size	Samples	
	U	Ra
Coarse[a]	6	19
Medium[b]	7	18
Fine[c]	5	24

[a]Plus 0.250 mm.
[b]Minus 0.250 plus 0.045 mm.
[c]Minus 0.045 mm.

or greater would cause a waste to be a hazardous waste because of radioactivity [3]. However, on 19 May 1980, the EPA deferred radiation limits on phosphogypsum [2], so at this time it cannot be stated that the phosphogypsum was a radiation hazard based on EPA criteria.

Sample G was low in radium compared to the other phosphogypsum stacks. This low content occurred because the phosphate rock that produced the phosphogypsum in Stack G contained about one-third uranium and radium that the phosphate rock that produced the phosphogypsum in the other stacks contained. Sample F is higher in radium than the other samples. We do not know, at this time, why this occurs.

ANOVA calculations were performed on the data in Table 9. Using all of the data, the ANOVA showed, among cores, a significant difference in radium content at the 99% confidence level, and showed that the difference in radium content was not significant with depth. The same was found when Samples C2, D, and I were excluded. When Samples A1, A2, and A3 were examined, no significant differences were indicated among samples or among depths. The same was true with Samples B1 and B2. This statistical analysis indicated that radium is uniformly distributed in each stack.

Table 10 shows uranium and thorium analyses of 3-m interval samples. Analysis of the data indicated that uranium is also uniformly distributed in each stack. Thorium data were insufficient for an accurate statistical analysis.

TABLE 14—*Average radium concentrations of phosphogypsum samples, pCi/g.*

Samples	Average
Composite	20.4
3-m interval	20.9
Composite (excluding C2, D, and I	20.2
3-m interval (excluding C2, D, and I)	20.3
All data: core, 3-m interval, and sized	20.5

Emission spectrographic analyses were performed on 13 core samples, on 90 3-m interval samples, and on 7 sized samples. This yielded 1780 individual analytical results for semiquantitative concentrations of 30 elements. These results are summarized in Table 11.

The averages shown in Table 11 were the sums of all concentrations detected for a given element divided by the total number of analyses of the cores in which the element was detected. Thus the data summarized concentrations only in cores where elements were detected. For example, 57 analyses of nickel in 11 cores averaged 2 μg/g of nickel. Two cores contained no nickel, but these zero values were not included in calculating the 2-μg/g average.

In addition to the emission spectrographic data summary in Table 11, the concentrations of each of 30 elements were tabulated by core versus depth. These tables are not included in this report because of the quantity of data. The emission spectrographic data, so tabulated, were statistically analyzed for 23 of the 30 elements listed in Table 11 by ANOVA at the 99% confidence level. The seven elements not analyzed were detected in less than eight samples, and their data precluded the use of analysis of variance.

In every case the ANOVA indicated that there were no significant differences in concentrations of the elements with depth. Eleven elements, aluminum, arsenic, iron, magnesium, molybdenum, potassium, sodium, tin, titanium, tungsten, and vanadium, showed a significant difference in concentrations among cores. The other twelve elements showed no significant difference in concentrations among cores. When considering a single phosphogypsum stack, B, and the eleven elements that showed a significant difference between cores, the ANOVA indicated no difference in concentrations with depth or between Cores B1 and B2.

These results indicated that trace elements were uniformly distributed in the phosphogypsum stacks. A uniform distribution of trace elements in the stacks would occur if the same quantities of trace elements were added to the stacks as were removed through leaching. However, three stacks, C, E, and F, are inactive. Stack C has been idle nine years. Stack E has been idle several months and Stack F has been idle twelve years. In spite of about 100 cm of rainfall a year [9] for nine and twelve years, Stacks C and F also showed no significant difference in concentrations of trace elements with depth. Thus, the results indicated that trace elements were not only uniformly distributed in the stacks but were not leached from the stacks in any significant amount. This also applied to sodium, potassium, copper, and nickel whose sulfates are soluble.

The elements, arsenic, barium, cadmium, chromium, lead, mercury, selenium, and silver, are listed as contaminants for characteristics of toxicity by the EPA [2]. Chromium, mercury, and selenium were not detected in the phosphogypsum. The detection limits for direct-current arc emission spectrographic analysis are 0.001% for chromium, 0.05% for mercury, and 0.10% for selenium. Barium, cadmium, lead, and silver were detected at concentrations far less than allowable by EPA requirements, even assuming that 100% of these elements would be

extracted by the EPA procedure. The average arsenic concentration was also less than allowable by EPA requirements. However, two cores, F and H, contained 124- and 113-μg/g arsenic, respectively. If 100% of the arsenic present was extracted by the EPA extraction procedure [2], the extracts from these cores would contain 6.20-μg/g and 5.65-μg/g arsenic, which exceeds the EPA allowable concentration of 5.0-μg/g arsenic. However, the previous analysis of the data indicated that the trace elements would not be leached from the phosphogypsum. Therefore, the phosphogypsum would not be a toxic hazardous waste. Further work is in progress to perform the EPA extraction procedure and confirm this conclusion. This will be reported in a subsequent publication.

Conclusions

Based on the research conducted at the Tuscaloosa Research Center, phosphogypsum was generated at a rate of 30 million metric tons per year in Florida. The amount of accumulated phosphogypsum in Florida was 304 million metric tons, and this quantity is projected to reach over 1 billion metric tons by the year 2000.

Phosphogypsum was not a corrosive hazardous waste. Its pH was greater than 2.0.

The radium concentration in phosphogypsum in Florida averaged 21 pCi/g, and its concentration was greatest in the fine sizes.

Thirty-nine elements were detected in phosphogypsum: 30 by emission spectrography, three radiologically, and six by chemical analyses.

The concentrations of elements listed by the EPA for toxic elements each average less than the allowable toxic elements criteria for toxic hazardous waste.

The concentrations of elements in phosphogypsum did not vary with depth.

Acknowledgments

The authors are indebted to advice and assistance in the study provided by Dr. David P. Borris, executive director, Florida Institute of Phosphate Research. The voluntary cooperation of the following Florida phosphate companies in assisting in this study is also greatfully acknowledged: Agrico Chemical Co.; American Cyanamid Co.; Borden Chemical Co.; CF Industries, Inc.; Conserve; Estech General Chemical; Farmland Industries; Gardinier, Inc.; International Minerals and Chemical Corp.; Occidental Chemical Co.; Royster Co.; U.S.S. Agri-Chemicals; and W. R. Grace and Co. Special appreciation is extended to the EPA radiation facility, Montgomery, AL, for radiological isotope analyses.

References

[1] Pressler, J. W., Gypsum, Bureau of Mines Mineral Commodity Profiles, Washington, DC, 1979, 11 pp.

[2] *Federal Register*, Vol. 45, No. 98, 19 May 1980, pp. 33086–33087, 33118, 33122–33131.

[3] *Federal Register*, Vol. 43, No. 243, 18 Dec. 1978, pp. 58957–58959.

[4] McConnel, D., *Apatite, Its Crystal Chemistry, Mineralogy, Utilization and Geologic and Biologic Occurrences*, Springer-Verlag, New York, 1973, 111 pp.
[5] Sauchelli, V., Ed., *Chemistry and Technology of Fertilizers*, American Chemical Society Monograph Series, Reinhold Publishing Corp., New York, 1965, 692 pp.
[6] Bridges, J. D., *Fertilizer Trends 1979*, Tennessee Valley Authority, National Fertilizer Development Center, Muscle Shoals, AL, Jan. 1980, 49 pp.
[7] Association of Florida Phosphate Chemists, *Methods Used and Adopted by the Association of Florida Phosphate Chemists*, 5th ed. Bartow, FL, 1970, pp. 80–82, 103–104.
[8] Douglas, G. S., Ed., "Radium by Radon Emanation Method," *Radioassay Procedures for Environmental Samples*, U.S. Public Health Service Publication No. 999-RH27, Rockville, MD, 1967, pp. (4-36)–(4-45).
[9] Zellars-Williams, Inc., "Water Recirculation System Balance of Central Florida Phosphate Mining, Mine I Calculations, 1974–1975 Rainfall Calculations," BuMines Open File Report No. 120–77, Tuscaloosa, AL, 1977, p. IV.

Alexander May[1] *and John W. Sweeney*[1]

Evaluation of Radium and Toxic Element Leaching Characteristics of Florida Phosphogypsum Stockpiles

REFERENCE: May A. and Sweeney, J. W., "**Evaluation of Radium and Toxic Element Leaching Characteristics of Florida Phosphogypsum Stockpiles,**" *The Chemistry and Technology of Gypsum, ASTM STP 861*, R. A. Kuntze, Ed., American Society for Testing and Materials, 1984, pp. 140–159.

ABSTRACT: The U.S. Bureau of Mines conducted studies to determine if phosphogypsum, a waste material from the processing of phosphate rock, contains hazardous toxic materials as defined by the Environmental Protection Agency (EPA) and whether leaching of these toxic materials and radium may occur. Samples of the phosphogypsum stockpiled material were evaluated using the EPA extraction procedure, atomic absorption, neutron activation, X-ray diffraction, and chemical and physical means. Radiological tests performed used both the germanium-lithium and emanation methods. The data show that the phosphogypsum stockpiles are not hazardous toxic waste as defined by EPA criteria. Trace elements and radium are not leached from the phosphogypsum stockpiles. Absorption of trace elements and radium by phosphogypsum is the major reason for their not being leached. The standard error of measurement of radium concentrations was 4.7 pCi/g.

KEY WORDS: gypsum, phosphoric acids, radium, byproduct gypsum, phosphogypsum, hazardous waste, phosphate fertilizer production

The U.S. Bureau of Mines has completed a two-year research study assessing potential environmental effects associated with phosphogypsum in Florida. Phosphogypsum and gypsum are both calcium sulfate dihydrate. The name "phosphogypsum" is used to designate the byproduct of phosphoric acid production, while "gypsum" refers to the natural mineral. The first phase [*1*] of the study developed baseline data to assess whether there were any environmental problems associated with the storage of phosphogypsum. The second phase, the subject of this report, evaluated the leaching characteristics of the phosphogypsum stockpiles.

The phosphate industry in Florida is a vital segment of the nation's economy and provides a critical mineral required for fertilizer production. In 1981, Florida

[1] Research chemist and supervisory mining engineer, respectively, Tuscaloosa Research Center, Bureau of Mines, P.O. Box L, University, AL 35486.

and North Carolina supplied 86% of the domestic and 33% of the world's phosphate requirement [2]. About 82% of the phosphate is converted into phosphoric acid, which is used to make fertilizers.

Phosphogypsum is the major byproduct of wet-process phosphoric acid production. Phosphate rock, which is composed of apatite minerals (calcium phosphates containing varying amounts of carbonate and fluoride), is digested with sulfuric acid and water to form phosphoric acid, phosphogypsum, and minor quantities of hydrofluoric acid.

The reaction of the phosphate rock to form gypsum, $CaSO_4 \cdot 2H_2O$, may be illustrated by

$$Ca_{10}(PO_4)_6F_2 + 10\ H_2SO_4 + 20\ H_2O \rightarrow 10\ CaSO_4 \cdot 2\ H_2O + 6\ H_3PO_4 + 2HF$$

In the Prayon process, commonly used in Florida, the phosphate rock, ground to pass a 150-μm (100-mesh) sieve, is treated with 30 to 46% phosphoric acid and 55 to 60% sulfuric acid. The rock and acid are circulated through reaction tanks to maintain the optimum time and temperature for the reaction and for the growth of phosphogypsum crystals. The phosphogypsum is filtered, washed with water, and pumped as a slurry to ponds from which the phosphogypsum settles to form the phosphogypsum stacks.

The hemihydrate process is similar but uses higher temperatures and acid concentrations in the reaction tanks. This favors the initial formation of hemihydrate. In subsequent crystallization tanks the hemihydrate is mixed with gypsum suspensions, where it recrystallizes as large crystals of the dihydrate; that is, as phosphogypsum [1].

By 1980 about 304 million metric tons of phosphogypsum had accumulated in Florida in 17 phosphogypsum stockpiles or stacks (Fig. 1). These piles occupied an average area of 920 km^2 (92 hectare) each and ranged from 9 to 43 m in height. Additional phosphogypsum is being generated at a rate of about 30 million metric tons per year, and the projected accumulation by the year 2000 will be over a billion metric tons [1].

The first phase of the Bureau's research [1] showed that phosphogypsum was not corrosive by Environmental Protection Agency (EPA) criteria. The study also presented evidence that phosphogypsum would not be toxic by EPA criteria and that trace elements and radium would not be leached from the stockpiles. These conclusions were obtained from statistical analyses of extensive quantities of spectrographic and radiological data. More direct confirmation of these conclusions was needed to decisively answer the question of leaching of toxic elements and radium from phosphogypsum stockpiles.

This investigation took a direct approach, that is, sampling and analyzing phosphogypsum at the bottom of the stockpiles and the underlying materials in the subsurface, to determine if leaching had occurred. In addition, the standard EPA extraction procedure was performed.

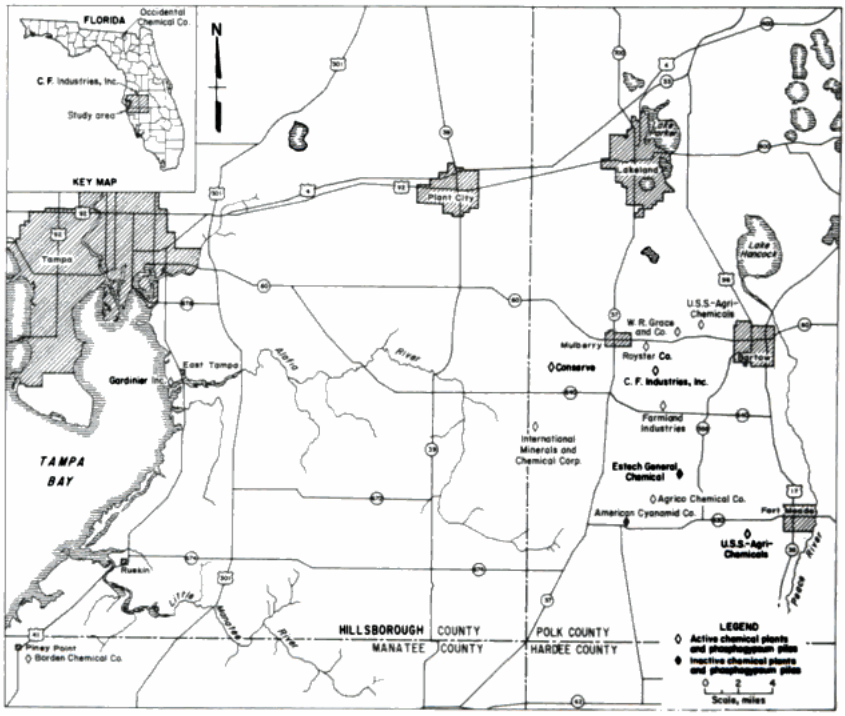

FIG. 1—*Location of phosphogypsum piles in Florida.*

Samples

Thirteen core samples were used from the earlier study of the environmental impact of phosphogypsum production [*1*]. The sample identifications are the same as in that work: A through I each represents an individual stockpile, and 1, 2, and 3 represent different cores on the same stockpile. Five additional core samples were obtained for this study. The new samples were taken only through a short section approximately 3 m above and 3 m below the interface with the ground surface. The samples contained phosphogypsum or soil. The sample identifications are the same as before: A, B, F, and H refer to the same stockpile as in Ref *1*; 1 and 2 refer to different cores on the same stockpile, but the samples are differentiated from the former samples by "-2," for example, F2-2. All sample depths are measured from the tops of the stockpiles of phosphogypsum.

In obtaining these five cores, the positions of the interfaces were determined by test holes. Then the drilling rig was moved about 6 m from the test holes to drill for the samples. In addition to depending on the position of the interfaces, chemical analyses were used to verify the nature of the samples.

Test Procedures

The leachabilities of toxic hazardous material were determined using the EPA extraction procedures [3]. The leachabilities of certain metals (copper, nickel, potassium, and sodium) that are not considered toxic were also determined. Samples were stirred 24 h in water and filtered; then the water-soluble concentrations were determined by atomic absorption. These metals form highly soluble sulfates that would be very susceptible to leaching and provide a test of the degree of ease of leaching within the phosphogypsum stacks.

Total concentrations of trace elements were determined by neutron activation analyses and atomic absorption. Radium concentrations were determined by the emanation method and by the germanium-lithium counting of natural radioactivity, corrected by reference to a National Bureau of Standards (NBS) uranium ore. Chemical analyses were performed by standard methods.

The permeability of phosphogypsum was also determined to help understand the effect of rainwater or leaching of trace elements. The standard variable-head method was modified in the following manner. One hundred grams of phosphogypsum was placed, as a slurry, in a glass tube 56.4 cm long and 1.80 cm in internal diameter. After settling and being compacted with a rod, the phosphogypsum column was 21.26 cm long with a density of 1.85 g/mL. A column of this density could support a weight equivalent to a water head of 16 m, which approximated the conditions within phosphogypsum stockpiles. Water was placed in the tube, and as the water seeped through the column of phosphogypsum, the water levels and time intervals were recorded.

Since the solubility of gypsum is only 0.2%, any rainwater seeping through a phosphogypsum stockpile would be saturated with gypsum. Leaching of trace elements would thus be due to a saturated gypsum solution, not to water alone. An X-ray diffraction analysis was performed to determine the trace elements present in saturated aqueous solutions of phosphogypsum. One thousand grams of phosphogypsum were stirred with 2000 mL of distilled deionized water for 24 h. The water was filtered and allowed to evaporate at room temperature. The crystals formed by evaporation were washed with water, air-dried again, and then dried a few minutes at 60°C before being analyzed by X-ray diffraction.

Neutron activation analyses were performed at the Oak Ridge National Laboratories, for both short and long half-life radionuclides, using irradiation times of 20 s and 30 min and counting times of 15 to 20 min, 1 day, 4 days, and 3 weeks.

Test Results

EPA Extraction Procedure

The EPA criteria defining hazardous and toxic waste were used as guidelines in this study. The EPA criterion for toxicity of wastes is based on an extraction procedure to identify toxic wastes likely to leach into the groundwater. The

hazardous nature of the waste is judged by the concentrations of specific contaminants in the extract. The contaminants listed by EPA for toxic consideration are eight metals and six chlorinated organic compounds [3].

Table 1 lists the EPA contaminants and the criteria that EPA has established to constitute a hazardous toxic waste. Table 2 shows the concentrations of the inorganic contaminants in the extract from the phosphogypsum samples. All of the organic compounds listed by EPA as hazardous toxic wastes were tested by the standard EPA procedure; none were detected. These included endrin, lindane, methoxychlor, toxaphene, 2,4-D silvex, and 2,4,5-TP silvex. All of the metals listed in Table 1 were found to be present in the extract at concentrations lower than allowed by EPA (as shown in Table 2). Therefore, by EPA definition phosphogypsum is not a hazardous toxic waste material. This confirms earlier research conclusions [1] that the leaching of trace elements from phosphogypsum is not significant in introducing hazardous toxic waste materials into the environment.

Phosphogypsum-Subsurface Material

Major Components—Five phosphogypsum-subsurface samples were obtained from cores by drilling through approximately the bottom 3 m of the phosphogypsum stacks and the top 3 m of the underlying subsurface soils. Chemical analyses were used to identify the nature of the samples and confirm that subsurface levels had been reached. The results of chemical analyses for the major components of the five samples are given in Table 3. The approximate mineral compositions of the samples are shown in Table 4. The approximate mineral

TABLE 1—*Maximum concentrations of contaminants for characteristics of EPA toxicity* [3].

Contaminant	Maximum Concentration, mg/L[a]
Arsenic	5.0
Barium	100.0
Cadmium	1.0
Chromium	5.0
Lead	5.0
Mercury	0.2
Selenium	1.0
Silver	5.0
Endrin (1,2,3,4,10,10-hexachloro-1,7-epoxy-1,4,4a,5,6,7,8, 8a-octahydro-1,4-endo, endo-5,8-dimethano naphthalene)	0.02
Lindane (1,2,3,4,5,6-hexachlorocyclohexane, gamma isomer)	0.4
Mathoxychlor (1,1,1-trichloro-2,2-bis [p-methoxyphenyl] ethane)	10.0
Toxaphene ($C_{10}H_{10-n}Cl_n$, technical chlorinated camphene, 67-69% Cl)	0.5
2,4-D (2,4-dichlorophenoxyacetic acid)	10.0
2,4,5-TP Silvex (2,4,5-trichlorophenoxypropionic acid)	1.0

[a] Maximum allowable concentrations in extract.

TABLE 2—*Concentrations of toxic elements in extract from EPA extraction procedures* [3].

Sample	Toxic Element, mg/L							
	Arsenic	Barium	Cadmium	Chromium	Lead	Mercury	Selenium	Silver
A1	0.020	0.2	0.01	0.04	0.01	0.000	0.002	0.08
A2	0.019	0.2	0.01	0.05	0.03	0.000	0.003	0.07
A3	0.029	0.0	0.02	0.06	0.00	0.000	0.005	0.10
B1	0.014	0.0	0.01	0.07	0.01	0.000	0.004	0.01
B2	0.011	0.2	0.01	0.01	0.00	0.001	0.003	0.04
C1	0.016	0.2	0.02	0.02	0.00	0.001	0.005	0.04
C2	0.007	0.4	0.03	0.05	0.00	0.001	0.003	0.10
D	0.009	0.0	0.01	0.11	0.01	0.001	0.003	0.09
E	0.005	0.2	0.03	0.03	0.03	0.001	0.004	0.06
F	0.002	0.1	0.01	0.01	0.04	0.001	0.002	0.05
G	0.005	0.3	0.01	0.01	0.01	0.001	0.002	0.08
H	0.018	0.3	0.01	0.05	0.00	0.001	0.003	0.04
I	0.019	0.2	0.01	0.02	0.01	0.004	0.002	0.07
Average	0.013	0.2	0.01	0.04	0.01	0.001	0.003	0.06

compositions of the samples were derived from the chemical compositions by calculating the amount of gypsum, sand and clay, and phosphate rock present.[2]

As shown in Table 3, the moisture content of subsurface material under the phosphogypsum was greater than that of the phosphogypsum. This indicates that the permeability of the subsurface material was less than that of the phosphogypsum. Thus, if trace elements were leached from the phosphogypsum, their concentrations should be increased in the subsurface material.

Minor Components—Table 5 gives the concentrations of minor components in the phosphogypsum and in the subsurface samples. Only potassium and chromium had greater concentrations in the subsurface material than in the phosphogypsum, possibly indicating that they were leached from the phosphogypsum.

Analyses of the subsurface material, before the phosphogypsum was accumulated, were not available. However, the subsurface material below the phosphogypsum consists of sand, clays, and phosphate rock. The concentrations of trace elements in the clays and phosphate rock (Table 6) may be used to estimate the concentration of trace elements present in the soil before the phosphogypsum was placed on top of it. For example, from Table 4, it can be seen that phosphate rock comprises 20% of the subsurface material. The concentration of a trace element previously present in the soil, as a result of the presence of phosphate rock, can be estimated as 20% of the value of the trace element shown in Table 6 (Column 3).

The values in Table 6 are the maximum values reported in the references

[2] Gypsum = percent $SO_3/0.465$; the factor 0.465 = fraction of sulfur trioxide in gypsum. Sand and clay = percent of silicate plus acid insoluble. Phosphate rock = percent of $P_2O_5/0.33$; the factor 0.33 is the fraction of phosphorus pentoxide in typical central Florida phosphate rock. Percentages were converted to the dry basis for these calculations.

TABLE 3—*Analyses of samples, major components.*[a]

Components	Samples					
	A1-2	B1-2	F1-2	F2-2	H2-2	Average
	PHOSPHOGYPSUM					
Sample depth, m	26–27	41–42	6–7	6–7	20–22	NAp
Analyses, %						
moisture[b]	2.9	3.0	5.5	12.8	17.8	8.4
combined water	18.8	14.4	17.9	15.1	15.3	16.3
silicon dioxide and acid insoluble	3.2	17.7	4.5	4.5	6.2	7.2
calcium oxide	31.1	26.9	29.4	28.0	25.1	28.1
sulfur trioxide	42.0	31.9	40.2	38.3	34.4	37.4
phosphorus pentoxide	0.8	3.7	0.6	0.5	0.5	1.2
aluminum	0.3	0.1	0.1	0.1	0.1	0.1
chlorine	0.0	0.0	0.0	0.0	0.0	0.0
fluorine	0.2	0.8	0.6	0.5	0.5	0.5
iron	0.0	0.1	0.1	0.0	0.1	0.1
magnesium	0.0	0.0	0.0	0.0	0.0	0.0
pH	4.5	4.5	4.5	5.3	4.6	4.7
Ratio, moles calcium oxide/moles sulfur trioxide	1.1	1.2	1.0	1.1	1.0	1.1
	MATERIAL UNDER PHOSPHOGYPSUM					
Sample depth, m	32–34	45–46	12–13	15–16	25–27	NAp
Analyses, %						
moisture[b]	17.9	14.9	18.9	28.9[c]	23.2	20.8
silicon dioxide and acid insoluble	67.9	80.1	69.7	17.6	46.0	56.3
calcium oxide	6.5	3.3	3.0	21.8	13.7	9.7
sulfur trioxide	1.6	0.6	0.0	2.1	0.6	1.0
phosphorus pentoxide	3.2	0.3	2.0	10.4	8.5	4.9
aluminum	1.2	0.1	0.9	0.5	0.8	0.7
chlorine	0.1	0.0	0.0	0.0	0.0	0.0[d]
fluorine	0.5	0.1	0.0	1.1	1.0	0.5
iron	0.3	0.3	0.2	0.7	1.1	0.5
magnesium	0.0	0.1	0.1	1.7	0.4	0.5
pH	4.0	5.0	5.6	6.8	5.4	5.4
Ratio, moles calcium oxide/moles sulfur trioxide	5.9	7.6	430[e]	14.6	31.5	98

[a] NAp = not applicable.
[b] This is referred to as "free water" in phosphogypsum or gypsum.
[c] This sample also contained 7.9 weight percent carbon dioxide.
[d] Without rounding off, this value is 0.02%.
[e] Based on 2.98% calcium oxide and 0.01% sulfur trioxide.

cited. The results show that the actual concentrations of arsenic, barium, cadmium, lead, mercury, potassium, selenium, silver, and sodium in the subsurface samples are lower than the concentrations of these metals estimated to be present with phosphate rock. Since these metals also are present in the clay, their estimated total concentration in the subsurface soil would be even greater. Therefore, these elements have not been leached from the phosphogypsum stacks. Copper also shows no significantly increased concentration, but nickel and chromium do. The nickel concentration is increased from 3 to 10 μg/g, and the

TABLE 4—*Approximate mineral compositions of samples, dry basis, weight percent.*

Mineral	Samples					
	A1-2	B1-2	F1-2	F2-2[a]	H2-2	Average
	PHOSPHOGYPSUM SAMPLES					
Gypsum[b]	93	71	91	94	90	88
Sand and clay[c]	3	18	5	5	8	8
Phosphate rock[d]	3	11	2	1	2	4
	SUBSURFACE SAMPLES					
Gypsum[b]	4	2	0	6	2	3
Sand and clay[c]	83	94	86	25	60	70
Phosphate rock[d]	12	1	7	44	34	20

[a] The subsurface sample also contained 7.9% carbon dioxide, equivalent to 25% limestone ($CaCO_3$).
[b] Gypsum = percent $SO_3/0.465$.
[c] Sand and clay = percent silicate and acid insoluble.
[d] Phosphate rock = percent $P_2O_5/0.33$.

TABLE 5—*Analyses of samples, minor components.*[a]

Components	Samples					
	A1-2	B1-2	F1-2	F2-2	H2-2	Average
	PHOSPHOGYPSUM					
Sample depth, m	26–27	41–42	6–7	6–7	20–22	NAp
Analyses, μg/g						
arsenic	3	2	3	2	8	4
barium	<10	<10	<10	<10	<10	<10
cadmium	3	3	4	4	3	3
chromium	15	20	19	21	30	21
copper	7	11	11	7	5	8
lead	12	13	9	7	2	9
mercury	<0.5	<0.5	<0.5	<0.5	<0.5	<0.5
nickel	17	13	12	10	12	13
potassium	86	42	24	20	63	47
selenium	1	<0.5	2	<0.5	1	<1
silver	<3	<3	<3	<3	<3	<3
sodium	4500	1300	180	150	490	1300
	MATERIAL UNDER PHOSPHOGYPSUM					
Sample depth, m	32–34	45–46	12–13	15–16	25–27	NAp
Analyses, μg/g						
arsenic	3	2	2	3	5	3
barium	<10	<10	<10	<10	<10	<10
cadmium	3	2	2	4	3	3
chromium	410	150	160	89	140	190
copper	2	1	1	5	5	3
lead	13	5	13	9	2	8
mercury	<0.5	<0.5	<0.5	<0.5	<0.5	<0.5
nickel	8	9	2	19	14	10
potassium	490	510	180	430	460	410
selenium	<0.5	<0.5	<0.5	1	1	<1
silver	<3	<3	<3	<3	<3	<3
sodium	400	130	410	1800	1900	930

[a] NAp = not applicable.

TABLE 6—*Trace element concentrations in subsurface samples, phosphate rock, and clay.*

Trace Element	In Subsurface Samples, μg/g[a]	In Phosphate Rock[b]		In Clay[b]	
		Concentration, μg/g	Reference	Concentration, μg/g	Reference
Arsenic	3	20	4	13	4
Barium	<10	70	4	580	4
Cadmium	3	30	4	0.3	4
Chromium	190	100	4	750	5
Copper	3	10	4	45	4
Lead	8	50	4	20	4
Mercury	<0.5	7	4	0.3	5
Nickel	10	15	4	68	4
Potassium	410	2000	4	30 000	5
Selenium	<1	7	4	0.6	4
Silver	<3	5	4	0.1	4
Sodium	930	5900	4	10 700	5

[a] Averages, Table 5.
[b] Maximum values in references cited.

chromium from 20 to 190 μg/g in subsurface samples compared to the background estimates for phosphate rock. Therefore, the chromium and nickel content of the clay also must be accounted for.

The same type of comparative projections can be made for the trace elements contained in the clay fraction. The amount of clay present is not as easily or as accurately determined as the phosphate rock. It can be estimated from the iron, magnesium, potassium, silicon, and sodium present, remembering that much of the silicon exists as sand (silicate) and must be excluded from the estimate. The clay fraction was estimated by dividing the concentrations (on a dry basis) of aluminum, iron, magnesium, potassium, and sodium (Tables 3 and 5) by the concentrations of each of these elements in normally occurring clay (Table 6). This produced an average value of 16% clay in the subsurface samples.

Taking 16% of the background concentrations (Table 6, Column 4) gives 7-μg/g copper and 11-μg/g nickel. This exceeds the actual level found in the subsurface samples. Therefore, copper and nickel have not been leached from the phosphogypsum. The total chromium background (using Columns 3 and 4 in Table 6) was estimated to be 140 μg/g. Actually, 190 μg/g was found in the subsurface sample, but the difference, 50 μg/g, was not considered significant because it was less than one standard deviation of the average of the subsurface chromium analyses.

It was concluded that none of the metallic elements would be leached from the phosphogypsum.

Radium Analyses—Results of the radium analyses are shown in Table 7. The samples tested by the two different laboratories were identical. EPA analyzed its samples by the emanation method, while the Oak Ridge National Laboratory

TABLE 7—*Radium analyses, dry basis.*[a]

Components	Samples					
	A1-2	B1-2	F1-2	F2-2	H2-2	Average
	PHOSPHOGYPSUM					
Sample depth, m	26–27	41–42	6–7	6–7	20–22	NAp
Radium, pCi/g						
ORNL[b]	18.2	9.2	41.3	19.8	24.6	22.6
EPA[c]	15.7	10.4	54.1	16.6	11.3	21.6
Average	17.0	9.8	47.7	18.2	18.0	22.1
	MATERIAL UNDER PHOSPHOGYPSUM					
Sample depth, m	32–34	45–46	12–13	15–16	25–27	NAp
Radium, pCi/g						
ORNL[b]	11.2	1.5	2.1	20.6	11.0	9.3
EPA[c]	9.9	1.7	2.7	13.9	11.4	7.9
Average	10.6	1.6	2.4	17.3	11.2	8.6

[a] NAp = not applicable.
[b] Analyzed by the Oak Ridge National Laboratory, Oak Ridge, TN.
[c] Analyzed by EPA Radiation Facility, Montgomery, AL.

used the germanium-lithium counting technique. The radium concentration in the phosphogypsum averaged 22.1 pCi/g, and the radium concentration in the subsurface material averaged 8.6 pCi/g.

Statistical analysis of the radium data is shown in the analysis of variance (ANOVA, Table 8). At the 99% confidence level, these results show a significant difference between the radium concentrations in phosphogypsum and in the subsurface material. They show no significant differences among the cores or between the Oak Ridge and EPA results. The standard error of measurement was 4.68 pCi/g for 20 analyses. This is near the standard error of 4.52 pCi/g

TABLE 8—*Analyses of variance of radium data (standard error = 4.68 pCi/g).*[a]

Source of Variation[b]	Degrees of Freedom	Sum of Squares	Mean Squares	F Ratio
G/S	1	913.952	913.952	41.71
CORE	4	784.053	196.013	8.95
LAB	1	6.962	6.962	0.32
G/S:CORE[c]	4	1292.803	323.200	14.75
G/S:LAB[c]	1	0.162	0.162	0.01
CORE:LAB[c]	4	108.133	27.033	1.23
Error	4	87.643	21.910	NAp
Total	19	3193.708	NAp	NAp

[a] G/S = in phosphogypsum versus material under phosphogypsum. CORE = among cores A1-2 through H2-2. LAB = Oak Ridge analyses versus EPA analyses. NAp = not applicable.
[b] Comparisons of radium concentrations.
[c] Interactions among main factors.

for 89 radium analyses previously reported [*1*]. These standard errors are both very near the 5 pCi/g proposed by the EPA as a maximum for radium in hazardous wastes and would be difficult to accurately assess in practice.

The background concentrations of radium in the subsurface material, before creation of the phosphogypsum piles, can be accurately estimated since long-term data are available [*4,6*]. Interest in radioactivity in Florida dates back to 1942 through 1948, when there was an urgent need to find domestic sources of uranium. In addition, there has been environmental concern about radium in Florida for the last 20 years, and considerable data have been published, some of which are shown in Table 9.

The material under the phosphogypsum piles consists of sand, clay, and phosphate rock. From the percentages of each of these materials (Table 4) and concentrations of radium in each material, the concentrations of radium in the subsurface material may be calculated. This is shown in Table 10. This method is analogous to the one used above to determine the background concentration of trace elements. These data were statistically analyzed (ANOVA and *F*-tests) for the background versus the measured radium concentrations under the phosphogypsum piles. No significant differences were found, and it was concluded that radium was not leached from the phosphogypsum.

Permeability

Table 11 gives the permeability data for seepage of water through phosphogypsum. The data were fitted by least squares linear regression to Eq 1

$$\ln h = a + b\,t \qquad (1)$$

where h is the water height in centimeters at time t in hours, and a and b are

TABLE 9—*Representative radium concentrations in Florida phosphate materials.*

Material	Radium, pCi/g
Background soil	1.5
Silt	1.1
Beach sand	0.9
Reclaimed soil	10 through 30
Overburden (excluding leach zone)	10
Leach zone material	40
Matrix	40 through 60
Wet phosphate rock	29 through 42
Dry phosphate rock [*4,6*]	38 through 48
Sand tailings	6.2 through 8.8
Gypsum	21 through 33

TABLE 10—*Radium concentration in material under phosphogypsum piles, dry basis, pCi/g.*

Source of Radium	Samples					Average
	A1-2	B1-2	F1-2	F2-2	H2-2	
From gypsum[a]	0.7	0.2	0.0	1.0	0.3	0.4
From sand[b]	0.7	0.8	0.8	0.2	0.5	0.6
From phosphate rock[c]	4.6	0.4	2.7	16.7	12.9	7.5
In material under phosphogypsum piles						
background[d]	6.0	1.4	3.5	17.9	13.7	8.5
observed[e]	10.6	1.6	2.4	17.3	11.2	8.6

[a] Percent gypsum (Table 4) divided by 100 times pCi/g radium in gypsum (Table 7).
[b] Percent sand and clay (Table 4) divided by 100 times pCi/g radium in sand (0.9, Table 9).
[c] Percent phosphate rocks (Table 4) divided by 100 times pCi/g radium in dry phosphate rock (38, Table 9).
[d] Sum of radium from gypsum, sand, and phosphate rock.
[e] From Table 7.

coefficients determined by the linear regression. The results gave

$$a = 7.869 \ln (\text{cm})$$

$$b = -1.120 \times 10^{-2}\ \text{h}^{-1}$$

The correlation coefficient of the linear regression was 0.9999. The permeability P of the phosphogypsum, derived from Eq 1 and Darcy's law [7], is given in Eq 2

$$P = -bL \tag{2}$$

where b is the coefficient in Eq 1 and L is the length, 21.26 cm, of the phosphogypsum column. The permeability was 0.24 cm/h of seepage.

TABLE 11—*Permeability data for water seepage through phosphogypsum.*

Time t, h	Water Height (h), cm[a]
0	56.0
18.53	45.9
42.67	35.1
63.44	27.7
71.25	25.2

[a] Height of water from bottom of phosphogypsum column.
NOTE: Length L of phosphogypsum column = 21.26 cm.

X-ray Diffraction

The X-ray diffraction analyses of water-soluble material from phosphogypsum showed only the presence of gypsum and a trace of hemihydrate. The sensitivity of this analysis was not sufficient to identify compounds of the trace elements.

Neutron Activation Analyses

Five phosphogypsum samples were analyzed by neutron activation analysis. This yielded quantitative results and the standard deviations for the concentrations of 44 elements. These analyses are presented in Table 12.

Factors Involved in Leaching

To help explain the results of this study and to aid in predicting the future stability of phosphogypsum stockpiles, the hydrology associated with the piles and the solubility and absorption of trace elements and radium were considered. How well the objectives of this investigation were met is also briefly considered.

Hydrology Associated with Phosphogypsum Piles

Phosphogypsum stockpiles in Florida are 200 to 2140 km^2 (20 to 214 hectare) in area, averaging 920 km^2 (92 hectare) [*1*]. The piles are formed by pumping phosphogypsum slurries from phosphoric acid plants to a system of ditches that direct the slurry within the piles. The slurries are directed to subdivided diked areas where the phosphogypsum rapidly settles. When the phosphogypsum builds up in an area, the dikes are adjusted to redirect the slurry to another area. In this manner terraces of phosphogypsum are formed. Figure 2 shows an interior-diked phosphogypsum pile. The clear supernatant water from the slurries of the phosphogypsum flows by gravity to holding ponds and is then reused.

These slurry areas make up only a small part of the phosphogypsum stockpile areas, and most of the remaining pile areas are fairly dry. Leaching in the settled portion of the pile would be due to rainwater passing downward through the pile.

Rainfall at Lakeland, FL, for 1974 was 112 cm. Of this amount, 66 cm fell during a 72-h period. There were 24 periods of rain of 3-h duration each, averaging 2.72 cm of rain [*8*]. The Soil Conservation Service (SCS) method [*9*] of estimating the quantity of runoff water was applied, resulting in 18 cm/year of runoff. Thus, the net amount of rainwater available to infiltrate the phosphogypsum was 94 cm in 1974. However, 1974 was an unusually dry year. Normal annual rainfall in the phosphate region is about 140 cm. Using the same runoff for a normal year results in a net available rainwater of 122 cm.

Evaporation usually exceeds rainfall on an annual basis in the Florida phosphate region [*8*]. However, the infiltration rate of water into dry soil or phosphogypsum is about 1.3 cm/h [*9*]. This greatly exceeds the evaporation rate.

TABLE 12—*Neutron activation analyses of phosphogypsum from Florida, μg/g.*[a]

Element	Average	Standard Deviation of Average
Aluminum	2000	540
Antimony	0.20	0.03
Arsenic	0.76 through 0.94	0.26 through 0.32
Barium	<210	<24
Bromine	<0.92	<0.12
Calcium	21 000	5700
Cerium	49	5.4
Cesium	0.03 through 0.07	0.01 through 0.02
Chlorine	<150	<4.7
Chromium	6.0	1.4
Cobalt	0.58	0.15
Copper	<82	<9.6
Dysprosium	<3.5	<0.20
Erbium	<330	<9.7
Europium	1.5	0.17
Gadolinium	130 through 170	51 through 59
Gallium	<3.0	<0.26
Gold	0.002 through 0.013	0.001 through 0.002
Hafnium	1.9	1.0
Indium	<0.14	<0.005
Iodine	0.90 through 3.8	0.20 through 0.90
Iron	860 through 1000	300 through 600
Lanthanum	39	4.6
Magnesium	<940	<27
Manganese	25	14
Mercury	0.28 through 0.40	0.25 through 0.28
Molybdenum	2.2 through 11	1.4 through 2.2
Neodymium	33	4.1
Potassium	200 through 230	83 through 94
Rubidium	0.72 through 3.2	0.45 through 0.96
Scandium	<0.40	0.16
Selenium	0.72 through 2.1	0.44 through 0.72
Silver	<1.3	<0.64
Sodium	520	79
Strontium	600	67
Tantalum	0.12	0.042
Terbium	1.0	0.14
Thorium	1.9	0.65
Titanium	440	140
Tungsten	<.91	<.060
Uranium	9.6	2.9
Vanadium	1.8 through 4.0	0.50 through 1.8
Ytterbium	2.6	0.45
Zinc	<340	<21

[a] Five samples, each a composite of cores of the depths shown: A1, 0 to 21 m; B1, 0 to 30 m; E, 0 to 27 m; F, 0 to 9 m; and H, 0 to 24 m.

FIG. 2—*Interior-diked phosphogypsum pile.*

Once moisture has penetrated into the piles, there is little evaporation from any appreciable depth. Taking a conservative viewpoint, evaporation was considered to be zero, so that the net water available to percolate through the phosphogypsum remains 122 cm/year for a normal year.

The sample used in the laboratory permeability test had the same characteristics as the phosphogypsum in the piles. It was formed by settling a phosphogypsum slurry, followed by compaction, which is the same way the stockpiles are created. The permeability figure that resulted from the tests was the saturated hydraulic conductivity since the sample was completely immersed in a column of water during the test. However, phosphogypsum in the piles is not saturated with water but contains an average of about 15% moisture. Permeability decreases drastically with decreases in moisture content because of the loss of water head. The unsaturated hydraulic conductivity would be 10% or less of the saturated value [*10*], or approximately 0.024 cm/h (2.0 m/year).

Seepage of water through the piles is not uniform. It is greatest during a rain but almost ceases during dry periods. This results in irregular moisture profiles in the piles, with wet and dry layers alternating within the piles. This moisture pattern has been observed previously [*1*].

The solubility of gypsum is 0.26%, and its density is 2.32 g/mL. From this,

the amount of phosphogypsum dissolved by rain was calculated to be a layer only 0.13 cm thick for each 122 cm, or year, of rain. At this rate it would require 6600 years of normal rainfall to dissolve a 9-m pile of phosphogypsum.

The normal annual amount of rainfall and the rate of seepage are sufficient to leach radium and the trace elements. However, this does not occur. The rate of movement of radium and trace elements is much less than the rate of seepage. The U.S. Nuclear Regulatory Commission reported [*10*] that radium moves at $\frac{1}{215}$ times the seepage rate. This was radium from a uranium tailings pond seeping through alluvium soil. The factor of $\frac{1}{215}$ is directly dependent on the absorption of radium by the soil. Radium sulfate has a solubility of only 2.1×10^{-6}%, is in the same crystal system as gypsum, and would be strongly absorbed by gypsum. Its rate of movement through gypsum would be at least as slow as its rate of movement through soil, or less than $\frac{3}{215}$ or 0.9 cm/year. It would require 2300 years for radium to migrate through a 21-m phosphogypsum stack, and by then the radium would have disintegrated to 37% of its original concentration, or 7.8 pCi/g. For comparison, EPA regulations on uranium tailings allow a maximum concentration of radium-226 of 15 pCi/g averaged over 15-cm thick layers of soil more than 15 cm below the surface [*11*].

Solubility of Compounds of Trace Elements

Evaporation of the leach water from 1000 g of phosphogypsum and X-ray diffraction of the resulting crystals did not identify any compounds of trace elements. Trace elements may exist as sulfates, such as mercuric sulfate, or as calcium salts, such as calcium selenate, in equilibrium with a saturated solution of calcium and sulfate ions from gypsum. Further isolation of trace elements by extraction, precipitation, ion exchange, or other means would so alter this equilibrium that the original amounts and types of compounds present would not be determined. Literature studies of phase equilibria in saturated gypsum solutions were used to identify possible trace element compounds.

Many compounds may be present in phosphogypsum piles, such as silicates, fluorides, phosphates, or chlorides. However, sulfate and calcium compounds would predominate because of the large excess of calcium and sulfate ions from the phosphogypsum. The specific compounds considered in this report are listed, by their formulas, in Table 13. These are all sulfates except the calcium compounds of arsenate, chromate, and selenate, which are the most probable compounds of these elements present. Potassium is considered as $K_2SO_4 \cdot CaSO_4 \cdot H_2O$ (syngenite), identified as the solid phase present in saturated $K_2SO_4 \cdot CaSO_4$ solutions [*12*]. Most of the solubilities were taken from Seidell [*13*].

The percent leached is determined by taking the quantities of each trace element leached, times 100, divided by the total quantities present. These quantities are also presented in Table 13. There is excellent linear correlation between the solubilities of copper, nickel, and cadmium sulfates and their respective percentages leached. The correlation coefficient was 0.9998. Increasing solubility

TABLE 13—*Comparison of total and leachable trace elements in phosphogypsum.*

Element	Average, μg/g[a] Total	Leached	Leached, % of total	Absorbed, % of total[b]	Axial ratios, A/A gypsum[c]	Solubility, % as element[d]	Compounds Whose Axial Ratios and Solubilities Were Considered
Arsenic	0.85[e]	0.24[g]	28	72	1.0	0.13	$CaHAsO_4 \cdot 2H_2O$
Barium	105[e]	3.2[g]	3	97	2.0	0.00023	$BaSO_4$
Cadmium	0.59[f]	0.28[g]	47	53	3.0	24	$CdSO_4 \cdot 8/3H_2O$
Chromium	6.0[f]	0.80[g]	13	87	1.7	5.6	$CaCrO_4 \cdot 2H_2O$
Copper	4.9[f]	0.25[f]	5	95	1.6	7.4	$CuSO_4 \cdot 5H_2O$
Lead	1.3[f]	0.36[g]	28	72	2.0	0.00031	$PbSO_4$
Mercury	0.34[e]	0.012[g]	4	96	1.8	3.40	$HgSO_4$
Nickel	6.3[f]	0.97[f]	15	85	2.4	11	$NiSO_4 \cdot 7H_2O$
Potassium	90[f]	47[f]	52	48	3.3	1.4	$K_2SO_4 \cdot CaSO_4 \cdot H_2O$
Selenium	1.4[e]	0.060[g]	4	96	1.0	3.0	$CaSeO_4 \cdot 2H_2O$
Silver	0.67[e]	0.96[g]	. . .[h]	. . .[h]	2.0	0.56	Ag_2SO_4
Sodium	404[f]	204[f]	50	50	3.0	7.1	$Na_2SO_4 \cdot 10H_2O$

[a] Averages from Samples D and F for sodium, potassium, copper, and nickel. Averages from Samples A1, B1, e, F, and H for all other elements.

[b] 100 minus percent leached.

[c] Crystallographic ratios *A*-axial-ratio/*A*-axial-ratio of gypsum. *A* gypsum = 0.413.

[d] Solubilities of compounds in the last column times fractions of elements (in the first column) in the compounds.

[e] Analysis by neutron activation.

[f] Analysis by atomic absorption.

[g] EPA extraction procedure.

[h] Indeterminate.

correlated highly with a greater percentage leached. The anions arsenate, chromate, and selenate yielded a linear correlation coefficient of −0.64, and barium, cadmium, chromium, copper, mercury, nickel, and selenium gave a coefficient of 0.89. Except for barium and lead, whose sulfates are very insoluble, the moisture content of phosphogypsum would supply sufficient water to dissolve all of the trace elements listed in Table 13. Solubility would not be a limiting factor in leaching trace elements, although barium and lead would require water seeping through the phosphogypsum stockpiles to supply sufficient water to dissolve their sulfates.

Absorption of Trace Elements on Phosphogypsum

Absorption of ions from a solution, by a solid in contact with the solution, is enhanced if both the solid and liquid phases contain the same ions. Molecular absorption may occur if the molecules in solution will fit into the crystal lattice of the solid.

All of the compounds in Table 13 contain either calcium or sulfate ions, in common with gypsum. The crystallographic lattice dimensions and axial ratios of each of these compounds were compared to those of gypsum. Data were obtained from the Powder Diffraction Standards Data File [*14*]. The conventions

stated by Dana [*15*] were used in selection of axial lengths corresponding to the *a*, *b*, and *c* axes. For orthorhombic and triclinic systems, the *c* axis is shorter than the *a* axis, and the *a* axis is shorter than the *b* axis, or $c < a < b$. For monoclinic systems, the *c* axis is shorter than the *a* axis dimension, or $c < a$. The *A* axial ratio is the quotient of the *a* axis dimension divided by the *b* axis dimension. In this report the *A* axial ratios of the compounds of the trace elements were divided by the *A* axial ratio of gypsum to give a number for each compound, indicative of the extent to which the crystal lattice of the compound matched that of gypsum. These numbers are listed in Table 13 in Column 6. The percent absorbed is defined as 100 minus the percent leached and is also given in Table 13. These data were fitted to Eq 3

$$S = 48.7 + 53.3\,R - 16.7\,R^2 \tag{3}$$

where *S* equals percent absorbed, and *R* equals the axial ratio relative to gypsum as defined. The correlation coefficient was 0.88, and the standard error of estimate was 10% absorption. This data indicate that absorption is a major factor.

Radium sulfate has an axial ratio relative to gypsum of 1.93. From Eq 3, the absorption of radium by phosphogypsum would be 89% of the amount of radium originally present. This indicates that very little radium would be leached.

Discussion

The three objectives of this investigation were to determine (1) if the phosphogypsum piles were hazardous toxic wastes, (2) if toxic elements were leached from phosphogypsum, and (3) if radium was leached.

The first objective involved performing the standard EPA extraction procedure and comparing the results with the EPA allowable concentrations. The findings showed that the phosphogypsum was not toxic.

The second objective involved comparing the estimated background concentrations of trace elements with the concentrations found in the subsurface samples. A difficulty encountered was in establishing the background concentrations. A firm estimate of these background concentrations was afforded through phosphorus pentoxide analyses of the samples. This established the amounts of phosphate rock in the samples. Since concentrations of trace elements in phosphate rock and the amounts of phosphate rock in the subsurface samples were available, the trace element concentrations in the background could be estimated. On this basis alone, only nickel and chromium may be leached. The same method of estimating background concentrations was applied using clay. It showed that nickel and chromium were not leached. It was concluded that toxic element concentrations were below EPA standards and were not being leached from phosphogypsum stockpiles.

The third objective was to determine if radium was being leached. Background concentrations of radium in many materials present in the phosphate mining area

have been previously determined. Using these data, it was found that radium concentrations in phosphogypsum significantly exceeded those in the subsurface samples. Also the radium concentrations in the subsurface samples were only equal to background. This indicated that radium was not leached.

Conclusions

1. Phosphogypsum stockpiles in Florida are not hazardous toxic wastes.
2. Trace elements are not leached from phosphogypsum stockpiles.
3. Radium is not leached from phosphogypsum stockpiles.
4. The standard error of measurement of radium concentration was 4.7 pCi/g.
5. Absorption of trace elements and radium by phosphogypsum is the major reason for their not being leached.

Acknowledgments

The authors wish to acknowledge the assistance of Dr. David P. Borris, Executive Director, Florida Institute of Phosphate Research (FIPR), for his advice and cooperation in the study under a Memorandum of Agreement between the Bureau of Mines and FIPR. The voluntary cooperation of the following Florida phosphate companies in assisting in this study is also gratefully acknowledged: Agrico Chemical Co., Estech General Chemical, Farmland Industries, Gardinier, Inc., and U.S.S. Agri-Chemical. Special appreciation is extended to the EPA radiation facility, Montgomery, AL, and the Oak Ridge National Laboratory, Oak Ridge, TN, for radium analyses.

References

[1] May, A. and Sweeney, J. W., "Assessment of Environmental Impacts Associated with Phosphogypsum in Florida," U.S. Bureau of Mines Report 8639, Tuscaloosa, AL, 1982, 19 pp.
[2] Stowasser, W. F., *Phosphate Rock, BuMines Minerals Yearbook 1981*, Vol. 1, U.S. Bureau of Mines, Washington, DC, 1982, pp. 649–666.
[3] *Federal Register*, Vol. 45, No. 98, May 19, 1980, pp. 33122, 33127–33131.
[4] National Academy of Sciences, *Redistribution of Assessory Elements in Mining and Mineral Processing, Part II. Uranium, Phosphate, and Alumina*, Washington, DC, 1979, pp. 55 and 71.
[5] Rankama, K. and Sahama, T. G., *Geochemistry*, University Chicago Press, Chicago, IL, 1950, p. 226.
[6] U.S. Environmental Protection Agency, "Final Areawide Environmental Impact Statement, Central Florida Phosphate Industry," EPA 904/9-78-026(B), Vol. 2, Atlanta, GA, Nov. 1978, p. 1.53.
[7] Wenzel, L. K., "Methods of Determining the Permeability of Water-Bearing Materials," U.S. Geological Survey Water Supply Paper 887, Washington, DC, 1942, pp. 50–87.
[8] Zellars-Williams, "Water Recirculation System Balance of Central Florida Phosphate Mining," BuMines OFR 120-77, NTIS PB 270 359, U.S. Bureau of Mines, Tuscaloosa, AL, Jan. 1977, 83 pp.
[9] Haan, C. T. and Barfield, B. J., "Hydrology and Sedimentology of Surface Mined Lands," University of Kentucky, Lexington, KY, 1978, pp. 65–72.

[10] U.S. Nuclear Regulatory Milling," Project M-25, Appendices A–F, NUREG-0706, Vol. 2, Washington, DC, Sept. 1980, pp. E-5 and E-21.
[11] *Federal Register*, Vol. 48, No. 3, Jan. 5, 1983, p. 602.
[12] Hill, A. E., *Journal of the American Chemical Society*, Vol. 56, 1934, pp. 1071–1078.
[13] Seidell, A., *Solubilities of Inorganic and Metal Organic Compounds*, 3rd ed., D. Van Nostrand Co., Inc., New York, 1940, 1698 pp.
[14] Joint Committee on Powder Diffraction Standards, Data Cards 25-138, 24-1035, 20-187, 11-646, 1-0382, 28-739, 11-647, 1-0403, 5-0577, 13-519, 16-479, 27-1403, 21-816, compiled by the International Centre for Diffraction Data, Swarthmore, PA, dates vary.
[15] Hurlbut, C. S., Jr., *Dana's Manual of Mineralogy*, 18th ed., Wiley, New York, 1971, pp. 81, 89, 94.

Franz Wirsching[1]

Drying and Agglomeration of Flue Gas Gypsum

REFERENCE: Wirsching, F., **"Drying and Agglomeration of Flue Gas Gypsum,"** *The Chemistry and Technology of Gypsum, ASTM STP 861*, R. A. Kuntze, Ed., American Society for Testing and Materials, 1984, pp. 160–173.

ABSTRACT: Flue gas gypsum is obtained as a moist finely divided powder from the desulfurization of combustion gases in power plants. From its upgrading by drying and agglomeration, a material is produced very similar in its properties to that of natural gypsum. The drying is carried out very successfully by using rapid driers. Agglomeration can be done by the process of briquetting, compaction, or pelletizing. Briquetting, the most reliable of the agglomeration processes, will be described in more detail. Flue gas gypsum briquets can be used by both the gypsum and the cement industry. In case of a surplus, these briquets can easily be stored in the open, especially during winter months. This puts the power plant operator in a position whereby he can produce by-product gypsum with a variety of application properties and at the same time contribute to the gypsum being reliably and economically utilized.

KEY WORDS: gypsum, drying, agglomeration, briquetting, flue gas gypsum, by-product of desulfurization, processing of flue gas gypsum, flue gas gypsum briquets

Industrial countries, such as Japan, the United States, and the Federal Republic of Germany, today desulfurize the combustion gases of large combustion plants including, in particular, power stations. Of all the numerous desulfurization processes "wet purification" with limestone ($CaCO_3$), calcium hydroxide ($Ca(OH)_2$), or calcium oxide (CaO) has so far proved to be the best and is extensively used. The end product after desulfurization is a mixture of calcium sulfite and calcium sulfate, or after oxidation with oxygen from the air, calcium sulfate dihydrate ($CaSO_4 \cdot 2H_2O$), so-called flue gas gypsum. Reactions taking place in desulfurization can be represented by the following equations, as shown in Fig. 1.

Flue gas gypsum is obtained as finely divided crystals in an aqueous reaction medium. Depending on the process, the size and shape of the crystals vary from 1 to 200 μm and from a cubic to a rod shaped structure, as shown in Figs. 2a

[1]Manager of research and development, Gebr. Knauf Westdeutsche Gipswerke, Zentrallaboratorium, 8715 Iphofen, Federal Republic of Germany.

I $SO_2 + CaCO_3 + \frac{1}{2} H_2O \longrightarrow CaSO_3 \cdot \frac{1}{2} H_2O + CO_2$
(gas) (solid suspension) (solid suspension)

II $CaSO_3 \cdot \frac{1}{2} H_2O + SO_2 + H_2O \longrightarrow Ca(HSO_3)_2 + \frac{1}{2} H_2O$
(solid suspension) (gas) (in solution)

III $Ca(HSO_3)_2 + O_2 + 2H_2O \longrightarrow CaSO_4 \cdot 2H_2O + H_2SO_4$
(in solution) (solid suspension)

FIG. 1—*Reactions of sulfur dioxide with limestone to produce flue gas gypsum.*

and b. After filtration the flue gas gypsum occurs as a moist finely divided powder with a free water content of approximately 10%.

Flue gas gypsum is an end product that can be used industrially. When used as a substitute for natural gypsum by the gypsum industry or the cement industry, however, its moist finely divided particle size and structure can often be disadvantageous. This causes problems with handling or with intermediate storage, or when natural gypsum is used alternately with flue gas gypsum, or even with the application of different types of flue gas gypsum. The thixotropic behavior of finely divided flue gas gypsum makes it impossible for the gypsum industry to use it, for instance, in the manufacture of machine-applied gypsum plaster, which is widely used in central Europe. In an effort to overcome this problem a process has been developed for drying and agglomerating flue gas gypsum. The dry, lumpy flue gas gypsum obtained can be applied in the same way as natural gypsum.

Basics for Drying Flue Gas Gypsum

Moist finely divided flue gas gypsum has a free water content of approximately 10% in the form of adsorbed surface water. Furthermore, as a calcium sulfate dihydrate it contains about 20% chemically bonded water—water of crystallization or combined water. Flue gas gypsum has no hygroscopic water.

Initially only the surface water is removed when the flue gas gypsum is heated, and subsequent heating will effect the removal of the combined water. These heating processes can be designed to follow one another in direct succession, but remain quite distinct from one another. In the first step—referred to as the drying process—the adsorbed surface water can be completely removed. In a second step, quite distinct from the drying stage, the combined water is removed. In gypsum technology this second step is referred to as "calcination."

The energy levels of the two stages are quite distinct from each other, so that proper reaction steps will produce a completely dry flue gas gypsum without removal of any of the combined water.

Laboratory tests on the drying and calcination of moist finely divided flue gas gypsum in relation to temperature and time have shown that the drying behavior

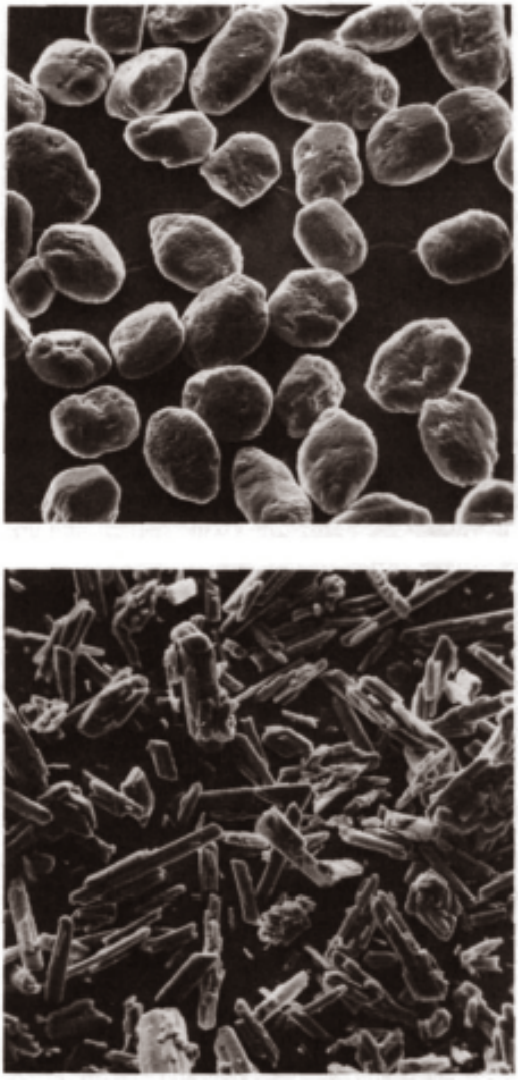

FIG. 2—(a) *Particle structure of flue gas gypsum: cubic shaped, bulk density 1.2 ton/m³ and* (b) *particle structure of flue gas gypsum: rod shaped, bulk density 0.5 ton/m³.*

curves of these two steps are quite distinct from each other. Such behavior curves, based on different temperatures, are shown in Fig. 3. From this it becomes apparent that at temperatures below 70°C (158°F) the gypsum is only dried. At temperatures above 70°C, up to about 90°C (194°F), the gypsum is first dried completely, and subsequently calcination occurs. The curves are of a stepped shape. The two processes merge only above a temperature of 90°C. The next paragraph explains how the drying of flue gas gypsum is accomplished on an industrial scale.

The Technique of Drying Flue Gas Gypsum

In the industrial drying of flue gas gypsum the aim is also to preserve the combined water and entirely remove the surface water. It is moreover necessary to carry out drying with the lowest possible energy consumption and within a short period of time, while achieving high production. Cocurrent drying units are suitable for this, in which the hot gases cocurrently come into direct contact with the moist finely divided flue gas gypsum. Since the process of calcination only starts at temperatures above 70°C (158°F) and after a certain residence time, care should be taken that such conditions are not attained during the drying process. It was established that there is a direct relationship between exhaust gas temperature and the drying and calcination (Fig. 4). From this it follows that calcination of the flue gas gypsum can be avoided by limiting the outlet gas

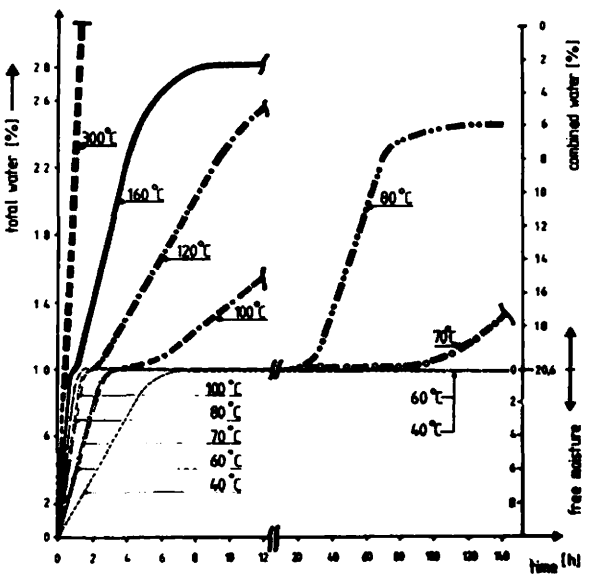

FIG. 3—*Drying behavior curves of flue gas gypsum in relation to temperature and time.*

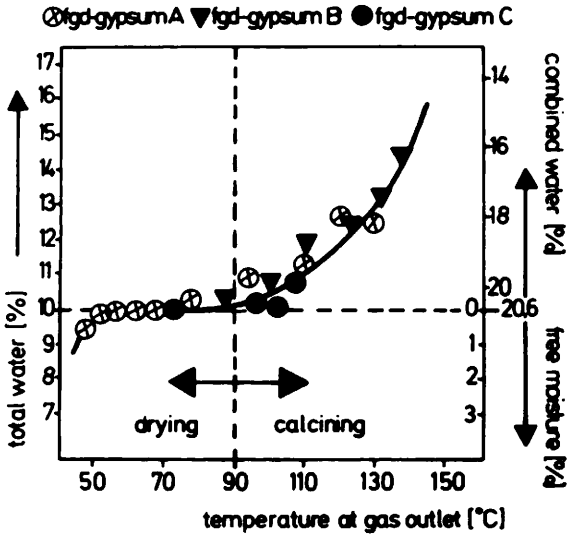

FIG. 4—*Relationship between exhaust gas temperature and drying and calcination of the flue gas gypsum.*

temperature to below 90°C (194°F) at the same time carrying out the drying process to its full.

In choosing the type of drier for drying the flue gas gypsum it was found that of all the cocurrent driers available, such as rapid driers, flash driers, or contact driers, the directly heated cocurrent rapid drier was the most suitable. Its design and mode of operation are described in Fig. 5.

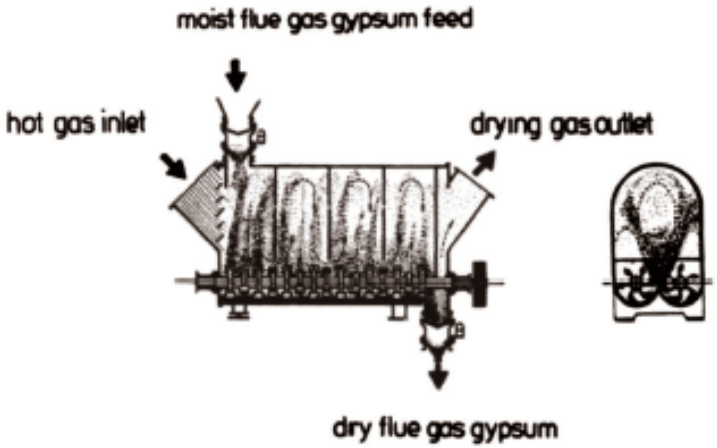

FIG. 5—*Rapid drier for drying flue gas gypsum.*

The rapid drier comprises a closed casing with two rotating shafts in the lower part. The moist finely divided flue gas gypsum is fed to the drier via a double flap valve above the hot gas inlet. The gypsum is moved upwards by the rotating shafts, and the hot gas stream transports it to the end of the drier. The hot gas enters at a temperature of about 400°C (752°F) and exits at a temperature of about 90°C (194°F), the residence time of the gypsum in the drier being 8 to 13 s. Under these conditions all the surface water evaporates. The dried flue gas gypsum is discharged together with the exhaust gas and separated from the gas in a cyclone. Another part of the dried gypsum is discharged at the end of the lower part of the drier. The process is controlled by the exhaust gas temperature. If the temperature rises the gypsum feed increases and vice versa.

A special advantage of the rapid drier is its simple and robust design. Furthermore, the shafts rotating at a speed of 100 to 200 rpm disperse the particle clusters often found to occur in the flue gas gypsum. If the drier stops suddenly, these shafts can easily be restarted, which prevents the drier from clogging or the material forming buildups or sticking inside it. Choking in the event of incomplete drying of the flue gas gypsum, for instance at start-up, is not possible. This ensures operational dependability of the rapid drier.

The dried flue gas gypsum can subsequently be calcined in kettles to hemihydrate for the manufacture of gypsum plasterboard as it is done especially in North America and in Japan. For its use in the cement industry or in the manufacture of machine-applied plaster or hand-applied plaster the dry flue gas gypsum first has to be agglomerated. This will be explained in the next section.

Agglomeration of Flue Gas Gypsum

Agglomeration of finely divided gypsum, such as phosphogypsum or flue gas gypsum, into a lumpy product can be done by any one of the following processes:

(1) agglomeration by means of pelletizers,
(2) agglomeration by means of extrusion presses, and
(3) agglomeration by means of compacting presses.

These processes are briefly discussed below. Technically and economically the compacting press was found to be the best for the agglomeration of flue gas gypsum.

Agglomeration by Means of Pelletizers

Pellets are produced when the flue gas gypsum is agglomerized in pelletizers (Fig. 6). A bonding agent is required for this type of agglomeration, for instance calcium sulfate hemihydrate, which is added to the moist finely divided flue gas gypsum. At least 25% of hemihydrate and the adequate amount of water for hydration has to be added to ensure that the pellets will have the required strength. The moist flue gas gypsum does not have to be dried first. The pellets produced

FIG. 6—*Agglomeration of flue gas gypsum by means of pelletizers producing pellets.*

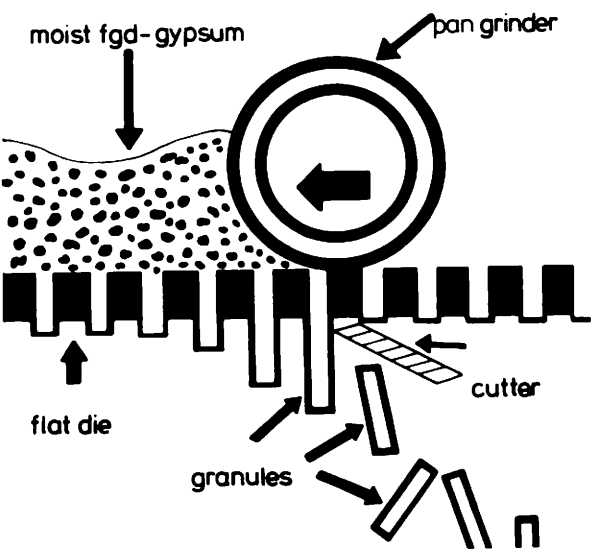

FIG. 7—*Agglomeration of flue gas gypsum by means of an extrusion press producing granules.*

are 10 to 25 mm in diameter, have a free water content of 8 to 10%, and an apparent density of about 1.6 g/cm^3.

Agglomeration by Means of Extrusion Presses

Granules are produced when the flue gas gypsum is agglomerated by means of an extrusion press (Fig. 7). The starting material is the moist, finely divided flue gas gypsum with a moisture content of 8 to 15% depending on the size distribution and the structure of the particles. The moist flue gas gypsum is squeezed through a flat die by means of a pan grinder. The granules obtained are cylindrical and have a diameter of 10 to 25 mm. Initially the granules are moist and of low strength.

The granules have to be dried immediately to achieve a higher strength. Belt driers are very suitable for this since, mechanically, they do not put much strain on the fresh soft granules. The dried granules have an apparent density of approximately 1.8 g/cm^3.

Agglomeration by Compacting Presses

The manufacture of briquets by agglomeration with a compacting press [*1*] is a process recently developed to produce a lumpy flue gas gypsum. When the process was being developed, it became apparent that the finely divided flue gypsum would have to be in the dry state. By using suitably designed press rollers, such as corrugated pass rollers closed at the ends (cigar-shaped), as shown in Fig. 8, flue gas gypsum briquets can be produced that have a point strength of more than 500 N and an apparent density of 2.15 g/cm^3. Natural gypsum has an apparent density of 2.3 g/cm^3. These flue gas gypsum briquets

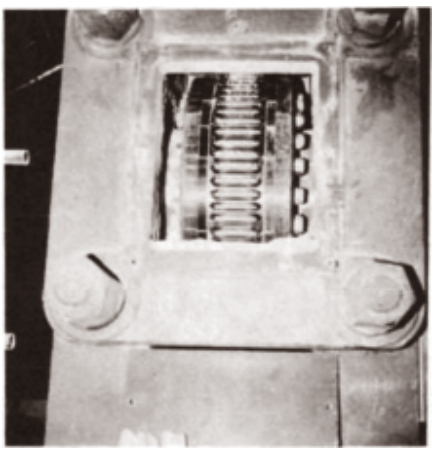

FIG. 8—*Cigar-shaped corrugated press roller of a compacting press.*

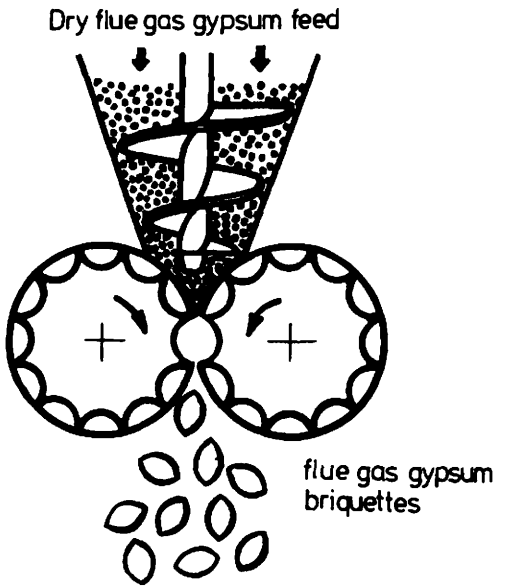

FIG. 9—*Agglomeration of flue gas gypsum by means of a compacting press producing briquets.*

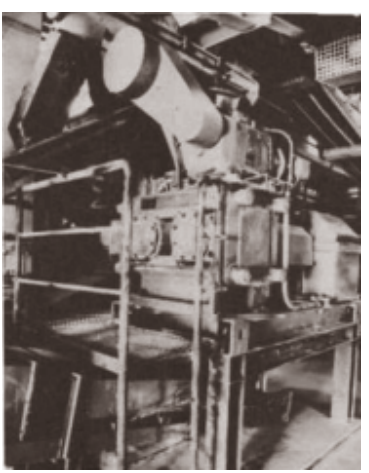

FIG. 10—*Compacting press in operation, capacity 4 ton/h.*

FIG. 11—*Flue gas gypsum briquets in storage.*

are therefore very much like a product made from natural gypsum. Because of their high strength and high density the briquets are exceptionally abrasion-resistant and can be stored in the open. Neither frost nor rain have any disturbing effect on them.

A further advantage of this process is that no bonding agents or additives are needed to agglomerate the finely divided flue gas gypsum. Also it was found that the briquets easily detach from the mold without any leftover material sticking to the press. Wear and tear of the rollers are slight because of the relatively soft gypsum grain (Mohs hardness 2). The operational dependability of the process has proved to be very good. The following figures show the process of compaction (Fig. 9), a compacting press in operation (Fig. 10), and flue gas gypsum briquets in storage (Fig. 11).

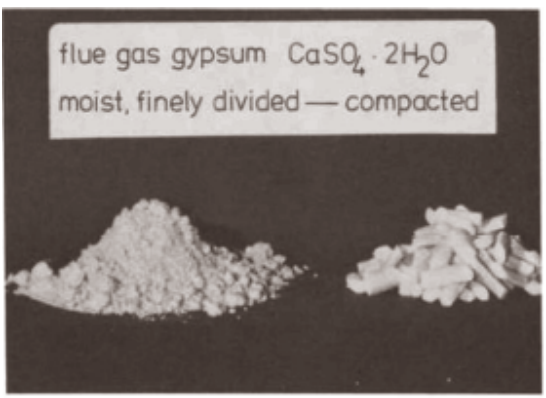

FIG. 12—*Comparison of finely divided flue gas gypsum and compacted flue gas gypsum.*

Figure 12 shows a comparison of finely divided flue gas gypsum with compacted flue gas gypsum. Special difficulties are caused by the very different bulk densities of the moist finely divided flue gas gypsum from approximately 0.5 to 1.2 ton/m^3. The process of compaction will overcome this deficiency and will produce a uniform product with a bulk density of about 1.0 to 1.1 ton/m^3.

From what has been said, and considering all the flue gas gypsum agglomeration processes, it can be concluded that if a compacting press is used for compaction a product is obtained that is of a lumpy structure very similar to that of lumpy natural gypsum.

Analyzing Compacted Flue Gas Gypsum

Tests carried out on compacted flue gas gypsum showed that nothing was left of the gypsum particles' initial size and shape. Scanning electron micrographs revealed that the flue gas gypsum briquets were of a solid structure, and the original gypsum crystals had intergrown into a rocklike body, as shown in Figs. 13 and 14. The original structure of the crystals could no longer be detected even after fine grinding of the briquets. Thus, the unfavorable particle size and shape of the flue gas gypsum were successfully dealt with by compaction under high pressure, and the flue gas gypsum could be used in the same way as natural gypsum. Besides, its thixotropic properties were thus completely eliminated.

It is mainly the monoclinic structure of the calcium sulfate dihydrate lattice that makes it possible for flue gas gypsum to be compacted without having to use bonding agents or additives, while the original particle size and structure are completely changed.

For the same reason it was possible to compact finely divided flue gas gypsum

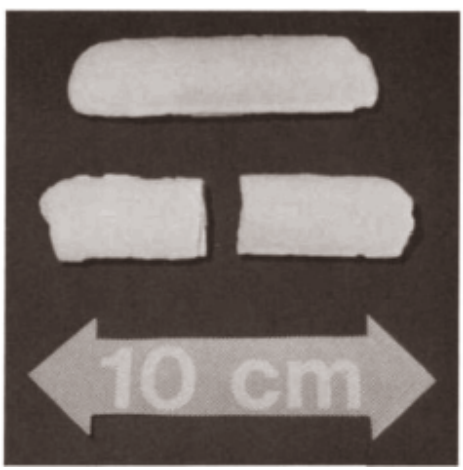

FIG. 13—*Flue gas gypsum briquets in original size.*

FIG. 14—*Scanning electron micrograph of the surface of a broken briquet: size and shape of the flue gas gypsum particles have disappeared.*

hemihydrate and get the same results. Calcium sulfate hemihydrate has a rhombohedral lattice arrangement with hollow channels containing water loosely bound. High pressure causes these particles also to intergrow.

So far this type of compaction has not been carried out successfully with anhydrous calcium sulfate because of its rhombic lattice arrangements and very dense ionic packing.

Technical Details of Drying and Compaction

Figure 15 schematically shows a plant for the processing of flue gas gypsum by drying and compaction, developed by Gebr. Knauf Westdeutsche Gipswerke, Iphofen, Federal Republic of Germany with the assistance of the Federal Ministry for Research and Technology, Federal Republic of Germany. This process is suitable for all types of flue gas gypsum.

At present four such plants are being built in the Federal Republic of Germany with a total capacity of 400.000 ton/*a* flue gas gypsum. These plants are to be commissioned in 1984 and 1985.

Particulars of the energy consumed by these plants are as follows:

1. Thermal energy for drying flue gas gypsum with a moisture content of 10%: 130.000 kcal/ton $CaSO_4 \cdot 2H_2O$ dry 550.000 kJ/ton $CaSO_4 \cdot 2H_2O$ dry.

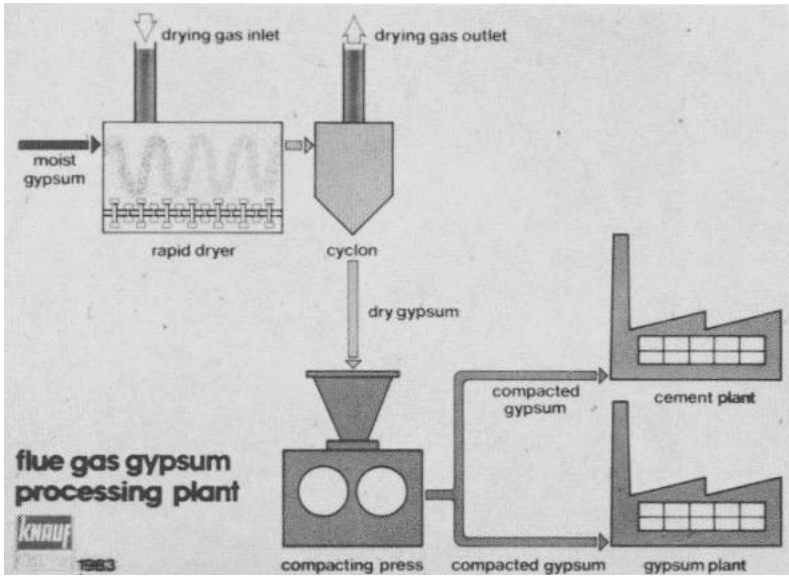

FIG. 15—*Schematic view of a processing plant for the compaction and drying of flue gas gypsum.*

2. Electrical energy for drying flue gas gypsum: 12 kWh/ton $CaSO_4 \cdot 2H_2O$ dry.
3. Electrical energy for compacting flue gas gypsum: 10 kWh/ton $CaSO_4 \cdot 2H_2O$ dry.

The thermal energy, in particular for drying the flue gas gypsum, is considerable being 130.000 kcal/ton or 550.000 kJ/ton. Attempts to cut down on this high energy consumption have led to utilizing waste heat, in the form of flue gas heat, from the power plant for drying the flue gas gypsum. Various tests were carried out successfully in a joint venture by Steinkohlen-Elektrizitäts-Aktiengesellschaft (STEAG) and Knauf in a pilot plant at the Haniel power station, Bottrop, Federal Republic of Germany. The plant produced 1.2 ton/h of dry gypsum.

In summary, it can be claimed that this process for the drying and compaction of flue gas gypsum clears the way for economically processing flue gas gypsum in combination with the power generated in the power plant (though without depending on the plant actually being in operation) and manufacturing a material that can be suitably utilized.

Reference

[1] Gebr. Knauf Westdeutsche Gipswerke, U.S. Patent No. 4,173,610, 20 Dec. 1977.

Summary

The papers in this publication may be divided into two parts; one dealing with procedures to determine the chemical composition and the physical properties of gypsum and gypsum products, and the other dealing with issues associated with the utilization of by-product gypsums.

Kocman has developed a rapid and precise X-ray fluorescence method for the multi-element analysis of gypsum and its products. Specimens of gypsum are calcined and fused into flat transparent disks, with sodium tetraborate flux. This flux was chosen because it produces and reduces clear transparent disks without the high incidence of gas entrainment and cracking. However, the use of sodium tetraborate prohibits sodium analysis by this method. Elements susceptible to analysis are calcium, sulfur, magnesium, strontium, silicon, aluminum, iron, potassium, phosphorus, and chlorine. The instrument used in the study was a Philips PW-1400 wavelength dispersive spectrometer equipped with four crystals (LiF, Ge, PET, TlAP). The analytical method is suitable for gypsum rock, hemihydrate, anhydrite, wallboard cores, gypsum bricks, gypsum plasters, quickset fillers, specialty gypsums, gypsum-based flooring cements, and other gypsum products.

Green describes a rapid and accurate polarizing microscope procedure for the qualitative analysis of gypsum, its dehydration products, and some common impurities. Gypsum may be identified by the refractive indices, oblique extinction angle, birefringence index, and a blue dispersion staining color. Natural anhydrite generally appears as blocky crystals with distinctive refractive indices, birefringence index, and parallel extinction. Beta hemihydrate has the same shape as the original dihydrate but is porous and cloudy instead of clear and solid. Alpha hemihydrate has characteristic refractive indices, a specific birefringence index, and its color changes from orange to blue when rotated. Deadburned gypsum has a similar refractive index to natural anhydrite but may be identified by dispersion colors of red and blue. Soluble anhydrite is the one species difficult to identify on the polarizing microscope. Silica has the same birefringence as gypsum, but its refractive index is higher and it has a yellow dispersion color. Limestone may be identified by its very high birefringence index whereby calcite may be distinguished from dolomite by color.

Goswami and Chandra identify sources of error in the determination of sulfur trioxide in gypsum by the precipitation of barium sulfate, and recommend a

revision of Section 12 of ASTM Chemical Analysis of Gypsum and Gypsum Products (C 471). The authors argue that the ASTM method, in using 50 mL of 1 + 5 hydrochloric acid as solvent for a 0.5-g specimen of gypsum and 20 mL of 10% barium chloride solution to precipitate, provides too high a concentration of both acid and chloride ions. The method also does not specify the final volume of solution before precipitation nor the use and type of filtering crucible. Lowering the quantities of hydrochloric acid and barium chloride used would reduce occlusion of chloride ions, coprecipitation of barium chloride and Ca^{++}, and solubility of barium sulfate in acidic solution. The authors recommend the following:

1. Reduce the initial amount of hydrochloric acid used as solvent to 25 mL of 1 + 5 hydrochloric acid for the 0.5-g test specimen.
2. Use 20 mL of 6% barium chloride solution (preferably old).
3. Make the volume of the reaction solution up to 400 to 500 mL before precipitation of barium sulfate.
4. Use filtering crucibles.

Karmazsin's paper describes a simple apparatus for measuring the degree of hydration of plaster and gypsum rock. The reactor consists of a vertical stainless steel cylinder capable of holding six small stainless steel sample tubes that are suspended from the removable roof of the cylinder by a stainless steel thermocouple well. The cylinder is fitted with a heater controlled by an external thermocouple, and a reservoir containing water vapor at 81% relative humidity is connected to the reactor. The reactor may be used to determine accurately the amount of dihydrate in either gypsum rock or incompletely hydrated plaster.

The work of Turk and Bounini on the mechanism of free-water uptake was intended to improve accuracy in the phase analysis of $CaSO_4 \cdot H_2O$ systems. The study determined that the amount of free moisture present is dependent on the physical structure of the sample as indicated by the adsorption and thermodynamic equilibria.

Drying conditions must leave these equilibria unaffected, that is, they must be in a region of the phase diagram where all calcium sulfate phases present remain stable. In microwave drying, this is accomplished by the selective absorption of microwave radiation energy to evaporate water. The study showed that microwave drying gives higher free moisture results than oven drying, indicating that more of the free moisture is removed from the pores of atmospheric calcined gypsum.

As Luckevich and Kuntze point out in their paper, the water demand of stucco is reduced by aging, which reduces the ability of the stucco to disintegrate. The objective of the work was to determine the relationship between water demand and particle size distribution resulting from changes in disintegration during aging. Tests used in determining these relationships were particle size analysis and various types of consistency measurements. The experimental data indicate,

with all other factors constant, that there is an almost linear relationship between water demand and particle size distribution and that the particle size distribution is governed by disintegration.

When aridizing agents or surfactants are used, consistency ceases to be a direct function of disintegration alone, but appears to depend on surface properties and particle morphology. This suggests it may be possible to produce a stucco with low water demand without sacrificing the disintegration necessary to maintain the desired setting and strength properties.

The work of Koslowski and Ludwig on the retardation mechanism of citric acid shows that this retarder has a considerable effect on the microstructure of hardened gypsum. Thus increased additions of citric acid cause a linear increase in the average grain size and a broader grain size distribution. Also, there is a hyperbolic change of the grain shape from long-prismatic to compact, an increased uniformity of grain shape, and a change from sphaerolithic crystal growth to isolated crystals.

The rate of hydration also causes changes in the microstructure. A slow rate causes a more distinct change toward a compact crystal shape. Citric acid addition causes a decrease in the total porosity and an increase in the average pore diameter. As a result gypsum strength was found to decrease with increasing additions of citric acid.

Archer's work on flexural strength, nail pull resistance, and core hardness of gypsum board has demonstrated that maximum load causing failure can be determined with greater accuracy using a constant strain rate rather than a constant stress rate. The correlation of results from either procedure shows that core hardness and nail pull resistance tests provide very similar information on core properties. It is argued that the more sophisticated constant strain rate machines should replace the equipment presently conforming to ASTM Physical Testing of Gypsum Board Products, Gypsum Lath, Gypsum Partition Tile or Block, and Precast Reinforced Gypsum Slabs (C 473).

Wirsching's paper describes a successful industrial process for drying and agglomerating flue gas gypsum. The process is intended to overcome the problems of processing flue gas gypsum, which is available as a moist, finely divided powder exhibiting thixotropic properties when attempts are made to use it. The purpose of the drying stage is to remove the 10% adsorbed surface water, without driving off any of the water of crystallization, with the lowest possible energy consumption in the shortest possible time. The equipment for this process is available.

There is a choice of three methods for successfully agglomerating the finely divided gypsum: pelletizing, extruding, and compacting. Technically and economically the compacting press was found to be the best for the agglomeration of flue gas gypsum. The agglomerated synthetic product was found to be similar to crushed natural gypsum rock. The scanning electron microscope (SEM) was unable to detect the presence of the original crystal structure in the compacted material, so that the initial problems of unfavorable particle size and shape were

overcome. As a result, the flue gas gypsum could be used in the same way as natural gypsum, and the thixotropic properties were completely eliminated.

Pressler discussed the history of by-product gypsum (BPG) utilization from 1972 to 1981. Over these nine years, there was no great change in the annual consumption or end use of BPG, consumption ranging from 610 000 to 750 000 ton/year. Five of the six companies that sold BPG in 1981 produced phosphoric acid from phosphate rock and sulfuric acid, while the sixth plant manufactured titanium dioxide pigment from ilmenite. All six companies are located in agricultural areas of the southern United States where the beneficial use of gypsum in agriculture is well understood.

The major applications in this area are stimulation of legume crops, especially peanuts, improvement in fertilizer utilization, softening of clayey soil, and neutralization of alkaline and saline soils. The 630 000 tons of BPG sold in 1981 is a small proportion of the total 10.4 million tons of crude gypsum produced in the United States in that year. There are indications, however, that BPG use in the United States may be on the increase.

The paper of May and Sweeney reports on work conducted by the Bureau at its Tuscaloosa Research Center on the environmental impacts of phosphogypsum produced by the Florida phosphate industry. Some 304 million metric tons of phosphogypsum by-product from the manufacture of phosphoric acid have been stockpiled to date, and the industry continues to generate 30 million metric tons a year. Samples from approximately 300 m of drill core obtained from mine stockpiles were characterized by chemical analysis, X-ray diffraction, emission spectrography, radiology, and physical testing. The data obtained indicated that phosphogypsum is not a corrosive or toxic hazardous waste according to the definition of the Environmental Protection Agency (EPA).

Thirty-nine elements were detected in the phosphogypsum samples, but concentrations of the elements did not vary with depth within the stockpiles. Radium content averaged 21 pCi/g and varied inversely with particle size.

A second paper by May and Sweeney reports on the second phase of the phosphogypsum study, that is, evaluation of the leaching characteristics of radium and toxic components identified in the phosphogypsum stockpiles during Phase I of the study. This was done by comparing estimated background concentrations of trace elements with concentrations found in the subsurface samples. The study concluded that toxic elements and radium were not being leached from phosphogypsum stockpiles.

Richard A. Kuntze
Ontario Research Foundation,
Sheridan Park, Mississauga,
Ontario, Canada L5K 1B3, editor

Index

ISBN 0-8031-0219-4